

Electronic Thesis and Dissertation Repository

---

10-12-2017 10:00 AM

## Characterization of plant-spider mite interactions and establishment of tools for spider mite functional genetic studies

Nicolas Bensoussan, *The University of Western Ontario*

Supervisor: Vojislava Grbić, *The University of Western Ontario*

A thesis submitted in partial fulfillment of the requirements for the Doctor of Philosophy degree in Biology

© Nicolas Bensoussan 2017

Follow this and additional works at: <https://ir.lib.uwo.ca/etd>



Part of the [Agronomy and Crop Sciences Commons](#), [Biotechnology Commons](#), [Cell Biology Commons](#), [Entomology Commons](#), [Genetics Commons](#), and the [Molecular Genetics Commons](#)

---

### Recommended Citation

Bensoussan, Nicolas, "Characterization of plant-spider mite interactions and establishment of tools for spider mite functional genetic studies" (2017). *Electronic Thesis and Dissertation Repository*. 5015. <https://ir.lib.uwo.ca/etd/5015>

This Dissertation/Thesis is brought to you for free and open access by Scholarship@Western. It has been accepted for inclusion in Electronic Thesis and Dissertation Repository by an authorized administrator of Scholarship@Western. For more information, please contact [wlsadmin@uwo.ca](mailto:wlsadmin@uwo.ca).

## Abstract

The two-spotted spider mite, *Tetranychus urticae* Koch (Acari: Tetranychidae), is one of the most polyphagous herbivores feeding on cell contents of over 1100 plant species including more than 150 crops. However, despite its important pest status and a growing understanding of the molecular basis of its interactions with plant hosts, knowledge of the way mites interface with the plant while feeding and the plant damage directly inflicted by mites is lacking. Likewise, while the use of the reverse genetic tools in plants facilitated our understanding of the establishment of defense mechanisms against spider mite herbivory, such tools are lacking for spider mite, preventing the expansion of functional analysis to both sides of the interacting organisms.

First, using various microscopy methods, I uncovered several key features of *T. urticae* feeding. By following the stylet path within the plant tissue, I determined that the stylet penetrates the leaf either in between epidermal pavement cells or through a stomatal opening, without damaging the epidermal cellular layer. Recordings of mite feeding events established that the duration of mite feeding ranges from several minutes to more than half an hour, during which time, mites consume a single mesophyll cell in a pattern that is common to both bean and *Arabidopsis* plant hosts. In addition, this study determined that leaf chlorotic spots, a common symptom of mite herbivory, do not form as an immediate consequence of mite feeding.

Second, using a soaking delivery method of dsRNA, I successfully triggered the RNAi response in *TuVATPase* and *TuCOPB2* target genes, resulting in visible phenotypes that correlated with reduced mite fitness and silencing of the *VATPase* gene. In addition, using RNAi-associated phenotypes, I enhanced RNAi efficiency by mixing dyes with dsRNA, to preselect mites that successfully ingested dsRNA, and have established a minimum size of 400 nucleotides of dsRNA to achieve a potent RNAi in spider mite.

Overall, my findings established a cellular context of plant-spider mite interactions and contributed to the development of the efficient RNAi protocol, a critical step toward functional characterization in *T. urticae*.

## Keywords

*Tetranychus urticae*; *Arabidopsis*; bean; chlorosis; microscopy; plant-pest interactions; stylet; RNA interference; mite target genes; RNAi optimization; dsRNA size.

## Co-Authorship Statement

A section of Chapter 1, including RNAi mechanism and RNAi in Tetranychid mites was published in a review article: *International Organization for Biological and integrated Control*. I am co-author with Dr. Vojislava Grbić (VG) who helped me for editing the manuscript.

A version of Chapter 2 is published in the journal: *Frontiers in plant Science*. I am co-author with Maria Estrella Santamaria (MES), Vladimir Zhurov (VZ), Isabelle Diaz (ID), Miodrag Grbić (MG), and Vojislava Grbić (VG). VG and MG conceived and together with ID planned the study. NB and MS performed experimental procedures, and collected data. NB, VZ, MG, and VG performed analysis and wrote the manuscript.

A version of the Chapter 3 was published in *Plos One*. For this section of the published manuscript, I am co-author with Takeshi Suzuki (TS), Maria Andréa Nunés (MAN) and Pengyu Jin (PJ) who contributed significantly. I performed gene expression analysis for each mite phenotype by qPCR, and synthesized dsRNA. TS developed the soaking method, and analyzed mortality and fecundity. MAN, PJ and I performed soaking of the 13 inbred lines, monitored mite fitness (mortality; fecundity) and analyzed data.

The Chapter 4 is in progress for completion. As it stands, I am co-author with PJ. I designed dsRNA fragments and performed soaking. I monitored mite fitness and performed whole mount *in situ* hybridization. PJ and I further optimized the soaking method.

## Acknowledgments

I would like to express my gratitude to my supervisor Dr. Vojislava Grbić who guided me through my PhD. I appreciated her patience and encouragement for all these years. I would like to thank her for the trust and the autonomy she has given me. To Dr. Miodrag Grbić, for his help and creative mind that encouraged me to think bigger. I would like to thank my advisors, Dr. Mark Bernards and Dr. Denis Maxwell. Their help and opinions were valuable. To the Biotron and especially to Dr. Richard Gardiner, who helped me to develop my microcopy skills and histology techniques during my PhD.

I would like to thank all my lab members, past and present. To Biljana and Vlad for their help during my project and coffee breaks. To Kristie, Golnaz, Zaichao and Peng for their enthusiasm and time spent together. To Hooman, for his time spent in the lab and on the tennis court. To the former post docs, Maria, Andrea and Takeshi, for their support during my project and for the valuable skills I learned from them.

Thanks to the staff members, Carol, Diane and Arzie for their availability and support over the years.

I would like to thank my parents and family members for their understanding, patience and support. Thanks for helping during all these years, and belief in my capacity to achieve my goals.

Finally, to Maja, who supports me on a daily basis and gives me motivation to always go further.

# Table of Contents

Abstract.....	i
Co-Authorship Statement.....	iii
Acknowledgments.....	iv
List of Tables .....	ix
List of Figures.....	x
List of Appendices .....	xii
List of Abbreviations .....	xiii
Chapter 1.....	1
1 General introduction .....	1
1.1 The two-spotted spider mite – <i>Tetranychus urticae</i> (Koch).....	1
1.2 Feeding mechanism and digestive tract.....	3
1.3 Plant damage and cytological changes associated with feeding.....	6
1.4 Spider mite control strategy.....	8
1.5 RNA interference.....	9
1.6 RNAi pathways and biological function.....	10
1.7 Mechanism of RNAi through the exogenous application of dsRNA .....	11
1.8 RNAi as a tool for pest control.....	11
1.9 Factors influencing RNAi efficiency.....	13
1.9.1 dsRNA design.....	13
1.9.2 dsRNA delivery method .....	14
1.9.3 Gut Environment.....	16
1.9.4 RNAi in Tetranychid mites.....	16
1.10 Rationale and specific goal of my research .....	18
1.11 Reference .....	20
Chapter 2.....	30

2	Plant-herbivore interaction: dissection of the cellular pattern of <i>Tetranychus urticae</i> feeding on the host plant .....	30
2.1	Introduction.....	30
2.2	Material and Methods .....	33
2.2.1	Plant growth and material rearing.....	33
2.2.2	Monitoring of <i>T. urticae</i> feeding .....	33
2.2.3	<i>T. urticae</i> cuticular preparations .....	33
2.2.4	Phalloidin staining .....	33
2.2.5	Scanning electron microscopy .....	34
2.2.6	Trypan blue staining of plant tissue and quantification of damage caused by <i>T. urticae</i> feeding.....	34
2.2.7	Histological analysis of <i>T. urticae</i> stylet path through the plant tissue ....	35
2.3	Results.....	36
2.3.1	Determination of the <i>T. urticae</i> feeding event.....	36
2.3.2	Determination of <i>T. urticae</i> Feeding Pattern on Plant Tissue.....	38
2.3.3	<i>Tetranychus urticae</i> Feeding.....	44
2.4	Discussion.....	48
2.4.1	Mechanism of <i>T. urticae</i> feeding.....	48
2.4.2	Mechanism of <i>T. urticae</i> Feeding: Comparison with other Cell-Content Feeding Herbivores and Implications for the Host Plant Defenses .....	51
2.5	Reference .....	56
	Chapter 3.....	61
3	RNA interference in the two-spotted spider mite <i>Tetranychus urticae</i> through soaking in solution of dsRNA. ....	61
3.1	Introduction.....	61
3.2	Materials and Methods.....	63
3.2.1	<i>T. urticae</i> rearing conditions .....	63
3.2.2	Preparation of developmentally synchronized mites .....	63

3.2.3	dsRNA fragments.....	64
3.2.4	dsRNA preparation for <i>TuVATPase</i> .....	64
3.2.5	Soaking mites in solution of dsRNA .....	67
3.2.6	Analysis of RNAi efficiency in inbred lines.....	67
3.2.7	RT-qPCR .....	68
3.2.8	Data analysis of survival and fecundity .....	68
3.2.9	Data analysis of <i>TuVATPase</i> RNAi effect on inbred lines .....	69
3.2.10	Imaging .....	69
3.3	Results.....	69
3.3.1	Induction of RNAi in soaked mites .....	69
3.3.2	Differential RNAi response in <i>T. urticae</i> inbred lines.....	75
3.4	Discussion.....	83
3.5	Reference .....	86
Chapter 4.....		89
4	Towards the establishment of an optimized method for gene silencing in the two-spotted spider mite <i>Tetranychus urticae</i> .....	89
4.1	Introduction.....	89
4.2	Materials and Methods.....	91
4.2.1	<i>T. urticae</i> rearing conditions .....	91
4.2.2	Preparation of developmentally synchronized mites .....	91
4.2.3	dsRNA fragments.....	92
4.2.4	dsRNA synthesis.....	95
4.2.5	Localization of <i>COPB2</i> mRNA expression pattern using whole mount <i>in situ</i> hybridization .....	97
4.2.6	Soaking mite in solution of dsRNA .....	98
4.2.7	Data analysis of survival and fecundity .....	98
4.2.8	Analysis of dsRNA uptake.....	99



4.2.9	Analysis of RNAi efficiency using various dsRNA fragment length.....	99
4.2.10	dsRNA- <i>TuVATPase</i> mix.....	100
4.2.11	Imaging.....	100
4.3	Results.....	100
4.3.1	Induction of RNAi in dsRNA <i>TuCOPB2</i> soaked mites.....	100
4.3.2	Whole mount <i>in situ</i> hybridization .....	103
4.3.3	Testing the uniformity of the dsRNA uptake.....	103
4.3.4	The effect of dsRNA size on RNAi efficiency .....	106
4.4	Discussion.....	112
4.4.1	Induction of RNAi in dsRNA <i>TuCOPB2</i> soaked mites.....	112
4.4.2	Optimization of dsRNA soaking method and RNAi design.....	113
4.5	Reference .....	116
Chapter 5	.....	119
5	Summary and Discussion.....	119
5.1	<i>T. urticae</i> feeding and plant damage.....	119
5.2	RNAi establishment and further optimization in <i>T. urticae</i> through soaking in dsRNA .....	122
5.3	Reference .....	125
6	List of Appendices .....	128
Curriculum Vitae	.....	133

## List of Tables

Table 2.1: Distribution of trypan blue stained cells within bean and <i>Arabidopsis</i> leaf tissues resulting from <i>T. urticae</i> feeding for 10 min. ....	43
Table 3.1: Primers used in this study. ....	66
Table 4.1: Primers used in this study. ....	94

## List of Figures

Figure 1.1: <i>T. urticae</i> life cycle.....	2
Figure 1.2: Schematic representation of a sagittal section through <i>T. urticae</i> female.....	4
Figure 1.3: Mechanism of RNA interference in eukaryotic cell.....	12
Figure 1.4: Heatmap representing expression patterns of RNAi-associated genes at different developmental stages of <i>Tetranychus urticae</i> , based on the number of mapped RNAseq reads (Illumina). .....	17
Figure 2.1 <i>T. urticae</i> feeding duration and mouth-part organs. ....	37
Figure 2.2: Mite feeding event and plant damage.....	39
Figure 2.3: Bean and <i>Arabidopsis</i> leaves cell layer.....	41
Figure 2.4: Plant damage associated with spider mite feeding. ....	42
Figure 2.5: Interface between <i>T. urticae</i> and plant tissue during feeding.....	45
Figure 2.6: Model of the interactions between the plant and the cell-content feeding herbivores—the two-spotted spider mite and the aphid. ....	55
Figure 3.1: Fragment used for the synthesis of dsRNAs. ....	65
Figure 3.2: White phenotype associated with soaking in solution of dsRNA. ....	70
Figure 3.3: Dark phenotype associated with RNAi response to dsRNA. ....	72
Figure 3.4: Adult survivorship after soaking treatment in solution of dsRNA- <i>TuVATPase</i> separately for normal and dark-body mites. ....	73
Figure 3.5: Adult mite fecundity and <i>TuVATPase</i> gene expression after soaking treatment in solution of dsRNA- <i>TuVATPase</i> . ....	74
Figure 3.6: RNAi response in soaked <i>T. urticae</i> inbred lines. ....	77
Figure 3.7: Inbred line mortality after treatment with dsRNA- <i>TuVATPase</i> . ....	79
Figure 3.8: Inbred line fecundity after treatment with dsRNA- <i>TuVATPase</i> . ....	80

Figure 3.9: Dark mite frequency in the inbred lines and London reference population after treatment with dsRNA. ....	81
Figure 3.10: Scatter 3D function displaying RNAi response parameter as a collection of points, plotted using three-dimensional cartesian coordinates. ....	82
Figure 4.1: Fragments used for synthesis of dsRNAs.....	93
Figure 4.2: Schematic of the template preparation for dsRNA synthesis and mRNA DIG-labeled probes using the PCR method. ....	96
Figure 4.3: Mite phenotype associated with RNAi response to dsRNA- <i>TuCOPB2</i> .....	101
Figure 4.4: Adult survivorship after soaking treatment in solution of dsRNA- <i>TuVATPase</i> separately for normal and dark-body mites. ....	102
Figure 4.5: Adult mite fecundity after soaking treatment in solution of dsRNA- <i>TuCOPB2</i> . ....	104
Figure 4.6: Whole-mount in situ hybridization of <i>COPB2</i> gene expression pattern in <i>T. urticae</i> female. ....	105
Figure 4.7: Correlation between blue mite and RNAi response after soaking for 24 hours in solution containing dsRNA with blue dye. ....	107
Figure 4.8: The effect of dsRNA- <i>TuVATPase</i> sequence sizes and variability of gene regions targeted on RNAi efficiency. ....	109
Figure 4.9: The effect of dsRNA- <i>TuCOPB2</i> sequence sizes and variability of gene regions targeted on RNAi efficiency. ....	110
Figure 4.10: The effect of mixed dsRNA- <i>TuVATPase</i> fragments on RNAi efficiency. ....	111

## List of Appendices

Appendix 1: Brightfield and confocal microscopy observation of fecal pellets and crystals of guanine in <i>T. urticae</i> . .....	128
Appendix 2: Representative picture of a cryosection of a mite feeding on a bean leaf previously frozen and embedded in optimal cutting temperature compound (OCT compound). .....	129
Appendix 3: Representative picture of a microtome section of a mite feeding on a bean leaf previously frozen, fixed, dehydrated and embedded in paraffin. ....	130
Appendix 4: Expression pattern of selected genes, highly expressed in mite's head using whole-mount RNA <i>in situ</i> hybridization.....	132

## List of Abbreviations

°C	degree Celsius
µg	microgram
ng	nanogram
µl	microliter
µm	micrometer
bp	base pair
cDNA	complementary deoxyribonucleic acid
DIG	digoxigenin
DNA	deoxyribonucleic acid
dsRNA	double stranded ribonucleic acid
mRNA	messenger ribonucleic acid
PBS	phosphate-buffered saline
PCR	polymerase chain reaction
RNA	ribonucleic acid
SEM	scanning electron microscopy
RT-qPCR	quantitative reverse transcription PCR
v/v	volume/volume
DNase	deoxyribonuclease
BSA	bovine serum albumin
HRc	high resolution camera
SSC	saline-sodium citrate buffer
NBT	nitro blue tetrazolium
BCIP	5-bromo-4-chloro-3'-indolyphosphate p-toluidine salt

## Chapter 1

### 1 General introduction

#### 1.1 The two-spotted spider mite – *Tetranychus urticae* (Koch)

The two-spotted spider mite, *Tetranychus urticae* (Acari: Tetranychidae) belongs to a group of plant pests whose members produce abundant silk (hence the name “spider mites”). The first specimen described was collected by the German arachnologist and entomologist Carl Ludwig Koch in 1836 on a stinging nettle, *Urtica dioica* (Koch, 1836). *T. urticae* belongs to the phylum of the Arthropoda, which are characterized by a segmented body, jointed appendages and presence of a chitinous exoskeleton. Within the arthropods, *T. urticae* belongs to the subphylum *Chelicerata* that represents the second largest group of arthropods. In the group of Acari, which is separated from spiders, phytophagous mites belong to the order of Trombidiformes, with about 22 000 species described (Walter, 2004). Despite its small size (about 0.5 mm long), *T. urticae* is an economically important agricultural pest with a global distribution (Bolland et al., 1998). The *T. urticae* genome was sequenced and annotated, and is characterized by a small size of 90 Mb (Grbić et al., 2011).

The mode of reproduction follows parthogenesis, in which fertilized offsprings develop into females and unfertilized eggs develop into males (Olivier, 1971). The duration of the *T. urticae* life cycle from eggs to adults varies from about a week to several weeks depending on the temperature and humidity. Helle and Sabelis (1985), established a development time of about 7-8 days at 27.5-32.5°C. *T. urticae* development transits through four development stages with quiescent stages at the end of larval and nymphal development, called chrysalis, as shown in the Figure 1.1 (Boudreaux, 1963). The eggs hatch after about 4-day post oviposition into a larva that is recognizable by its 3 paired-legs. Subsequently, the larva passes through a quiescent stage, the protochrysalis emerges into a protonymph with 4 pairs of legs. The protonymph undergoes another molting to become deutonymph. The last quiescent stage is the teliochrysalys from which new molted adults emerge (Shih et al., 1976).

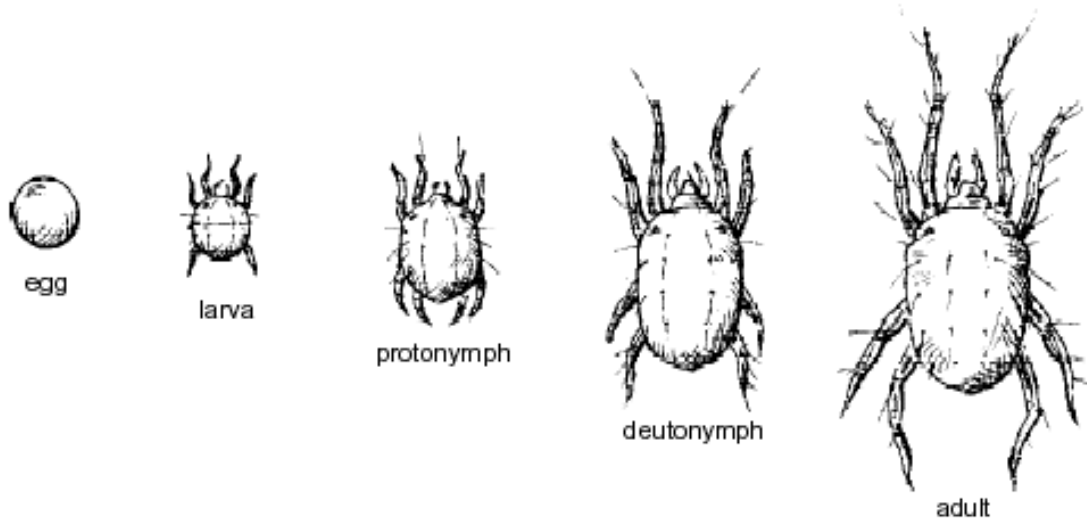


**Figure 1.1: The different development stages of *T. urticae*.** The larva hatches from egg. The remaining immatures are nymph (Illustration by D. Kidd).



## 1.2 Feeding mechanism and digestive tract

Since the 1940s, extensive studies have been carried out to depict mite anatomy and body structures associated with feeding. Bearing in mind the minute size of the mite, most of the reports on anatomic features used histological cross sections coupled with electron microscopy. Although, some nomenclature may vary between authors, a good agreement among reports regarding features of the mouthparts is established. A simplified description of a mite's body is described below and in Figure 1.2.

The mite body is divided in two functional domains: the gnathosoma, housing organs specialized in feeding (Becker, 1935), and the idiosoma, carrying the legs and organs dedicated in digestion, reproduction and excretion (Hammen, 1970). The gnathosoma is separated from the idiosoma by a flexible cuticule called circumcapitular furrow (Alberti, 2006; Grandjean, 1969). The gnathosoma is composed of two parts, the stylophore (STY; dorsal part of the gnathosoma), housing mobile elongated cheliceral digits (CHD; feeding tube), and the infracapitulum (ventral part of the gnathosoma), including the buccal cavity (BC), the pharynx (PH) and the pedipalps (PE) (André and Remacle, 1984; Mothes and Seitz, 1981b).

The stylophore is deeply inserted into the gnathosoma and a sclerotized invagination of the cuticule serves as the attachment site of a strong protractor muscle. The stylophore is flexible and independent from the infracapitulum where the protractor muscle is attached allowing a protraction of the stylophore. However, André and Remacle (1984), didn't observe any retractor muscles and postulated passive retraction of the stylophore. The stylophore bear a pair of feeding/piercing structure known as cheliceral digits (Alberti and Crooker, 1985; André and Remacle, 1984; Nuzzacci and De Lillo, 1991b; Summers et al., 1973). The two flexible cheliceral digits are strongly curves upward with, in each inner part, a specialized cuticule that allowed each digit to interlock by a tongue-and-groove shape (André and Remacle, 1984; Hislop and Jeppson, 1976; Summers et al., 1973). Transversal sections of cheliceral digits showed innervation and its rounded shape with a regular size except the narrowing at the tip, assumed to facilitate the piercing of plant tissues and cells (André and Remacle, 1984). When establishing the feeding

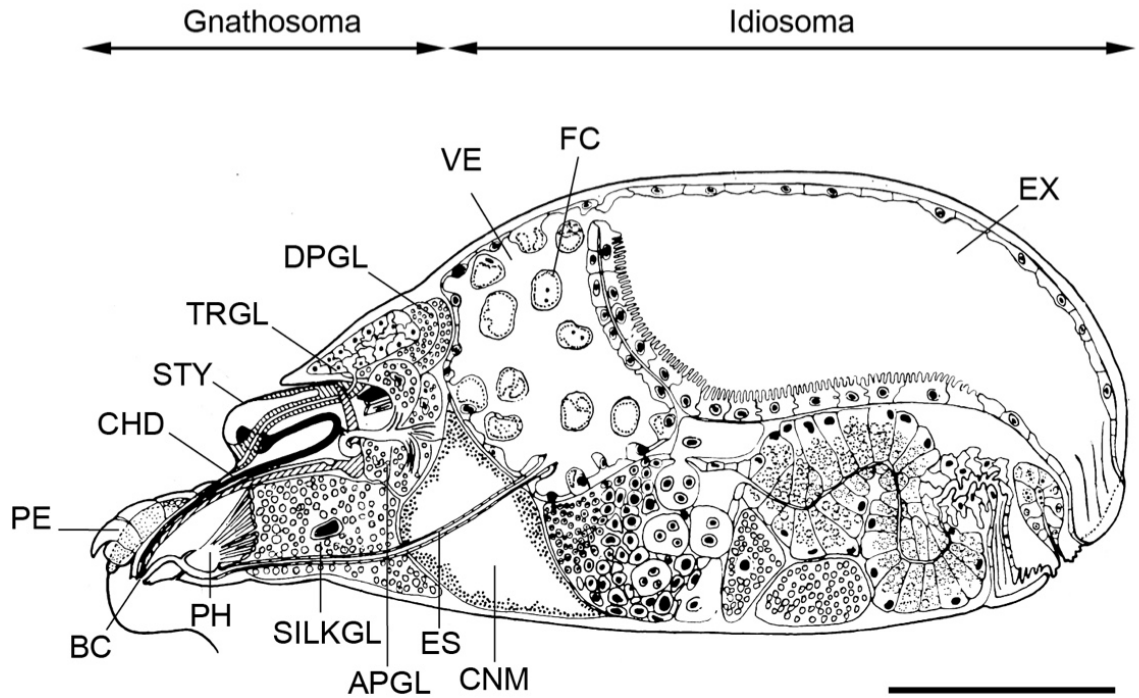


**Figure 1.2: Schematic representation of a sagittal section through *T. urticae* female.** Abbreviations: APGL: anterior podocephalic gland; BC: buccal cavity; CHD: cheliceral digit; CNM: central nervous mass; DPGL: dorsal podocephalic gland; ES: esophagus; EX: excretory organ; FC: floating cell; PE: pedipalps; PH: pharynx; SILKGL: silk gland; STY: stylophore; TRGL: tracheal gland; VE: ventriculus. Scale bar: 100  $\mu$ m. (Adapted from Alberti and Crooker (1985), with the permission of Elsevier).

process, a mite presses the infracapitulum in the contact with the leaf surface, using its pedipalps. The chemo- and mechano-sensing receptors that are presents within sensorial organ such as the setae (Mills, 1973), presumably help mites find a suitable feeding spot. In preparation for feeding, the protractor muscles contract and each cheliceral digit runs into the infracapitulum groove (rostral gutter), which helps interlock them in the narrowest part of the buccal cavity to form a hollow tube-stylet (Andre and Remacle, 1984; Summers et al., 1973). Once protracted, the stylet length ranges from 100  $\mu\text{m}$  in larval stages to about 150  $\mu\text{m}$  in adult female mites (Avery and Briggs, 1968; Ekka, 1969; Sances et al., 1979). The function of this tube remains unknown and it is still the subject of controversy among authors whether it can be used as a piercing structure to deliver salivary secretion into plant tissue and/or is used for the food uptake as well (André and Remacle, 1984; Hislop and Jeppson, 1976; Summers et al., 1973). Alternatively, the buccal cavity has been postulated to be the orifice by which the nutrient extruded from the epidermis is absorbed (Alberti and Crooker, 1985; Nuzzacci and De Lillo, 1991b).

Five glands (two paired of podocephalic glands: one anterior (APGL) and one dorsal (DPGL), two paired of coaxal glands and one unpaired tracheal gland (TRGL), including the silk glands (SILKGL)) have been identified in *T. urticae* and located in the dorsal part of the gnathosoma (Mills, 1973). Except for the silk glands, the functions of other glands are still unknown. However, Hammen (1980), has shown a salivary canal running from the infracapitulum to the tip of the gnathosoma, suggesting a role of two podocephalic glands in secretion. In the order Tenuipalpidae, the *Brevipalpus* mite presents similarites in anatomic features of the glands (Alberti et al., 2014). The authors have proposed a specific function for each of the prosomal glands. The anterior and dorsal podocephalic glands were proposed to be involved in producing saliva enzyme-secretions, while the coaxial glands are responsible of water, ions and osmoregulation secretions. Finally, the tracheal gland would be involved in the production of a lubricant facilitating the stylet to slide in the groove (Summers et al., 1973). Recent studies have demonstrated that *T. urticae* excretes salivary secretions via salivary glands (Jonckheere et al., 2016; Villarroel et al., 2016). It has been proposed that these secretions mediate suppression of plant defenses (Alba et al., 2015; Kant et al., 2008; Wybouw et al., 2015).

Regardless of the way mites ingest plant nutrients, the food is absorbed into the buccal cavity, through the pharynx (PH) that produces a sucking force and acts as a pump. The nutrients flow into the esophagus (ES), and are absorbed in the ventriculus (VE) that consists of large digestive “floating” cells (FC) in the midgut of the mite. The midgut is composed of the ventriculus above the nervous system (CNM) connected to the esophagus and the excretory system (EX). Two large cavities, the caeca specialized in digestion, fill most of the lateral part of mite body (Alberti and Crooker, 1985; Alberti and Storch, 1973). Large digestive “floating” cells are pinched from the ventriculus epithelium and are presumably involved in the absorption of the gut content by phagocytosis and pinocytosis (Mothes and Seitz, 1981a). These floating cells are transported into the excretory organ responsible for the elimination of food residue and nitrogenous wastes (Blauvelt, 1945). Two types of digestion product are excreted (Gasser, 1951; Hazan et al., 1974). Black balls located in the ventriculus and in the caeca, and white pellets located only in the excretory organ. Recently, these two types of residues were visualized under confocal microscope (Occhipinti and Maffei, 2013). These authors demonstrated that the black pellets contain chlorophyll and its degradation products while the white pellets are composed of the guanine residue (see also personal observation, Appendix 1).

### 1.3 Plant damage and cytological changes associated with feeding

*T. urticae* feeding causes extensive damage and important physiological changes in the host plant. They have been reported to feed on all aerial parts of the plant including cotyledon, leaves, stems, fruits and flowers. Although mites are mostly found at the abaxial side of the leaf (the underside that is shaded by the leaf itself), they are able to feed on both sides. The degree and the depth of injury are depending of several factors: 1) the length of the stylet, from 100 to 150 $\mu$ m 2) the feeding duration 3) mite population density and 4) host plant features (Avery and Briggs, 1968; Campbell et al., 1990; Ekka, 1969; Sances et al., 1979).

Reports on *T. urticae* feeding on strawberry plants have shown damage being restricted to the spongy mesophyll layer with minimal injuries to the uppermost palisade mesophyll

layer (Campbell et al., 1990; Sances et al., 1979). Similar conclusion were made with mites feeding on cucumber (Park and Lee, 2002). Also, a low mite density seems to affect mostly the spongy mesophyll, while with a high density of mites, both spongy and palisade mesophyll layers were affected (Sances et al., 1979).

Interestingly, the brown mites, *Bryobia rubrioculus*, feeding predominantly on the upper epidermis of almond leaves, caused damaged on the palisade layer, leaving the spongy layer unaffected (Summers and Stocking, 1972). The same authors evaluated the stylet length of *B. rubrioculus* to be 75  $\mu\text{m}$  long while the palisade layer is 90  $\mu\text{m}$  thick, leaving the spongy mesophyll layer unreachable for mites feeding from the upper epidermis. Also, it seems that, damage associated with feeding is localized within the mesophyll layer that is underneath the epidermis where the mite tends to settle. However, it is still unclear where the stylet is inserted in the epidermal cells. For instance, Avery and Briggs (1968) didn't observe epidermal damage and postulated that the stylet was inserted between the epidermal cells along the anticlinal walls. Similarly, no evidence of tissue damaged were observed to the lower epidermis of strawberry leaves (Sances et al., 1979). However, Campbell (1990) observed the presence of stylet holes through the periclinal walls of epidermal cells.

Although these studies represent the benchmark of *T. urticae* feeding pattern, these observations were made days or weeks post feeding, at the time when plant responses to mite feeding are triggered. As a consequence, these observations may be the combination of direct damage caused by mite feeding and plant responses, leaving the direct feeding injury unknown. For instance, changes to the stomatal apparatus reported by Sances et al., (1979) was not caused by direct *T. urticae* feeding, but rather resulted from injury to the spongy mesophyll layer that lead to reduced turgor in guard cells associated with plant's physiological response to mite feeding. Similarly, Mothes and Seitz (1982) reported a strong reduction of leaf thickness in bean leaves by 50%, 6 days post feeding. Likewise, several other reports (Avery and Briggs, 1968; Mothes and Seitz, 1981a; Tanigoshi and Davis, 1978) showed an extensive cell death in leaf tissue upon prolonged mite infestation, leaving the extent of leaf damage directly caused by mite feeding unknown. Furthermore, the presence of coagulated protoplasts, lack of cell content and

chloroplast abnormalities in cells that appear adjacent to the punctured cell (that may have been consumed by mite feeding) has been reported by Avery and Briggs (1968) and Tanigoshi and Davis (1978). In contrast, no morphological distortion in mesophyll cells adjacent to mite-damaged cells were observed in strawberry, suggesting that plant responses may differ in different species and may be dependent on their physiological state (Campbell et al., 1990; Sances et al., 1979).

## 1.4 Spider mite control strategy

*T. urticae*, is one of the most polyphagous arthropods, feeding on more than 1100 plant species including more than 150 agricultural crops that belong to more than 140 different families (Jeppson et al., 1975; Migeon and Dorkeld, 2006-2017). Despite increasing effort from the scientific community and growers, spider mite control remains challenging. Three main factors contribute to spider mite spread: pesticide resistance, crop practice and global warming. The current Integrated Pest Management (IPM; defined as a combination of existing pest management measures to decrease pests and reduce or minimize the use of pesticides) of spider mite relies on biological control using predatory mites and pesticides. However, while biological control is efficient under specific condition and low population density, *T. urticae* control requires utilization of pesticides. Unfortunately, *T. urticae* rapidly develops resistance to pesticides making mites the arthropod with the highest occurrence of pesticide resistance. This is due to its short life cycle, high fecundity and its specific mating system through which recessive resistance alleles are easily fixed via haploid males (Carrière, 2003; Denholm et al., 1998). Moreover, It has been evaluated that *T. urticae* can develop resistance to a new pesticide between 2 to 4 years (Van Leeuwen et al., 2015).

One mechanism of resistance is based on the modification of the targeted site due to a mutation that alters the interaction between the protein target and the pesticide (Li et al., 2006; Riga et al., 2017). The second mechanism consists of pesticide sequestration or enhancement of metabolism that prevent pesticide molecules from reaching their target (Roush and Tabashnik, 1990; Taylor and Feyereisen, 1996). In addition, major class of insecticides like the neonicotinoids (targeting acetylcholine receptor) do not have effect

on spider mites but affect mite predators, resulting in spider mite expansion. Also, damage caused by spider mite infestation coupled with an increase of mite population in warm weather is predicted to exacerbate plant damage as spider mites reproduce faster in high temperature. Likewise, drought-stress of host plants increases spider mite oviposition by two times (Ximénez-Embún et al., 2016).

## 1.5 RNA interference

Prior to the discovery and the characterization of RNAi mechanisms by Fire and Mello in 1998, the phenomena was initially reported in the petunia by Jorgensen and his team in an attempt to overexpressed the chalcone synthase gene (*chsA*), involved in anthocyanin production (Napoli et al., 1990). Unexpectedly, transgenic petunia carrying the *chsA* gene under the control of the strong promoter (35S) yielded petunia plants with white flowers or partially white with a pigmented background instead of purple flowers. The authors demonstrated that both endogenous and exogenous *chsA* transcripts were suppressed and that the reduction of mRNA transcript was not related to the reduction of the transcription efficiency, suggesting a “co-suppression” of homologous mRNA. A similar phenomenon was observed in the fungus *Neurospora crassa*, in an effort to increase the production of an orange pigment. The transformation of *N. crassa* wild-type (orange phenotype) by the carotenogenic albino-3 (*al-3*) or albino-1 (*al-1*) resulted in an albino phenotype in a few transformants in which transcripts levels were drastically reduced (Romano and Macino, 1992). The authors qualified this phenomenon in fungus as “quelling”.

In 1998, Fire and his colleagues demonstrated the nature of gene silencing by injecting double-stranded RNA (dsRNA) molecules into the body of the model organism *Caenorhabditis elegans* (Fire et al., 1998). They observed that injection of dsRNA was more efficient in reducing gene expression than sense mRNA or antisense mRNA single-strands. Furthermore, they discovered the systemic effect of gene silencing that could affect not only the injected animal but its progeny as well. This work was the first to elucidate the phenomena of gene silencing, for which the authors received the Nobel Prize in 2006.

Since the RNAi discovery, key elements underlying the RNAi mechanism were discovered. For instance, Hamilton (1999), identified small double stranded RNA molecules of about 25 nucleotides that were complementary to the targeted mRNA. They hypothesized that these small RNAs are the mediators of mRNA degradation. This hypothesis was verified in a series of experiments in which exogenous short-interfering dsRNA (siRNA) fragments of about 21 nucleotides long were able to trigger gene silencing in *Drosophila* embryo (Hammond et al., 2000) and mammalian cell lines (Elbashir et al., 2001). In the same time, the key enzyme responsible for the cleavage of dsRNA into a population of siRNAs was identified in *Drosophila melanogaster*. It is a type III RNase enzyme that is referred to as Dicer (for its dicing activity) (Bernstein et al., 2001; Hammond et al., 2000). Further, two proteins, Argonaute 1 (AGO1) and Argonaute 2 (AGO2) were identified in *Drosophila* to form a complex with the Dicer enzyme, yielding the RISC complex (RNAi-induced silencing complex), hypothesized to directly mediate the “slicing” activity (Hutvagner and Zamore, 2002; Martinez et al., 2002; Nykänen et al., 2001). However, only Argonaute 2 has been demonstrated to have the endonuclease activity (Liu et al., 2004).

## 1.6 RNAi pathways and biological function

Three main RNAi pathways associated with small RNAs have been characterized, each displaying specific function in eukaryotic organisms.

Micro RNAs (miRNA) are derived from long hairpin RNA encoded by the host genome. Its processing yields a single small non-coding RNA of about 22 nucleotides (Bartel, 2004). This endogenous RNAi is involved in gene regulation and functions as a repressor of either gene translation (Translation Gene Silencing; TGS; Djuranovic et al., 2012) or at the post transcriptional level (Post-Transcriptional Gene Silencing; PTGS; Bushati and Cohen, 2007; Leucci et al., 2013; Pillai et al., 2017). The Piwi-interacting short RNAs (piRNAs) mediated pathway has been demonstrated to be involved in silencing of transposable elements, preserving genome integrity (Aravin et al., 2007; Lee, 2015; Sienski et al., 2012).

Finally, the siRNA also called exogenous RNAi, is the pathway that has a role in protection against invading viral RNA (Ding, 2010; Ding and Voinnet, 2007). The



siRNA pathway can be manipulated through biotechnology to suppress a specific gene target by delivering dsRNA into the cell.

## 1.7 Mechanism of RNAi through the exogenous application of dsRNA

When exogenous dsRNA is introduced, dsRNA molecules are processed by the enzyme Dicer-2 into a population of uniformly sized siRNA molecules of 20 to 25 bp long and loaded into the RISC complex. siRNAs are subsequently recruited by the Argonaute proteins into a RISC complex that either cleaves the homologous mRNA or prevents its translation (Figure 1.3). This mechanism is particularly interesting, since the application of the exogenous dsRNA can be used to knock-down, in theory, any gene. Since RNAi depends on the complementarity between the target and dsRNA, the RNAi response is expected to be specific. For more than a decade, RNAi has been used as a reverse genetic tool (Lawson and Wolfe, 2011), therapeutic treatment (Aagaard and Rossi, 2007) and recently in plant-pest control (Baum et al., 2007). The use of RNAi in the control of plant-pests is based on the premise that if the targeted mRNA encodes an essential protein, its silencing leads to lethality. The sequence specificity of a dsRNA fragment used for the RNAi should secure effectiveness against a particular species without affecting other organisms.

## 1.8 RNAi as a tool for pest control

A potential use of RNAi in agricultural pest control has been established by Baum and Mao who independently demonstrated that artificial diets and transgenic plants can be used as delivery systems of dsRNA capable of silencing genes in insect pests (Baum et al., 2007; Mao et al., 2007). In the study done by Mao, transgenic plants were engineered to express hairpin dsRNA targeting the cytochrome P450 gene (*CYP6AE14*) of the cotton bollworm *Helicoverpa armigera* (CBW), involved in detoxification of the secondary metabolite gossypol that is produced by the cotton plant. When CBW was feed on transgenic *Arabidopsis thaliana* or *Nicotiana tobacum* that expressed dsRNA against P450, transcript levels of the target gene decreased in the insect midgut and larval growth was retarded. Moreover, the effects were intensified in the presence of gossypol.

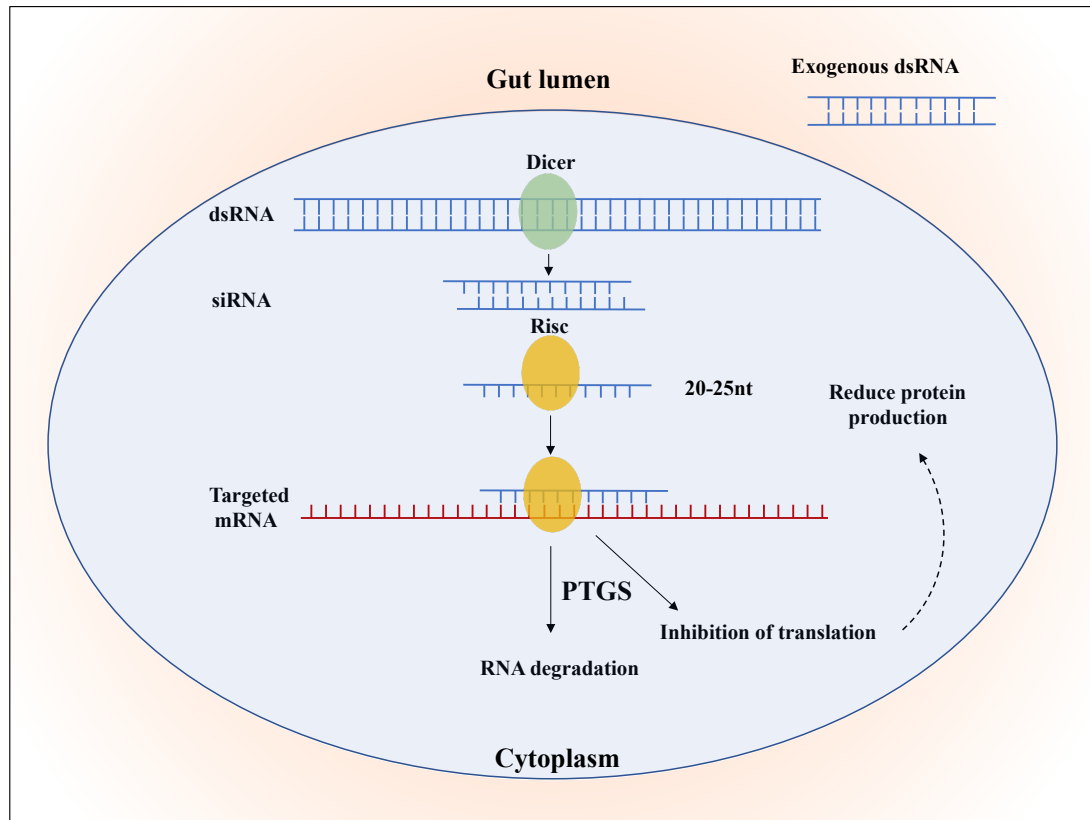


**Figure 1.3: Mechanism of RNA interference in eukaryotic cell.** Exogenous dsRNA triggers RNAi by activating Dicer enzyme that is going to cleave long dsRNA fragment into a population of short interfering RNAs (siRNAs) of 20 to 25 base pairs. siRNAs are loaded into a RISC complex that induces either degradation of complementary mRNA or its inhibition. This phenomenon is called Post Translation Gene Silencing, (PTGS). (adapted from Bensoussan and Grbić, 2017).

Baum and his team, designed an RNAi screen in which they tested 290 dsRNAs, targeting genes coding for proteins of vital function and supplied in artificial diet. They identified 14 genes that strongly responded to RNAi, causing increased larval mortality in the western corn rootworm, *Diabrotica virgifera virgifera* (WCR). Subsequently, corn plants were transformed to express dsRNA against the proton pump V-ATPase of WCR, one of the targets identified in the artificial diet screen. These plants showed significant reduction of root damage with low nodal injury upon WCR infestation, indicating the efficiency of the RNAi in crop protection (Baum et al., 2007). Although, these studies highlight the potential of RNAi as a promising tool to control pests, RNAi efficiency has been shown to be variable among insects and arthropods. Even though the RNAi machinery is conserved across insect and arthropods classes, RNAi responsiveness differs among orders (Bellés, 2010). For example, it has been reported that coleopterans are very sensitive to RNAi.

In contrast, RNAi responsiveness in lepidopterans has been reported to be low and variable between species, tissues, gene targets, delivery methods and required high concentration of dsRNA to trigger equivalent RNAi efficiency as in coleopterans (Ivashuta et al., 2015; Terenius et al., 2011). Moreover, factors including, but not limited to, RNAi design, dsRNA concentration, delivery method, targeted gene, life stage and expression level of RNAi machinery have been demonstrated to be critical (Bolognesi et al., 2012; Chu et al., 2014; Coleman et al., 2015; Huvenne and Smagghe, 2010; Ivashuta et al., 2015).

## 1.9 Factors influencing RNAi efficiency

### 1.9.1 dsRNA design

Factors including dsRNA fragment size, concentration and targeted mRNA region can profoundly affect the RNAi efficiency, which also dependent on the targeted gene and the organism tested. For instance, in the red flour beetle, *Tribolium castaneum*, long dsRNA with a minimal size of 70 nucleotides was required to achieve effective RNAi, in which the length was shown to be crucial for cell uptake (Miller et al., 2012). Furthermore, they demonstrated a dose-response between the concentration of dsRNA and the interference,

with optimal concentration of 0.01  $\mu\text{g}/\mu\text{l}$ , after which further increase of dsRNA concentration didn't increase RNAi potency.

In insects such as *Drosophila*, fragment sizes ranging from 21 to 592 base pairs have been tested for RNAi efficiency on S2 cells (Saleh et al., 2006). The authors clearly show a positive correlation between fragment size and increased RNAi efficiency. In addition, long dsRNAs were more efficient compare to siRNA when expressed in transgenic plants (Mao et al., 2011). Overall, most of the studies have shown that dsRNA of 100 to 600 bp are required for the successful RNAi. The region of mRNA sequence targeted by dsRNA can also influence RNAi efficiency. For instance, ingestion of dsRNA designed against the 3' end of the apoptosis gene *AelAP1* of the mosquito *Aedes aegypti*, showed greater effect than dsRNA against the 5' end region (Pridgeon et al., 2008). However, no differences were observed between dsRNA designed either against the 5' or 3' ends of the targeted gap gene *hunchback*, a key regulator in the anteroposterior patterning in the pea aphid, *Acyrtosiphon pisum* (Mao and Zeng, 2012).

These studies point out the variability of RNAi sensitivity when designing dsRNA intrinsic to the target and the organism. Also, they hint at a need to design several fragments, each targeting different parts of the mRNA, which can also be used to test the experimental reproducibility. Also, *in silico* analysis of the targeted sequence must be performed prior to synthesizing dsRNA to avoid off-target effects from sequence match between population of siRNA (product from dsRNA cleavage) and mRNA from undesired targets (Du et al., 2005; Jackson et al., 2003). Although, to date, no consensus about the degree of sequence mismatch between siRNA derived from dsRNA and off targeted mRNA has been established.

### 1.9.2 dsRNA delivery method

Several methods have been developed to deliver dsRNA, including but not limited to: injection, feeding on artificial diet, transgenic plant expressing dsRNA, and soaking which consists of the immersion of the organism or cell culture into solution containing dsRNA (Yu et al., 2013). Injection was the first method used to deliver dsRNA and was done in *D. melanogaster* in the attempt to silence the *frizzled* gene (Kennerdell and

Carthew, 1998). The advantages associated with this method is the high silencing efficiency of the target gene and the control of the amount of dsRNA delivered into the body. However, variation of RNAi response has been observed when compared between delivery methods on the same organism (Terenius et al., 2011). Injection of dsRNA was more efficient to silence *apn* gene in *Spodoptera litura* compare to the interference from feeding on hairpin-loop transformed plants as a result of a lower concentration of delivered dsRNA with feeding (Rajagopal et al., 2002).

In contrast, ingestion of dsRNA through oral delivery was more efficient than injection when a continuous feeding was applied in the Cotton Bollworm, *Helicoverpa armigera* (Yang and Han, 2014). The development of the oral delivery method was introduced as an alternative of injection, that is time consuming and subject to mechanical damage that is often lethal (Liu et al., 2010), or that induces an immune response (Han et al., 1999). Also, injection of dsRNA or small RNAs were widely used as a reverse genetics tool, while non-invasive methods of dsRNA delivery, such as soaking or feeding, are more suitable for the development of RNAi as biopesticide. Moreover, oral delivery is convenient, less invasive, and can be used as high-throughput screen. The first demonstration of RNAi through oral delivery was done in *C. elegans* feeding on *Escherichia coli* transformed to express dsRNAs (Timmons and Fire, 1998).

Also, several studies have shown the potential of using artificial diet mixed with dsRNA for oral delivery. It was successful to trigger RNAi in whiteflies, aphids and honey bees (Aronstein et al., 2006; Ghanim et al., 2007; Whyard et al., 2009; Wuriyangan et al., 2011). Oral delivery through feeding on transgenic plants expressing dsRNA was efficient to trigger RNAi in Coleopteran (Baum et al., 2007), Lepidoptera (Dai et al., 2008), *Helicoverpa* (Bally et al., 2016), and in Hemiptera (Zha et al., 2011).

Soaking in a solution of dsRNA has been used to deliver dsRNA into nematodes (Conte et al., 2015; Tabara et al., 1998) and arthropods (Li et al., 2015; March and Bentley, 2007; Timmons and Fire, 1998). Recently, RNAi-based efforts to control the mite honey bee parasite, *Varroa destructor*, have been reported by Campbell in 2010. In this study, injection and soaking mites in solution of dsRNA, were assessed. Soaking mites in a

solution of dsRNA resulted in 87% transcript level downregulation compare to 97% when injected, albeit rather associated with high mortality due to the mechanical stress.

### 1.9.3 Gut Environment

Although the oral delivery of dsRNA may provide an advantage to follow a natural ingestion route through the gut, the ability of dsRNA to be ingested and absorbed by epithelium gut cells can influence RNAi potency. Moreover, the spatio-temporal expression of key components of the RNAi machinery can also affect RNAi efficiency and its ability to spread through the body (Chintapalli et al., 2007; Rinkevich and Scott, 2013). Recently, there is increasing evidence of the presence of nuclease in the gut and hemolymph in arthropods that, this could result in dsRNA degradation prior to cell uptake and a lack of potent RNAi in some species (Allen and Walker, 2012; Garbutt et al., 2013; Wynant et al., 2014). Interestingly, the elimination of the nuclease activity in the potato beetle, *Leptinotarsa decemlineata*, increased RNAi efficiency (Spit et al., 2017). In addition to the presence of nucleases, extreme gut pH can provide a deleterious environment to dsRNA stability (Lomate and Bonning, 2016). However, an acidic gut environment has been shown to be required for SID-2 activity in dsRNA cell uptake in *Drosophila* S2 cells (McEwan et al., 2012).

### 1.9.4 RNAi in Tetranychid mites

The genome of *T. urticae* contains genes encoding for a complete set of RNAi processing machinery, including two Dicer homologs, pasha, Drosha and components of the RISC complex (including seven orthologs of both *Argonaute* and *Piwi* genes; Grbić et al., 2011). In contrast to other arthropods and similar to *Caenorhabditis elegans*, *T. urticae* possesses five copies of the RNA-dependent RNA polymerase (RdRp) required for the systemic spread of RNAi responses. Expression levels of these genes in different *T. urticae* developmental stages are shown in Figure 1.4, suggesting that RNAi machinery is potentially efficient throughout spider mite development. Thus, screening for RNAi target genes is not limited to a specific developmental stage in spider mites.

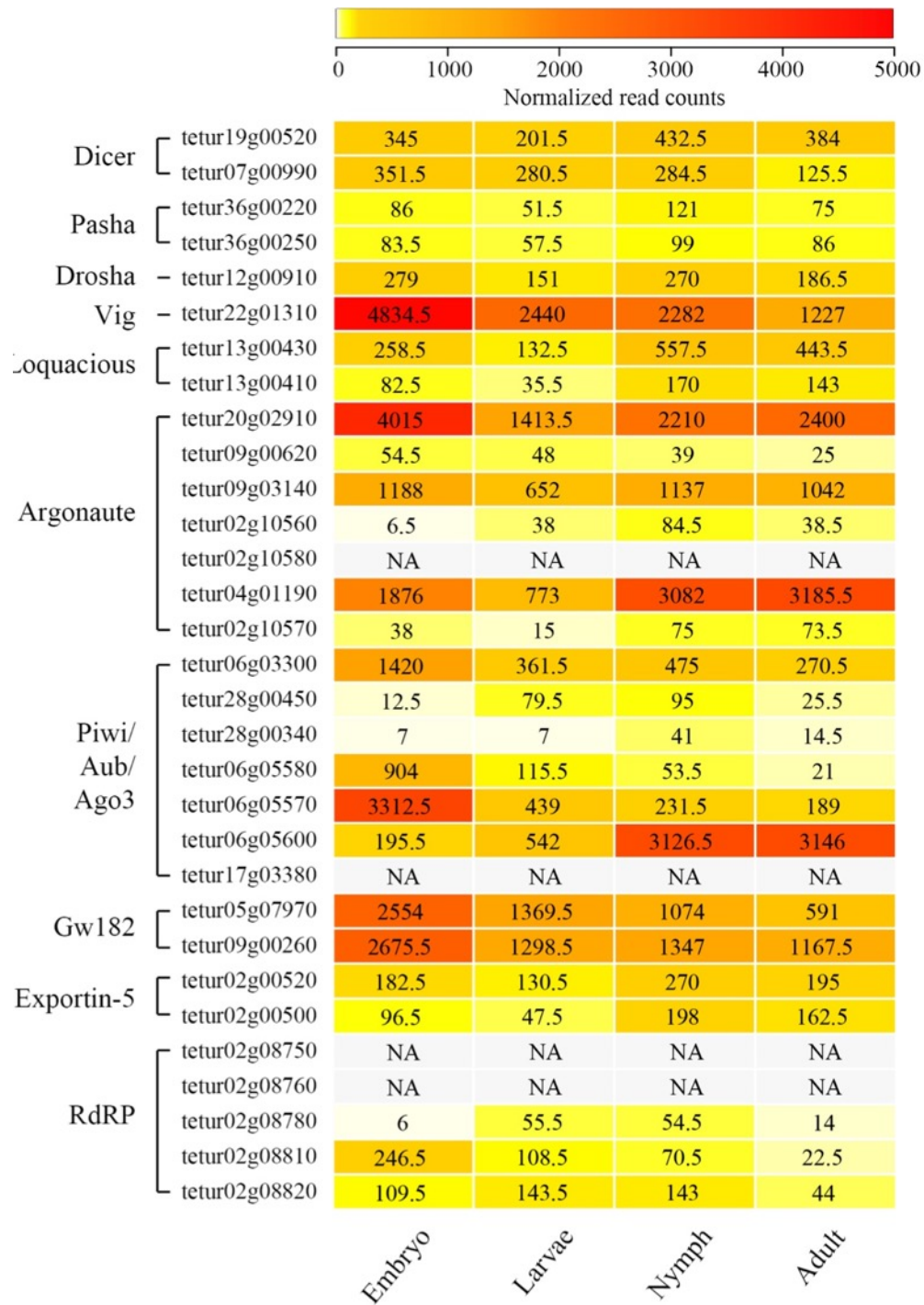


**Figure 1.4: Heatmap representing expression patterns of RNAi-associated genes at different developmental stages of *Tetranychus urticae*, based on the number of mapped RNAseq reads (Illumina). Boxes are colored yellow for low expression and red for high expression (see scale at the top). Row labels are tetur IDs grouped by gene function. Column labels are the developmental stages of *T. urticae*. (Adapted from Bensoussan et al., 2017).**

Khila and Grbić (2007) demonstrated that parental RNAi can silence the expression of the homeobox gene, *Distal-less (Dll)*. Injection of either *Tu-Dll*-specific dsRNA or siRNA into adult female mites resulted in offspring with truncated and fused leg segments. This study was the first to demonstrate that RNAi could be a valid reverse genetic approach in *T. urticae*. However, compared to other arthropods, for example *Tribolium* and *Oncopeltus*, dsRNA injection is not a viable delivery method for *T. urticae*, as females are less than 0.5 mm in length. Recently, Kwon et al., (2013) reported an alternative method for the administration of dsRNA to *T. urticae*. They developed a protocol for oral delivery of dsRNA using bean leaf discs that floated on a solution containing dsRNA. Using this method, they were successful in decreasing the expression levels of several genes involved in mite metabolism and physiology, resulting in mite mortality five days post feeding. Even though this method may not be practical for high throughput screens of potential mite targets, as it requires large quantities of dsRNA that must be replaced daily, it has been useful as a reverse genetics tool. For example, application of this dsRNA delivery method in the red mite, *Pannonychus citri*, has been successful in down-regulating the chitinase (*PcCht1*) gene by almost 60%. Associated with the reduced expression of this target gene was lethality that resulted from larval molting failure (Xia et al., 2016). Similarly, oral delivery of dsRNA to the carmine spider mite, *Tetranychus cinnabarinus*, was successful in down-regulating an esterase (*TCE2*) whose expression was implicated in acaricide resistance. The exogenous application of acaricides to the dsRNA-treated mites increased their effectiveness, indicating the correlation between the expression of *TCE2* gene and acaricides resistance (Shi et al., 2016). These examples reinforce the feasibility of using RNAi as a reverse genetics tool for functional studies of mite biology, and as a tool for the development of new mite management strategies.

## 1.10 Rationale and specific goals of my research

*T. urticae* is one of the most polyphagous herbivores feeding on cell contents of over 1100 plant species including more than 150 crops. It is being established as a model



chelicerate herbivore with tools that enable tracking of reciprocal responses in plant-spider mite interactions. However, despite their important pest status and a growing understanding of the molecular basis of interactions with plant hosts, knowledge of the way mites interface with the plant while feeding and the plant damage directly inflicted by mites is lacking. In addition, a critical step in the analysis of spider mite gene function is the availability of efficient reverse genetic tool. To further promote the establishment and use of *T. urticae* as a model herbivore, the objectives of my work were:

- 1) To characterize plant damage that directly results from mite feeding at a cellular level and duration of a feeding event.
- 2) To investigate the *T. urticae* stylet pathway while feeding on host plants.
- 3) To establish RNA interference in *T. urticae* through soaking of adult female mites in the solution of dsRNA against the target gene *VATPase*.
- 4) To further optimize the soaking method and RNAi design in *T. urticae* using dsRNA against *VATPase* and *COPB2*.

## 1.11 Reference

- Aagaard, L., and Rossi, J. J. (2007). RNAi therapeutics: Principles, prospects and challenges. *Adv. Drug Deliv. Rev.* 59, 75–86.
- Alba, J. M., Schimmel, B. C. J., Glas, J. J., Ataide, L. M. S., Pappas, M. L., Villarroel, C. A., et al. (2015). Spider mites suppress tomato defenses downstream of jasmonate and salicylate independently of hormonal crosstalk. *New Phytol.* 205, 828–840.
- Alberti, G. (2006). On some fundamental characteristics in acarine morphology. *Atti della Accad. Naz. Ital. di Entomol.* R.A. LIII, 315–360.
- Alberti, G., and Crooker, A. (1985). “Internal anatomy,” in *Spider mites: their biology, natural enemies and control.*, eds. W. Helle and M. W. Sabelis (Elsevier Ltd), 29–62.
- Alberti, G., and Kitajima, E. W. (2014). Anatomy and Fine Structure of Brevipalpus Mites (Tenuipalpidae) - Economically Important Plant-Virus Vectors. Stuttgart: Schweizerbart.
- Alberti, G., and Storch, V. (1973). Zur Feinstruktur der “Munddrüsen” von Schnabelmilben (Bdellidae, Trombidiformes). *Z. Wiss. Zool.* 186, 149–160.
- Allen, M. L., and Walker, W. B. (2012). Saliva of *Lygus lineolaris* digests double stranded ribonucleic acids. *J. Insect Physiol.* 58, 391–396.
- André, H. M., and Remacle, C. (1984). Comparative and functional morphology of the gnathosoma of *Tetranychus urticae* (Acari: Tetranychidae). *Acarologia.* 25, 179–190.
- Aravin, A. A., Hannon, G. J., and Brennecke, J. (2007). The piwi-piRNA pathway provides an adaptive defense in the transposon arms race. *Science.* 318, 761–764.
- Aronstein, K., Pankiw, T., and Saldivar, E. (2006). SID-I is implicated in systemic gene silencing in the honey bee. *J. Apic. Res.* 45, 20–24.
- Avery, D. J., and Briggs, J. B. (1968). The aetiology and development of damage in young fruit trees infested with fruit tree red spider mite, *Panonychus ulmi* (Koch). *Ann. Appl. Biol.* 61, 277–288.
- Bally, J., McIntyre, G. J., Doran, R. L., Lee, K., Perez, A., Jung, H., et al. (2016). In-plant protection against *Helicoverpa armigera* by production of long hpRNA in chloroplasts. *Front. Plant Sci.* 7, 1453.
- Bartel, D. P. (2004). MicroRNAs: genomics, biogenesis, mechanism, and function. *Cell.* 116, 281–297.

- Baum, J. A., Bogaert, T., Clinton, W., Heck, G. R., Feldmann, P., Ilagan, O., et al. (2007). Control of coleopteran insect pests through RNA interference. *Nat Biotech.* 25, 1322–1326.
- Becker, E. (1935). Die Mundwerkzeuge de *Tetranychus telarius* (L.) und deren Funktionin Beziehung zur chemischen Bekämpfung des letzteren. *Rev. Zool.* 14, 637–554.
- Bellés, X. (2010). Beyond *Drosophila*: RNAi in vivo and functional genomics in insects. *Annu. Rev. Entomol.* 55, 111–128.
- Bensoussan, N., and Grbić, V. (2017). RNA interference in the two-spotted spider mite *Tetranychus urticae*. *Int. Organ. Biol. Integr. Control.* 124, 200–206.
- Bernstein, E., Caudy, A. A., Hammond, S. M., and Hannon, G. J. (2001). Role for a bidentate ribonuclease in the initiation step of RNA interference. *Nature.* 409, 363–366.
- Blauvelt, W. (1945). The internal anatomy of the common spider mite (*Tetranychus telarius* L.). *Agri. Exp. Stn.* 270, 1–35.
- Bolland, H. R., Gutierrez, J., and Flechtmann, C. H. (1998). World catalogue of the spider mite family:(Acari: Tetranychidae). *Brill.* Leiden; Boston.
- Bolognesi, R., Ramaseshadri, P., Anderson, J., Bachman, P., Clinton, W., Flannagan, R., et al. (2012). Characterizing the mechanism of action of double-stranded RNA activity against western corn rootworm (*Diabrotica virgifera virgifera* LeConte). *PLoS One* 7, e47534.
- Boudreaux, H. B. (1963). Biological Aspects of Some Phytophagous Mites. *Annu. Rev. Entomol.* 8, 137–154.
- Brusca, R. C., and Brusca, G. J. (2003). *Invertebrates*. Sunderland, MA: Sinauer Associates.
- Bushati, N., and Cohen, S. M. (2007). microRNA Functions. *Annu. Rev. Cell Dev. Biol.* 23, 175–205.
- Campbell, E. M., Budge, G. E., and Bowman, A. S. (2010). Gene-knockdown in the honey bee mite *Varroa destructor* by a non-invasive approach: studies on a glutathione S-transferase. *Parasit. Vectors.* 3, 73.
- Campbell, R. J., Grayson, R. L., and Marini, R. P. (1990). Surface and ultrastructural feeding injury to strawberry leaves by the twospotted spider mite. *Hortscience.* 25, 948–951.
- Carrière, Y. (2003). Haplodiploidy, sex, and the evolution of pesticide resistance. *J. Econ. Entomol.* 96, 1626–1640.

- Chintapalli, V. R., Wang, J., and Dow, J. A. T. (2007). Using FlyAtlas to identify better *Drosophila melanogaster* models of human disease. *Nat Genet.* 39, 715–720.
- Chu, C.C., Sun, W., Spencer, J. L., Pittendrigh, B. R., and Seufferheld, M. J. (2014). Differential effects of RNAi treatments on field populations of the western corn rootworm. *Pestic. Biochem. Physiol.* 110, 1–6.
- Coleman, A. D., Wouters, R. H. M., Mugford, S. T., and Hogenhout, S. A. (2015). Persistence and transgenerational effect of plant-mediated RNAi in aphids. *J. Exp. Bot.* 66, 541–548.
- Conte, D., MacNeil, L. T., Walhout, A. J. M., and Mello, C. C. (2015). “RNA Interference in *Caenorhabditis elegans*,” in *Current Protocols in Molecular Biology* (Hoboken, NJ, USA: John Wiley & Sons, Inc.), 26.3.1-26.3.30.
- Dai, H., Ma, L., Wang, J., Jiang, R., Wang, Z., and Fei, J. (2008). Knockdown of ecdysis-triggering hormone gene with a binary UAS/GAL4 RNA interference system leads to lethal ecdysis deficiency in silkworm. *Acta Biochim. Biophys. Sin. (Shanghai)*. 40, 790–5.
- Denholm, I., Horowitz, A. R., Cahill, M., and Ishaaya, I. (1998). “Management of Resistance to Novel Insecticides” in *Insecticides with Novel Modes of Action: Mechanisms and Application*,” eds. I. Ishaaya and D. Degheele (Berlin, Heidelberg: Springer Berlin Heidelberg), 260–282.
- Ding, S. W. (2010). RNA-based antiviral immunity. *Nat Rev Immunol.* 10, 632–644.
- Ding, S. W., and Voinnet, O. (2007). Antiviral Immunity Directed by Small RNAs. *Cell.* 130, 413–426.
- Djuranovic, S., Nahvi, A., and Green, R. (2012). miRNA-Mediated gene silencing by translational repression followed by mRNA deadenylation and decay. *Science.* 336, 237–240.
- Du, Q., Thonberg, H., Wang, J., Wahlestedt, C., and Liang, Z. (2005). A systematic analysis of the silencing effects of an active siRNA at all single-nucleotide mismatched target sites. *Nucleic Acids Res.* 33, 1671–1677.
- Ekka, I. (1969). The Rearing of the Two-Spotted Spider Mite (*Tetranychus urticae* Koch) on Artificial Diets. Ph.D thesis. McGill University.
- Elbashir, S. M., Harborth, J., Lendeckel, W., Yalcin, A., Weber, K., and Tuschl, T. (2001). Duplexes of 21-nucleotide RNAs mediate RNA interference in cultured mammalian cells. *Nature.* 411, 494–498.
- Fire, A., Xu, S., Montgomery, M. K., Kostas, S. A., Driver, S. E., and Mello, C. C. (1998). Potent and specific genetic interference by double-stranded RNA in *Caenorhabditis elegans*. *Nature.* 391, 806–811.

- Garbutt, J. S., Bellés, X., Richards, E. H., and Reynolds, S. E. (2013). Persistence of double-stranded RNA in insect hemolymph as a potential determiner of RNA interference success: Evidence from *Manduca sexta* and *Blattella germanica*. *J. Insect Physiol.* 59, 171–178.
- Gasser, R. (1951). Zur Kenntnis der gemeinen Spinnmilbe *Tetranychus Urticae* Koch: Mitteilung 1: Morphologie, Anatomie, Biologie und Oekologie. *Rull Soc Ent Suisse.* 24, 217–262.
- Ghanim, M., Kontsedalov, S., and Czosnek, H. (2007). Tissue-specific gene silencing by RNA interference in the whitefly *Bemisia tabaci* (Gennadius). *Insect Biochem. Mol. Biol.* 37, 732–738.
- Grandjean, F. (1969). Stasis. Actinopiline. Explanation of my mites classification into three major groups. Terminology of -soma. *Acarologia.* 11, 796–827.
- Grbić, M., Van Leeuwen, T., Clark, R. M., Rombauts, S., Rouzé, P., Grbić, V., et al. (2011). The genome of *Tetranychus urticae* reveals herbivorous pest adaptations. *Nature.* 479, 487–492.
- Hamilton, A. J. (1999). A Species of small antisense RNA in posttranscriptional gene silencing in plants. *Science.* 286, 950–952.
- Hammen, L. van der. (1970). General notes on the fundamental structure of the gnathosoma. *Acarologia* 12, 16–22.
- Hammen, L. van der (1980). *Glossary of acarological terminology. Vol. 1: General terminology.* The Hague: Dr. W. Junk, B. V.
- Hammond, S. M., Bernstein, E., Beach, D., and Hannon, G. J. (2000). An RNA-directed nuclease mediates post-transcriptional gene silencing in *Drosophila* cells. *Nature.* 404, 293–296.
- Han, Y. S., Chun, J., Schwartz, A., Nelson, S., and Paskewitz, S. M. (1999). Induction of mosquito hemolymph proteins in response to immune challenge and wounding. *Dev. Comp. Immunol.* 23, 553–562.
- Hazan, A., Gerson, U., and Tahori, A. S. (1974). Spider mite webbing. I. The production of webbing under various environmental conditions. *Acarologia.* 16, 68–84.
- Helle, W., and Sabelis, M. W. (1985). *Spider mites: their biology, natural enemies and control.* eds. W. Helle and M. W. Sabelis Amsterdam: Elsevier Ltd.
- Hislop, R. G., and Jeppson, L. R. (1976). Morphology of the mouthparts of several species of phytophagous mites. *Ann. Entomol. Soc. Am.* 69, 1125–1135.
- Hutvagner, G., and Zamore, P. D. (2002). A microRNA in a Multiple-Turnover RNAi Enzyme Complex. *Science.* 297, 2056–2060.

- Huvenne, H., and Smagghe, G. (2010). Mechanisms of dsRNA uptake in insects and potential of RNAi for pest control: A review. *J. Insect Physiol.* 56, 227–235.
- Ivashuta, S., Zhang, Y., Wiggins, B. E., Ramaseshadri, P., Segers, G. C., Johnson, S., et al. (2015). Environmental RNAi in herbivorous insects. *RNA.* 21, 840–850.
- Jackson, A. L., Bartz, S. R., Schelter, J., Kobayashi, S. V., Burchard, J., Mao, M., et al. (2003). Expression profiling reveals off-target gene regulation by RNAi. *Nat Biotech.* 21, 635–637.
- Jeppson, L. R., Keifer, H. H., and Baker, E. W. (1975). *Mites injurious to economic plants*. Berkeley: University of California Press.
- Jonckheere, W., Dermauw, W., Zhurov, V., Wybouw, N., Van den Bulcke, J., Villarroel, C. A., et al. (2016). The Salivary Protein Repertoire of the Polyphagous Spider Mite *Tetranychus urticae*: A Quest for Effectors. *Mol. Cell. Proteomics.* 15, 3594–3613.
- Kant, M. R., Sabelis, M. W., Haring, M. A., and Schuurink, R. C. (2008). Intraspecific variation in a generalist herbivore accounts for differential induction and impact of host plant defences. *Proc. R. Soc. B Biol. Sci.* 275, 443–452.
- Kennerdell, J. R., and Carthew, R. W. (1998). Use of dsRNA-mediated genetic interference to demonstrate that *frizzled* and *frizzled 2* act in the wingless pathway. *Cell.* 95, 1017–1026.
- Khila, A., and Grbić, M. (2007). Gene silencing in the spider mite *Tetranychus urticae*: dsRNA and siRNA parental silencing of the Distal-less gene. *Dev. Genes Evol.* 217, 241–251.
- Koch, C. L. (1836). *Tetranychus urticae*. *Dtsch. Crustac. Myriapoda, Arachn.* 1, 10.
- Kwon, D. H., Park, J. H., and Lee, S. H. (2013). Screening of lethal genes for feeding RNAi by leaf disc-mediated systematic delivery of dsRNA in *Tetranychus urticae*. *Pestic. Biochem. Physiol.* 105, 69–75.
- Lawson, N. D., and Wolfe, S. A. (2011). Forward and reverse genetic approaches for the analysis of vertebrate development in the zebrafish. *Dev. Cell.* 21, 48–64.
- Lee, Y. C. G. (2015). The Role of piRNA-mediated epigenetic silencing in the population dynamics of transposable elements in *Drosophila melanogaster*. *PLOS Genet.* 11, e1005269.
- Leucci, E., Patella, F., Waage, J., Holmstrøm, K., Lindow, M., Porse, B., et al. (2013). microRNA-9 targets the long non-coding RNA *MALAT1* for degradation in the nucleus. *Sci. Rep.* 3, 2535.
- Li, H., Guan, R., Guo, H., and Miao, X. (2015). New insights into an RNAi approach for plant defence against piercing-sucking and stem-borer insect pests. *Plant. Cell*

- Environ.* 38, 2277–2285.
- Li, X., Schuler, M. A., and Berenbaum, M. R. (2006). Molecular mechanisms of metabolic resistance to synthetic and natural xenobiotics. *Annu. Rev. Entomol.* 52, 231–253.
- Liu, J., Carmell, M. A., Rivas, F. V, Marsden, C. G., Thomson, J. M., Song, J.-J., et al. (2004). Argonaute2 is the catalytic engine of mammalian RNAi. *Science.* 305, 1437–1441.
- Liu, S., Ding, Z., Zhang, C., Yang, B., and Liu, Z. (2010). Gene knockdown by intrathoracic injection of double-stranded RNA in the brown planthopper, *Nilaparvata lugens*. *Insect Biochem. Mol. Biol.* 40, 666–671.
- Lomate, P. R., and Bonning, B. C. (2016). Distinct properties of proteases and nucleases in the gut, salivary gland and saliva of southern green stink bug, *Nezara viridula*. *Sci.Rep.* 6, 27587.
- Mao, J., and Zeng, F. (2012). Feeding-based RNA interference of *gap* gene is lethal to the pea aphid, *Acyrtosiphon pisum*. *PLoS One* 7, e48718.
- Mao, Y.-B., Cai, W.-J., Wang, J.-W., Hong, G.-J., Tao, X.-Y., Wang, L.-J., et al. (2007). Silencing a cotton bollworm P450 monooxygenase gene by plant-mediated RNAi impairs larval tolerance of gossypol. *Nat Biotech.* 25, 1307–1313.
- March, J. C., and Bentley, W. E. (2007). RNAi-based tuning of cell cycling in *Drosophila* S2 cells—effects on recombinant protein yield. *Appl. Microbiol. Biotechnol.* 73, 1128–1135.
- Martinez, J., Patkaniowska, A., Urlaub, H., Lührmann, R., and Tuschl, T. (2002). Single-stranded antisense siRNAs guide target RNA cleavage in RNAi. *Cell.* 110, 563–574.
- McEwan, D. L., Weisman, A. S., and Hunter, C. P. (2012). Uptake of extracellular double-stranded RNA by SID-2. *Mol. Cell.* 47, 746–754.
- Migeon, A., and Dorkeld, F. (2006-2014). Spider Mites Web: a comprehensive database for the Tetranychidae. Available online at: <http://www.montpellier.inra.fr/CBGP/spmweb>
- Miller, S. C., Miyata, K., Brown, S. J., and Tomoyasu, Y. (2012). Dissecting systemic RNA interference in the red flour beetle *Tribolium castaneum*: parameters affecting the efficiency of RNAi. *PLoS One* 7, e47431.
- Mills, L. R. (1973). Structure of dorsal setae in the two-spotted spider mite *Tetranychus urticae* Koch, 1836. *Acarologia.* 15, 649–658.
- Mothes, U., and Seitz, K. a. (1981a). Fine structure and function of the prosomal glands of the two-spotted spider mite, *Tetranychus urticae* (Acari, Tetranychidae). *Cell*

*Tissue Res.* 221, 339–349.

- Mothes, U., and Seitz, K. A. (1981b). Functional microscopic anatomy of the digestive system of *Tetranychus urticae* (Acari, Tetranychidae). *Acarologia*. 22, 257–270.
- Napoli, C., Lemieux, C., and Jorgensen, R. (1990). Introduction of a chimeric chalcone synthase gene into petunia results in reversible co-suppression of homologous genes in trans. *Plant Cell*. 2, 279–289.
- Nuzzacci, G., and De Lillo, E. (1991b). “Fine structure and functions of the mouthparts involved in the feeding mechanisms in *Tetranychus urticae* Koch (Tetranychoidae: Tetranychidae),” in *Modern Acarology: Proceedings of the VIII International Congress of Acarology*, eds F. Dusbabek and V. Bukva (The Hague: Academia Prague and SPB Academic), 301–303.
- Nykänen, A., Haley, B., and Zamore, P. D. (2001). ATP Requirements and Small Interfering RNA Structure in the RNA Interference Pathway. *Cell* 107, 309–321.
- Occhipinti, A., and Maffei, M. E. (2013). Chlorophyll and its degradation products in the two-spotted spider mite, *Tetranychus urticae*: observations using epifluorescence and confocal laser scanning microscopy. *Exp. Appl. Acarol.* 61, 213–219.
- Olivier, J. H. (1971). Parthenogenesis in mites and ticks (Arachnida: Acari). *Am. Zool.* 11, 283–299.
- Park, Y.-L., and Lee, J.-H. (2002). Leaf cell and tissue damage of cucumber caused by twospotted spider mite (Acari: Tetranychidae). *J. Econ. Entomol.* 95, 952–7.
- Pillai, R. S., Bhattacharyya, S. N., and Filipowicz, W. (2017). Repression of protein synthesis by miRNAs: how many mechanisms? *Trends Cell Biol.* 17, 118–126.
- Pridgeon, J. W., Zhao, L., Becnel, J. J., Strickman, D. A., Clark, G. G., and Linthicum, K. J. (2008). Topically applied *AaeIAP1* double-stranded RNA kills female adults of *Aedes aegypti*. *J. Med. Entomol.* 45, 414–20.
- Rajagopal, R., Sivakumar, S., Agrawal, N., Malhotra, P., and Bhatnagar, R. K. (2002). Silencing of midgut aminopeptidase N of *Spodoptera litura* by double-stranded RNA establishes its role as *Bacillus thuringiensis* toxin receptor. *J. Biol. Chem.* 277, 46849–46851.
- Riga, M., Bajda, S., Themistokleous, C., Papadaki, S., Palzewicz, M., Dermauw, W., et al. (2017). The relative contribution of target-site mutations in complex acaricide resistant phenotypes as assessed by marker assisted backcrossing in *Tetranychus urticae*. *Sci. Rep.* 7, 9202.
- Rinkevich, F. D., and Scott, J. G. (2013). Limitations of RNAi of  $\alpha 6$  nicotinic acetylcholine receptor subunits for assessing the *in vivo* sensitivity to spinosad. *Insect Sci.* 20, 101–108.



- Romano, N., and Macino, G. (1992). Quelling: transient inactivation of gene expression in *Neurospora crassa* by transformation with homologous sequences. *Mol. Microbiol.* 6, 3343–3353.
- Roush, T., and Tabashnik, B. (1990). *Pesticide Resistance in Arthropods.* , eds. R. T. Roush and B. E. Tabashnik Boston, MA: Springer US.
- Saleh, M.-C., van Rij, R. P., Hekele, A., Gillis, A., Foley, E., O’Farrell, P. H., et al. (2006). The endocytic pathway mediates cell entry of dsRNA to induce RNAi silencing. *Nat Cell Biol.* 8, 793–802.
- Sances, F. V, Wyman, J. A., and Ting, I. P. (1979). Morphological responses of strawberry leaves to infestations of twospotted spider mite. *J. Econ. Entomol.* 72, 710–713.
- Shi, L., Wei, P., Wang, X., Shen, G., Zhang, J., Xiao, W., et al. (2016). Functional analysis of esterase *TCE2* Gene from *Tetranychus cinnabarinus* (Boisduval) involved in acaricide resistance. *Sci. Rep.* 6, 18646.
- Shih, C. T., Poe, S. L., and Cromroy, H. L. (1976). Biology, life table, and intrinsic rate of increase of *Tetranychus urticae*. *Ann. Entomol. Soc. Am.* 69, 362–364.
- Sienski, G., Dönertas, D., and Brennecke, J. (2012). Transcriptional silencing of transposons by piwi and maelstrom and its impact on chromatin state and gene expression. *Cell.* 151, 964–980.
- Spit, J., Philips, A., Wynant, N., Santos, D., Plaetinck, G., and Vanden Broeck, J. (2017). Knockdown of nuclease activity in the gut enhances RNAi efficiency in the Colorado potato beetle, *Leptinotarsa decemlineata*, but not in the desert locust, *Schistocerca gregaria*. *Insect Biochem. Mol. Biol.* 81, 103–116.
- Summers, F., Gonzales, R., and Witt, R. (1973). The mouthparts of *Bryobia rubrioculus* (Sch.) (Acarina: Tetranychidae). *Proc. Entomol. Soc. Washing.* 75, 96–11.
- Summers, F. M., and Stocking, C. R. (1972). Some immediate effects on almond leaves of feeding some by *Bryobia rubrioculus* (Scheuten). *Acarologia.* 14, 170–178.
- Tabara, H., Grishok, A., and Mello, C. C. (1998). RNAi in *C. elegans*: Soaking in the genome sequence. *Science.* 282, 430–431.
- Tanigoshi, L. K., and Davis, R. W. (1978). An ultrastructural study of *Tetranychus mcdanieli* feeding injury to the leaves of “Red Delicious” apple (Acari: Tetranychidae). *Int. J. Acarol.* 4, 47–51.
- Taylor, M., and Feyereisen, R. (1996). Molecular biology and evolution of resistance of toxicants. *Mol. Biol. Evol.* 13, 719–34.

- Terenius, O., Papanicolaou, A., Garbutt, J. S., Eleftherianos, I., Huvenne, H., Kanginakudru, S., et al. (2011). RNA interference in Lepidoptera: An overview of successful and unsuccessful studies and implications for experimental design. *J. Insect Physiol.* 57, 231–245.
- Timmons, L., and Fire, A. (1998). *Specific interference by ingested dsRNA.* *Nature.* 395, 854.
- Van Leeuwen, T., Tirry, L., Yamamoto, A., Nauen, R., and Dermauw, W. (2015). The economic importance of acaricides in the control of phytophagous mites and an update on recent acaricide mode of action research. *Pestic. Biochem. Physiol.* 121, 12–21.
- Villarroel, C. A., Jonckheere, W., Alba, J. M., Glas, J. J., Dermauw, W., Haring, M. A., et al. (2016). Salivary proteins of spider mites suppress defenses in *Nicotiana benthamiana* and promote mite reproduction. *Plant J.* 86, 119–131.
- Walter, D. E. (2004). “Hidden in Plain Sight. Mites in the Canopy.,” in *Forest Canopies: Second Edition*, 224–241.
- Whyard, S., Singh, A. D., and Wong, S. (2009). Ingested double-stranded RNAs can act as species-specific insecticides. *Insect Biochem. Mol. Biol.* 39, 824–832.
- Wuriyangan, H., Rosa, C., and Falk, B. W. (2011). Oral delivery of double-stranded RNAs and siRNAs induces RNAi effects in the potato/tomato psyllid, *Bactericera cockerelli*. *PLoS One* 6, e27736.
- Wybouw, N., Zhurov, V., Martel, C., Bruinsma, K. A., Hendrickx, F., Grbić, V., et al. (2015). Adaptation of a polyphagous herbivore to a novel host plant extensively shapes the transcriptome of herbivore and host. *Mol. Ecol.* 24, 4647–4663.
- Wynant, N., Santos, D., Verdonck, R., Spit, J., Van Wielendaele, P., and Vanden Broeck, J. (2014). Identification, functional characterization and phylogenetic analysis of double stranded RNA degrading enzymes present in the gut of the desert locust, *Schistocerca gregaria*. *Insect Biochem. Mol. Biol.* 46, 1–8.
- Xia, W.-K., Shen, X.-M., Ding, T.-B., Niu, J.-Z., Zhong, R., Liao, C.-Y., et al. (2016). Functional analysis of a chitinase gene during the larval-nymph transition in *Panonychus citri* by RNA interference. *Exp. Appl. Acarol.* 70, 1–15.
- Ximénez-Embún, M. G., Ortego, F., and Castañera, P. (2016). Drought-Stressed Tomato Plants Trigger Bottom-Up Effects on the Invasive *Tetranychus evansi*. *PLoS One* 11, e0145275.
- Yang, J., and Han, Z. (2014). Optimisation of RNA interference-mediated gene silencing in *Helicoverpa armigera*. *Austral Entomol.* 53, 83–88.

- Yu, N., Christiaens, O., Liu, J., Niu, J., Cappelle, K., Caccia, S., et al. (2013). Delivery of dsRNA for RNAi in insects: an overview and future directions. *Insect Sci.* 20, 4–14.
- Zha, W., Peng, X., Chen, R., Du, B., Zhu, L., and He, G. (2011). Knockdown of midgut genes by dsRNA-transgenic plant-mediated RNA interference in the hemipteran insect *Nilaparvata lugens*. *PLoS One* 6, e20504.

## Chapter 2

### 2 Plant-herbivore interaction: dissection of the cellular pattern of *Tetranychus urticae* feeding on the host plant

#### 2.1 Introduction

The chelicerates are the second largest arthropod group comprised of horseshoe crabs, scorpions, spiders, mites, and ticks (Brusca and Brusca, 2003). Horseshoe crabs, scorpions and spiders are predators that use pre-oral digestion as a shared digestive strategy. These organisms secrete digestive enzymes, originating from the midgut, into their prey to aid in the pre-oral digestion and liquefaction of prey tissues before ingestion by morphologically diverse mouthparts (Cohen, 1995). Ticks and mites belong to the Acari, the most diverse group within chelicerates, with over 40,000 identified species. This group exhibits a plethora of different lifestyles ranging from parasitic to predatory to plant-feeding. Predatory Acari, similar to other chelicerate predators, utilize secreted proteins to facilitate the consumption of their prey. However, these digestive enzymes originate from salivary secretions rather than from the midgut (Cohen, 1995).

Phytophagous mites represent a complex assemblage of saprophagous, fungivorous and herbivorous species (Krantz and Lindquist, 1979). Among them, Tetranychidae (spider mites), Tenuipalpidae (false spider mites), and some Eriophyoidea mites are exclusively phytophagous and include major agricultural pests. A common feature of the mouth apparatus of these mites includes the formation of the elongated cheliceral stylet that allowed adaptation to a piercing mode of feeding, in which the stylet is used to penetrate the host tissue to allow the consumption of the cells contents. While Tetranychidae and Tenuipalpidae mites have a single, long and retractable stylet (Alberti and Kitajima, 2014), Eriophyoid mites have several stylets that are not retractable. Instead, Eriophyoid mites penetrate their stylets into the plant tissue by telescoping the palpal tissue that surrounds the stylet bundle (Krantz and Lindquist, 1979).

*Tetranychus urticae* Koch (Acari: Tetranychidae), the two-spotted spider mite (*T. urticae*), is one of the most polyphagous herbivores that feeds on over 1100 plant species,

including more than 150 crop species (Jeppson et al., 1975; Migeon and Dorkeld, 2006–2017). Similarly to phloem-feeding insects, this chelicerate pest has mouthparts adapted for a “sucking” mode of feeding, but exactly how *T. urticae* feeds on plant tissues remains controversial. In contrast to phloem-feeding herbivores that “suck” the sap from a plant's vascular system, *T. urticae* feeds on cells within the leaf mesophyll (Park and Lee, 2002). Associated with this difference in feeding preference is the length of the *T. urticae* stylet that ranges from 100  $\mu\text{m}$  in larvae to  $\sim 150$   $\mu\text{m}$  in the adult female mites (Avery and Briggs, 1968; Ekka, 1969; Sances et al., 1979), relative to the much longer stylets of phloem-feeding insects that can reach up to 800  $\mu\text{m}$  (Pointeau et al., 2012). The *T. urticae* stylet is a tube formed by the interlocking of two cheliceral digits with a single canal of  $\sim 2$   $\mu\text{m}$  in diameter (André and Remacle, 1984). This contrasts the more elaborate structure of stylets in phloem-feeding insects (e.g., aphids and psyllids), which consist of two canals: a feeding canal that transports the plant nutritive sap, and the salivary canal that allows secretion from the insect's salivary glands into the plant tissue (Tjallingii and Esch, 1993; Garzo et al., 2012). While the function of a stylet as a piercing-feeding organ is clearly described in phloem-feeding insects, its role in *T. urticae* feeding is still unclear. It is not known if *T. urticae* use their stylet to transport both the saliva and the plant nutritive fluid (Summers et al., 1973; Hislop and Jeppson, 1976; André and Remacle, 1984), or if they use the stylet to pierce the plant tissues, deliver salivary secretions, and then use the buccal cavity to directly ingest the nutritive fluid originating from mesophyll cells that is proposed to be extruded to the surface by capillary action (Alberti and Crooker, 1985; Nuzzaci and De Lillo, 1991a).

Spider mites most frequently feed on leaf tissues, causing the formation of chlorotic spots that are associated with an extensive collapse of the mesophyll layer (Sances et al., 1979; Park and Lee, 2002). Ultrastructural studies of damaged plant tissue identified cells that were either plasmolysed, empty, collapsed, or had coagulated contents (Tanigoshi and Davis, 1978; Albrigo et al., 1981; Campbell et al., 1990). As cell wall disruption was associated with some of the affected cells, the observed damage was attributed to stylet penetration and mite feeding. In addition, it has been estimated that mites damage  $\sim 20$  clustered cells per minute directly leading to the formation of a chlorotic spot (Liesering, 1960). While these studies provide a benchmark for our understanding of the *T. urticae*-

plant relationship, some conclusions were inferred from the observation of the *T. urticae* feeding behavior or its long-term consequence on plant tissues, rather than on the direct and immediate analysis of plant-mite interface. For example, the assessment of plant damage was based on the analysis of leaf tissues that were exposed to mite herbivory for days, hindering the ability to distinguish between plant damage that directly resulted from mite feeding and damage that was a cumulative result of both mite feeding and plant's response to it. In addition, the number of cells consumed by mites was estimated based on the movement of *T. urticae*'s mandibular plate and the assumption that every movement corresponds to the insertion of the stylet into an independent cell (Liesering, 1960).

*T. urticae* is being established as a model chelicerate pest. Its genome was recently sequenced (Grbic et al., 2011) and several plant-*T. urticae* interaction experimental systems were established (Zhurov et al., 2014; Martel et al., 2015; Wybouw et al., 2015; Diaz-Riquelme et al., 2016). The ability to track the whole-genome reciprocal responses in plant-*T. urticae* interactions allows dissection of molecular mechanisms underlying plant responses to mite herbivory. In addition, recent work indicated that the *T. urticae* and related mites can manipulate plant defense responses, suggesting that there is an elaborate interaction between these herbivores and their plant hosts, and an evolutionary arms-race between their genomes (Kant et al., 2008; Alba et al., 2014; Wybouw et al., 2015; Villarroel et al., 2016; Jonckheere et al., 2016). In this context, the knowledge of spider mite feeding at the cellular level, using direct observations, becomes critical for understanding cellular interactions and signaling underlying mite feeding and plant-induced responses. Here, I characterized plant damage that directly results from mite feeding at a cellular level and the interface between the mite and the plant during the feeding process. I show that *T. urticae* uses its stylet to penetrate into the leaf mesophyll, where it consumes individual cells without damaging epidermal cell layer. In addition, I show that the consumption rate of plant cells is much lower than previously estimated and that mite feeding *per se* does not result in the formation of chlorotic spots

This study establishes the cellular context for the plant-spider mite interactions required for our understanding of the cell signaling associated with spider mite feeding.

## 2.2 Material and Methods

### 2.2.1 Plant growth and material rearing

The bean, *Phaseolus vulgaris*, cultivar California Red Kidney (Stokes, Thorold, ON), and *Arabidopsis thaliana* (Columbia-0) plants were grown from seed in peat–vermiculite growing mix (Premier Pro-mix BX; Premier Tech) at 24°C, under 100–150  $\mu\text{M}$  m–2s–1 cool-white fluorescent light and 16/8 h (light/dark) photoperiod. The reference spider mite strain, *Tetranychus urticae* (London), was reared on bean plants under the same conditions.

### 2.2.2 Monitoring of *T. urticae* feeding

To estimate the amount of time that spider mites spend at a feeding site, mites were first starved for 12 h and then 10 female mites were placed on either a bean or *Arabidopsis* leaf disk of 1.5 cm in diameter. Mite feeding was recorded under a dissecting microscope fitted with the Canon EOS Rebel T5i camera (Canon, Japan).

### 2.2.3 *T. urticae* cuticular preparations

Adult spider mites were starved for 12 h and were placed in 100% ethanol overnight. The following day, mites were transferred to a slide containing a drop of a mix of Hoyer's medium and lactic acid (1:1, v/v). The slides were incubated overnight at 60°C and were viewed using a Zeiss Axiophot microscope (Carl Zeiss AG, Germany) fitted with a Zeiss AxioCam Color HRc CCD Camera 412-312 (Carl Zeiss AG, Germany).

### 2.2.4 Phalloidin staining

Spider mite adults were collected and fixed in 4% formaldehyde in 0.1 M phosphate buffer saline (pH 7.4) overnight at 4°C. Mites were washed twice in 0.1 M phosphate buffer. Approximately 100 spider mites suspended in 100  $\mu\text{l}$  of phosphate buffer saline were incubated with 50  $\mu\text{l}$  of phalloidin 546 (Alexa Fluor® 546 Phalloidin, ThermoFisher Scientific, USA) overnight at 4°C (Jiang et al., 2007). Phalloidin stained actin filaments were visualized using a Zeiss Axiophot confocal microscope (Carl Zeiss AG, Germany) using the following settings: Excitation: 543 nm, Filter: Ch1, LP 560; Image size: 2048 x 2048 pixels representing an area of  $460.6 \times 460.6 \mu\text{m}$ .

### 2.2.5 Scanning electron microscopy

Spider mites were fixed overnight in 2.5% (v/w) glutaraldehyde (Electron Microscopy Sciences, USA) in 0.1 M sodium phosphate buffer (pH 7.2). Fixed mites were washed three times in 0.1 M sodium phosphate buffer (pH 7.2) and were dehydrated in a graded ethanol series of increasing concentration for 10 min at each concentration—50, 70, 80, 90, 95, 100%, and 100% (v/v in H<sub>2</sub>O). The specimens were further dried in a graded series of hexamethyldisilazane (HMDS; Sigma, USA) diluted with 100% ethanol (v/v) to 25, 50, 80, 100, 100% for 10 min at each step, followed by air-drying in a fume hood for 1 h (Bray et al., 1993). Individual spider mites were mounted onto SEM stubs using an eyelash probe before coating them with gold particles in the sputter (Technics Hummer VI Sputter Coat Unit, Anatech, USA). Samples were examined with a Hitachi S-3400N electron microscope (Hitachi Science Systems, Tokyo, Japan) operated at a voltage of 5 kV.

### 2.2.6 Trypan blue staining of plant tissue and quantification of damage caused by *T. urticae* feeding

Trypan blue staining was performed according to Keogh et al. (1980), with some modifications. Adult female mites were allowed to feed on either the adaxial or abaxial side of the *Arabidopsis* or bean leaf piece of 1 cm<sup>2</sup> for 10 min, as described above. Subsequently, leaves were submerged in trypan blue solution (1:1:1:1 v/v, lactic acid, phenol, glycerol, water, and 1% trypan blue) diluted with 95% ethanol (1:2 v/v) in a 15-mL conical polypropylene tube, and were placed in a boiling water bath. *Arabidopsis* leaves were boiled for a minute and bean leaves for 5 min. The tissue was left in the staining solution overnight at room temperature. Subsequently, leaves were cleared with a chloral hydrate solution (2.5 g/mL diluted in water; Sigma, USA) for ~6 h with two changes of the solution. Cleared leaves were either prepared for imaging or sectioning. Leaves for imaging were mounted in 50% glycerol in 0.1 M sodium phosphate buffer at pH 7.0 and observed by light or confocal microscopy using a Zeiss Axiophot microscope (Carl Zeiss AG, Germany) fitted with a Carl Zeiss AxioCam Color HRc CCD Camera 412-312 (Carl Zeiss AG, Germany). For confocal imaging, the tissue was excited with a 543 nm HeNe laser line and bi-directional scanning was used to scan leaf tissue regions



in sections of  $230 \times 230 \mu\text{m}$  at a  $2048 \times 2048$  pixel resolution. Sectioning of the trypan blue-stained and cleared plant tissues: Trypan blue-stained bean tissue was prepared for sectioning by fixing the sample in 10% glutaraldehyde solution in 0.1 M sodium phosphate buffer (pH 7.0) overnight. Leaf tissue was manually dehydrated in an ethanol series up to 70% (v/v in  $\text{H}_2\text{O}$ ). Further dehydration and paraffin embedding was performed in a tissue processor (Leica ASP300TP). Embedded leaf tissue was sectioned on a microtome (Leica RM2255 Microtome) at a thickness of  $10 \mu\text{m}$ . Sections were dewaxed in two 10 min changes of 100% xylene, were mounted with Permount™ Mounting Medium (Fisher, USA) and were examined under a Carl Zeiss AxioCam Color HRc CCD Camera 412-312. Several attempts to paraffin-embed trypan blue-stained *Arabidopsis* leaves resulted in an excessive tissue disruption. Instead, a free-hand sectioning of *Arabidopsis* tissue had to be performed. Briefly, a surgical blade (Feather, No. 23) was used to cut leaf sections of  $100\text{--}150 \mu\text{m}$  in thickness under the dissecting microscope. Leaf sections were mounted flat between layers of 2% agar (w/v in  $\text{H}_2\text{O}$ ) to provide physical support for the leaf tissue. The agar embedded tissue was excised, mounted in 50% glycerol (v/v in  $\text{H}_2\text{O}$ ) and observed under a light microscope using a Zeiss Axiophot microscope (Carl Zeiss AG, Germany) fitted with a Carl Zeiss AxioCam Color HRc CCD Camera 412-312 (Carl Zeiss AG, Germany).

### 2.2.7 Histological analysis of *T. urticae* stylet path through the plant tissue

Fully expanded adult bean or *Arabidopsis* leaves were cut into small pieces ( $0.4 \times 0.8$  cm) that were placed on wet cotton with either adaxial or abaxial sides exposed and then infested with 50 mites that were starved for 12 h. Mites were allowed to feed for 10 min. Next, leaf pieces (with mites still feeding on them) were submerged in liquid nitrogen in order to fix mites in their natural feeding position. Frozen leaf pieces were transferred to a solution of 2.5% (v/v) glutaraldehyde in 0.1 M sodium phosphate buffer at pH 7. After 24 h, the tissues were gently washed in 0.1 M sodium phosphate buffer at pH 7 and dehydrated in a graded alcohol series: 25, 50, 75, 95, 100% and 100% (v/v in  $\text{H}_2\text{O}$ ), for 15 min in each solution. Leaf pieces with mites still attached were embedded in LR White resin (Electron Microscopy Science, USA) and were cured overnight at  $55^\circ\text{C}$ .

Specimens were cut with a Reichert Ultracut S ultramicrotome (Leica, Austria) into 1  $\mu\text{m}$  serial sections using a glass knife. Sections were stained with toluidine blue, 0.5% (w/v) in 0.1% (w/v)  $\text{Na}_2\text{CO}_3$  in water, for 5 min on a slide warmer at 60°C and dried overnight at room temperature. Cross sections of mite-free plant leaves were prepared in parallel as controls.

## 2.3 Results

### 2.3.1 Determination of the *T. urticae* feeding event

In order to determine the immediate consequence of mite herbivory on plants damage, I first had to establish the timing of a mite's feeding event. A feeding event was defined as a process that is initiated by a mite's settlement at a particular leaf spot and is terminated when the mite raises its head away from the leaf surface. An example of a feeding initiation event is shown in the Supplemental Movie S1, beginning at 0 min 31 s, while a termination event can be seen at 5 min 2 s in the Supplemental Movie S2. The whole feeding event of this mite is shown in Supplemental Movie S3, which captures the mite feeding for over 12 min (See movies in supplemental data in: Bensoussan et al., 2016). In addition, two other mites that were continuously feeding are captured within the same frame. An analysis of 27 independent feeding events revealed a wide distribution of durations, ranging from as short as several minutes to over half an hour, with an average duration of mite feeding event of 13 min 22 s (Figure 2.1A).

During feeding, mites move their stylophore (Sty in Figure 2.1B) leading to stylet protrusion and penetration into the plant tissue. The stylet, not directly visible as mites feed, is a tube composed of two movable cheliceral digits (Chd in Figures 2.1Bv–viii). Each cheliceral digit is attached dorsally to a retractable and extrudable stylophore. While feeding, protracted cheliceral digits slide into grooves formed by the rostral gutter (Rg; seen in the inset in Figure 2.1Bi) to interlock together and form the stylet—a hollow tube—at the buccal cavity level (Bc in Figure 2.1B). Besides the stylet and buccal cavity, the spider mite feeding apparatus is composed of the propharynx (Pr), pharynx (Ph), esophagus (Es), and midgut (Figure 2.1B). Ventrally, a small opening through the cuticle,

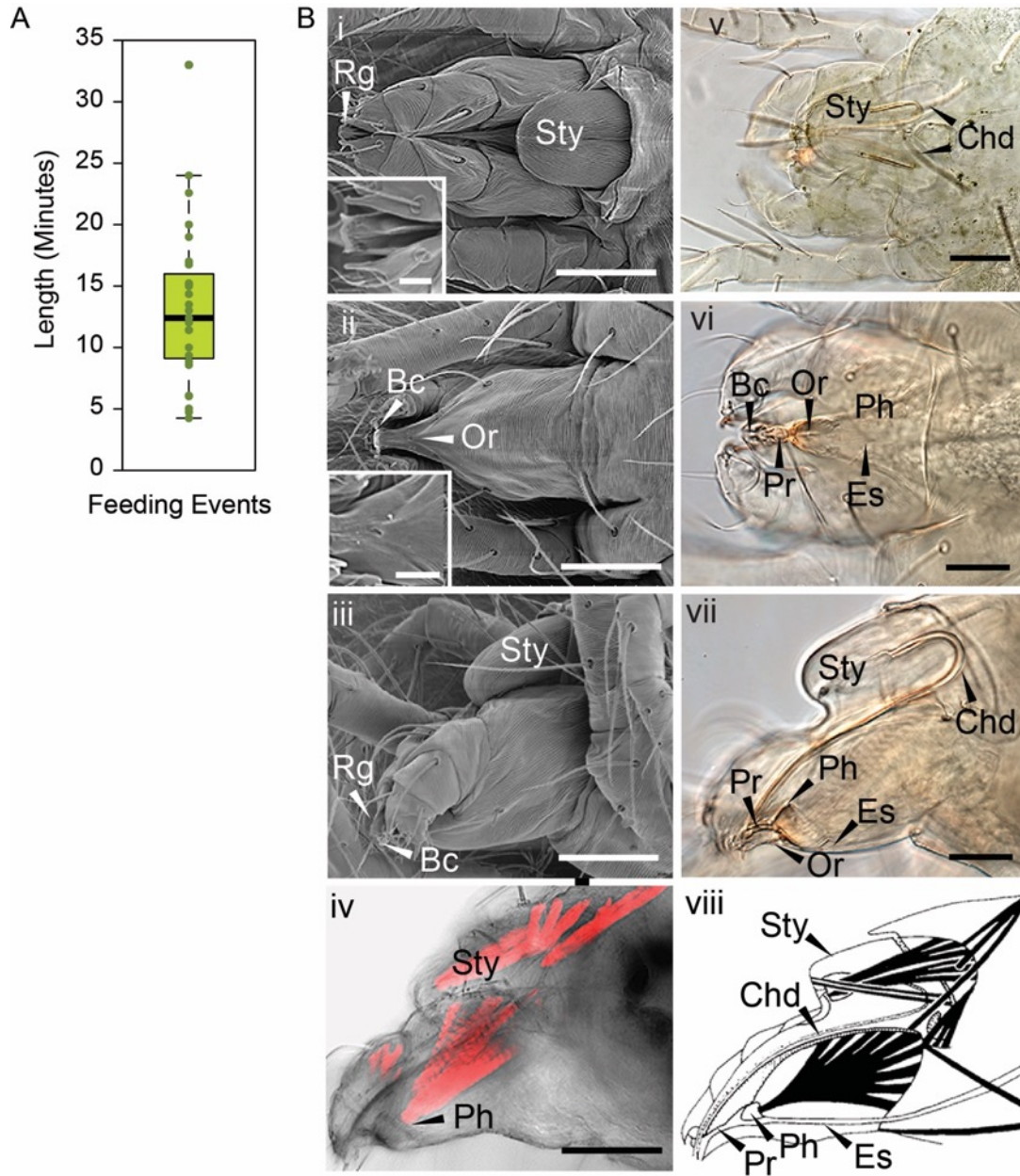


**Figure 2.1** *T. urticae* feeding duration and mouth-part organs. (A) Duration of individual mite feeding events in minutes ( $n = 27$ ). (B), *T. urticae* mouth parts. i–iii, SEM imaging and v–vii, brightfield of mite gnathosoma. i and v, dorsal view with inset close up view of the rostral gutter (Rg); ii and vi, ventral view with inset close up view of the inferior oral commissure (Or); iii and vii lateral view; iv: phalloidin staining of actin filaments and viii: schematic representation of muscles associated with the mouth parts. Sty, stylophore; Bc, buccal cavity; ChD, Cheliceral digits; Es, Esophagus; Ph, Pharynx; Pr, Propharynx; scale bars: in inset i and ii, 10  $\mu$ m; in iv (i–iv and vi–viii), 50  $\mu$ m; in v, 50  $\mu$ m. (C–F), Mite feeding and plant damage.

referred to as the inferior oral commissure (Or) can be observed (see inset in Figure 2.1Bii). This aperture was hypothesized to help the suction flow caused by the pharyngeal pump (Nuzzaci and De Lillo, 1991b). Both the stylophore and the pharynx are connected to head muscles that control their movements (Figures 2.1Biv, viii). While the movement of the pharyngeal pump cannot be observed, the pulsing of the mite opistosoma (the posterior part of the body) is readily visible as mites feed (Supplemental Movies 1–3).

No visual plant damage can be observed following mite feeding. A representative feeding event is shown in Figures 2.2A, B. Once feeding is completed (this particular one lasted for 10 min), no macroscopic change can be observed at the site (Figures 2.2C, D). Thus, chlorotic spots that eventually form on infested leaves (see Figure 2.2F in inset) are not an immediate consequence of mite feeding. A similar duration of feeding with a lack of visible damage was also observed after mite feeding on the *Arabidopsis* leaves (data not shown). Thus, mites spend minutes feeding at the same leaf spot, without causing visual damage to plant tissue.

### 2.3.2 Determination of *T. urticae* Feeding Pattern on Plant Tissue

The frequency of stylophore movement associated with mite feeding led to the proposition that mites consume ~20 plant cells per minute (Liesering, 1960). To determine the extent of leaf damage occurring during a single mite feeding event, I allowed mites to feed on leaves for 10 min, after which I immediately stained the leaf tissue with trypan blue vital stain, to identify the number and the pattern of dead cells. As host-plant preference may affect mite feeding patterns, I infested both bean leaves (preferred host for the population used in this study) and *Arabidopsis* leaves (a non-preferred host) with mites. In addition, since mites normally feed from both adaxial and abaxial leaf surfaces, I examined plant damage in a controlled experimental set-up that allowed mites to exclusively feed from only one of these surfaces. This allowed me to determine if accessing the leaf tissue from different epidermal surfaces has an effect on feeding patterns. Bean and *Arabidopsis* leaves have cell layers typical of dicotyledonous plants: the adaxial (upper) epidermis (ad), the palisade mesophyll (pm), the spongy mesophyll (sm), and the abaxial (lower) epidermis (ab) (Figure 2.3A). I used

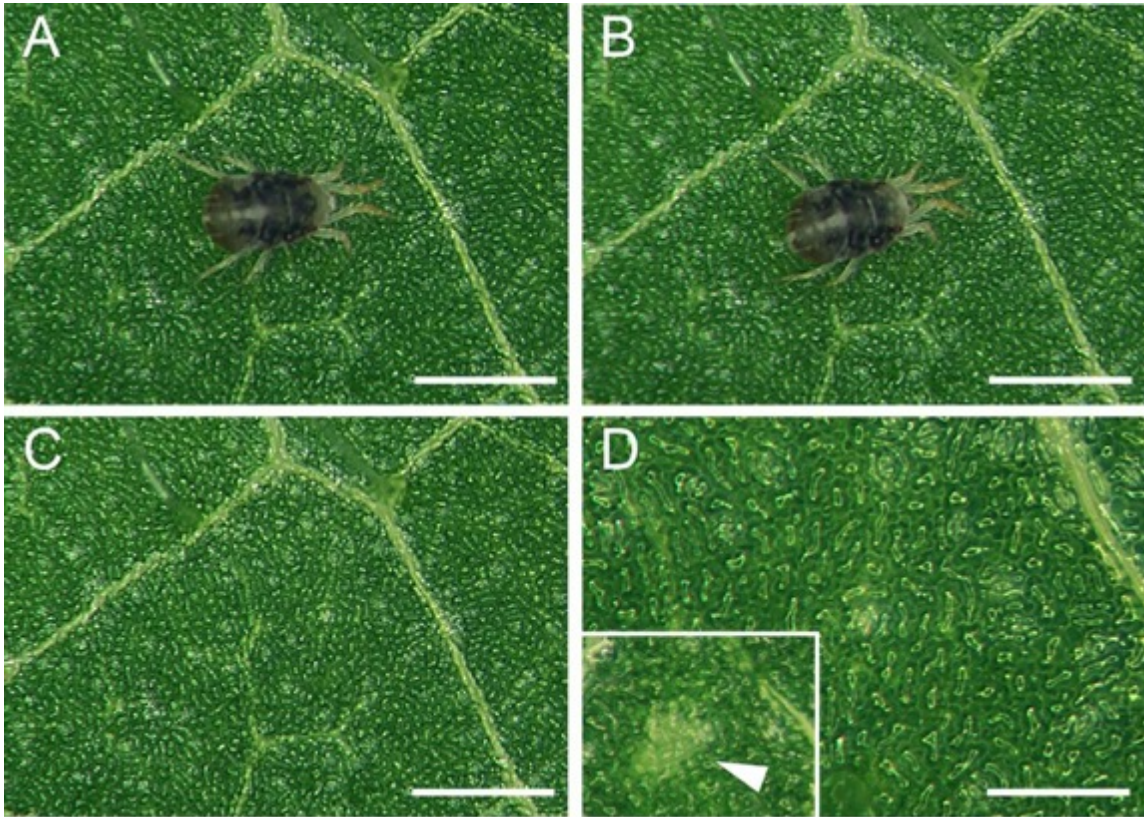


**Figure 2.2: Mite feeding event and plant damage.** (A), Mite at the beginning of the feeding event. (B), Mite at the end of the feeding event. (C, D) Feeding site. F inset, a typical chlorotic spot (arrow head). Scale bars: 500  $\mu\text{m}$  in (A–C); 250  $\mu\text{m}$  in (D) (main panel and inset).

both histological and optical sectioning to observe cells that were damaged as a result of mite feeding, Figure 2.3A. The epidermal layers are cellular monolayers containing densely packed pavement cells, trichomes, and stomata. Stomata consist of two guard cells that form an opening through the epidermal layers that allow gas exchange between the leaf mesophyll and atmosphere. Below the adaxial epidermis is the palisade mesophyll, a monolayer in both bean and *Arabidopsis* leaves that is composed of densely packed cylindrical cells. Located further ventrally is the spongy mesophyll that is characterized by a multilayer of oval and sparsely packed cells that are interspaced with large volumes of the air space. The spongy mesophyll is in direct contact with the abaxial epidermis, which forms the most ventral leaf boundary. I used trypan blue to distinguish intact cells from those with disrupted cell membranes, since only damaged cells accumulate the dye and appear blue under a bright field microscope. To ensure that all cells that could have been damaged during a 10-min mite feeding were visualized, I examined the leaf tissue in both transverse and longitudinal serial sections after mite feeding (Figures 2.4A–D).

When mites fed from the adaxial epidermis, the trypan blue staining was most frequently restricted to the palisade parenchyma that is in direct contact with the upper epidermis (86% of the total number of feeding events on bean leaves and 77% on *Arabidopsis* leaves, Table 2.1 and Figures 2.4A, C). The frequency of feeding events involving multiple cells negatively correlated with the number of dead cells. On bean and *Arabidopsis* leaves respectively, two stained cells were observed in 13 and 20% feeding events, and three stained cells were observed in 1 and 3% of feeding events. Thus, when placed on the adaxial epidermis, mites usually damaged a single palisade cell that was immediately below the epidermis. However, the epidermis was not damaged (Table 2.1 and Figures 2.4A, C).

When mites fed from the abaxial epidermis (where *T. urticae* preferentially feeds), the damage most frequently occurred in the layer immediately adjacent to the lower epidermis, the spongy parenchyma, in both bean and *Arabidopsis* leaves (76% of feeding events on bean and 69% on *Arabidopsis* involved a single cell in the spongy layer, Table

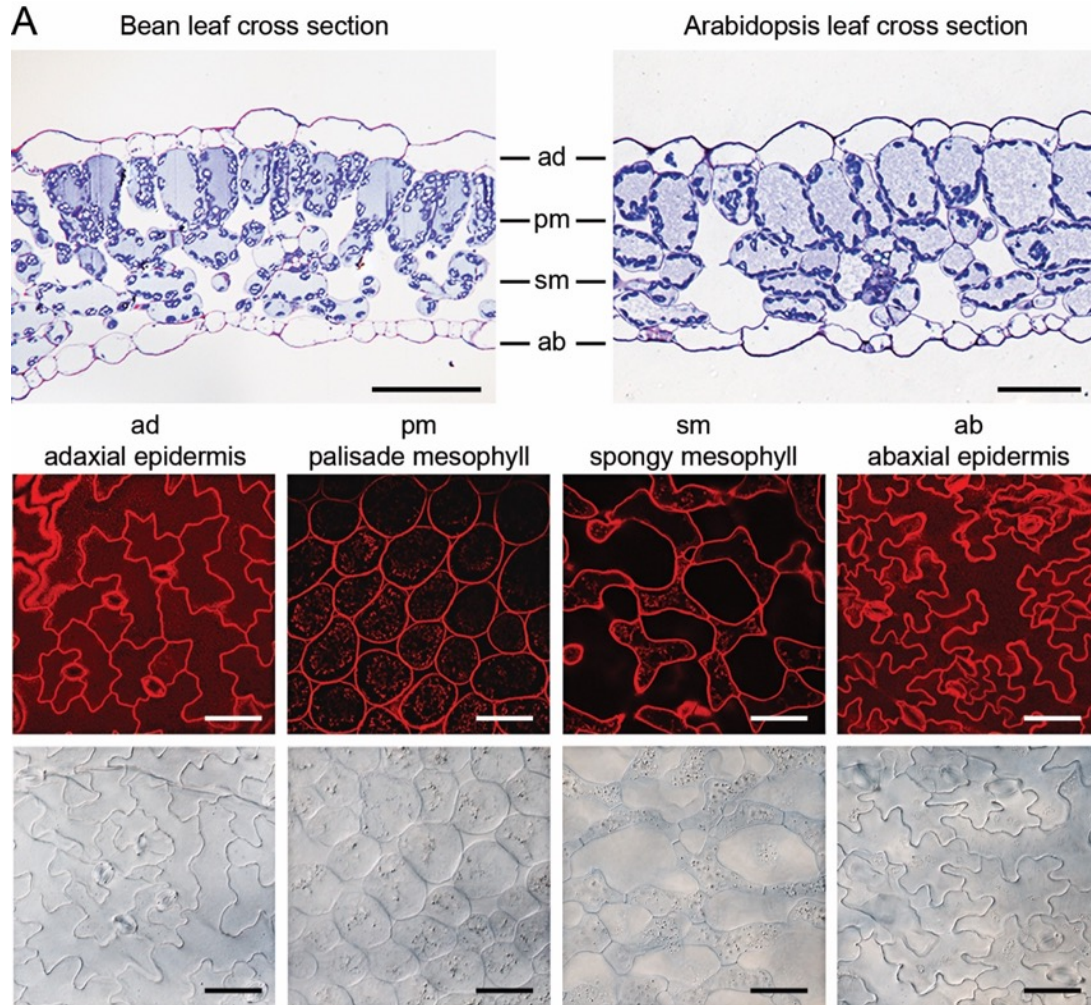


**Figure 2.3: Bean and *Arabidopsis* leaves cell layer.** (A), Longitudinal cross sections of bean and *Arabidopsis* leaves stained with toluidine blue (on the top) and *Arabidopsis* optical sections (at the bottom) visualized using confocal (upper row) and brightfield (lower row) microscopy. ad, adaxial epidermis; pm, palisade mesophyll; sm, spongy mesophyll; ab, abaxial epidermis. Scale bars: 50  $\mu\text{m}$  in all panels.

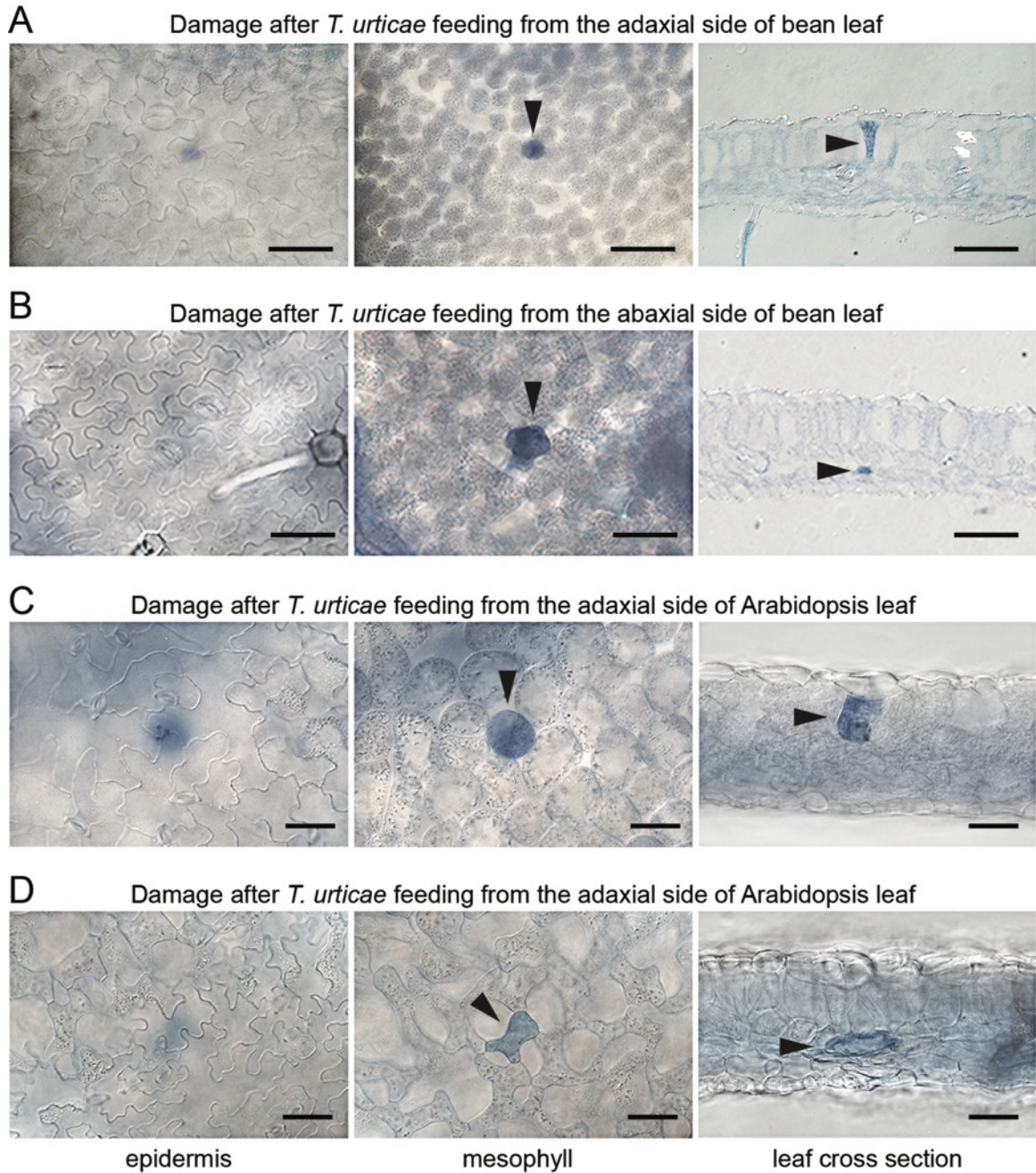


**Figure 2.4: Plant damage associated with spider mite feeding.** (A–D), Representative images of damaged cells within trypan blue stained bean and Arabidopsis leaves after spider mite feeding for 10 min. Damaged cells appear blue and are marked with arrowheads in optical and cross sections. Scale bars: 50  $\mu\text{m}$  in (A) through (E).



**Table 2.1: Distribution of trypan blue stained cells within bean and *Arabidopsis* leaf tissues resulting from *T. urticae* feeding for 10 min.**

Leaf surface exposed	<i>Arabidopsis</i>		Bean	
	Upper	Lower	Upper	Lower
<b>Number of damaged cells (%)</b>				
1	77	69	86	76
2	20	29	13	23
3	3	2	1	1
<b>Cell type (%)</b>				
Epidermis	0	0	0	0
Palisade mesophyll (only)	73	16	85	21
Spongy mesophyll (only)	8	64	8	62
Palisade and spongy mesophyll	19	20	7	17
<b>Samples analyzed (n)</b>	95	119	221	207

2.1 and Figures 2.4B, D). Feeding that resulted in staining of two or three cells was observed in 24 and 31% of cases in bean and *Arabidopsis* leaves, respectively. Thus, spider mite feeding events (restricted to a 10-min period) most frequently resulted in the trypan blue staining of a single mesophyll cell that was adjacent to the epidermal layer that mites stand on, regardless of the plant host. This pattern suggests that mites: (a) do not have a preference for the cell type within the mesophyll, and (b) feed on internal leaf tissue cells without an apparent disturbance of the epidermal layer.

### 2.3.3 *Tetranychus urticae* Feeding

A lack of trypan blue staining within the epidermal cellular layers and the observed cell death of mesophyll cells resulting from mite feeding raises the question of stylet penetration through the plant tissue. Given these observations, at least two possible stylet paths are conceivable. First, the stylet can transverse epidermal cells, however, since the stylet is only 2  $\mu\text{m}$  in diameter, the resulting damage may not affect cell viability. Consequently, epidermal cells remain colorless upon trypan blue staining. Alternatively, the stylet does not penetrate, but transverses the epidermal layer in between cells.

To distinguish between these possibilities, I had to reconstitute stylet pathway within the leaf tissue. Given that mites retract their stylet upon disturbance, I first had to develop a tissue preparation method that supports histological analysis of plant tissues with mites (and their stylets) in a feeding position (see Material and Methods). My first step was to find a good fixation method to keep mites in feeding position without disturbing stylet movement. I used different concentration and combination of chemical fixative, physical techniques such as  $\text{CO}_2$  incubation and finally immersion in liquid nitrogen. This last technique was the most efficient in preserving mites in feeding position on plant tissue. Next, I tested different histological methods in order to section internal leaf tissue and observe the stylet path. I tested cryosectioning, which consists of embedding frozen tissue in a compound suitable for sectioning at very low temperature (-20; -30°C). However, this technique was not suitable as it caused mechanical distortion and tissue compression/extension from the blade (Appendix 2). I next tried paraffin embedding of frozen tissue that was previously fixed and dehydrated for microtome sectioning. The

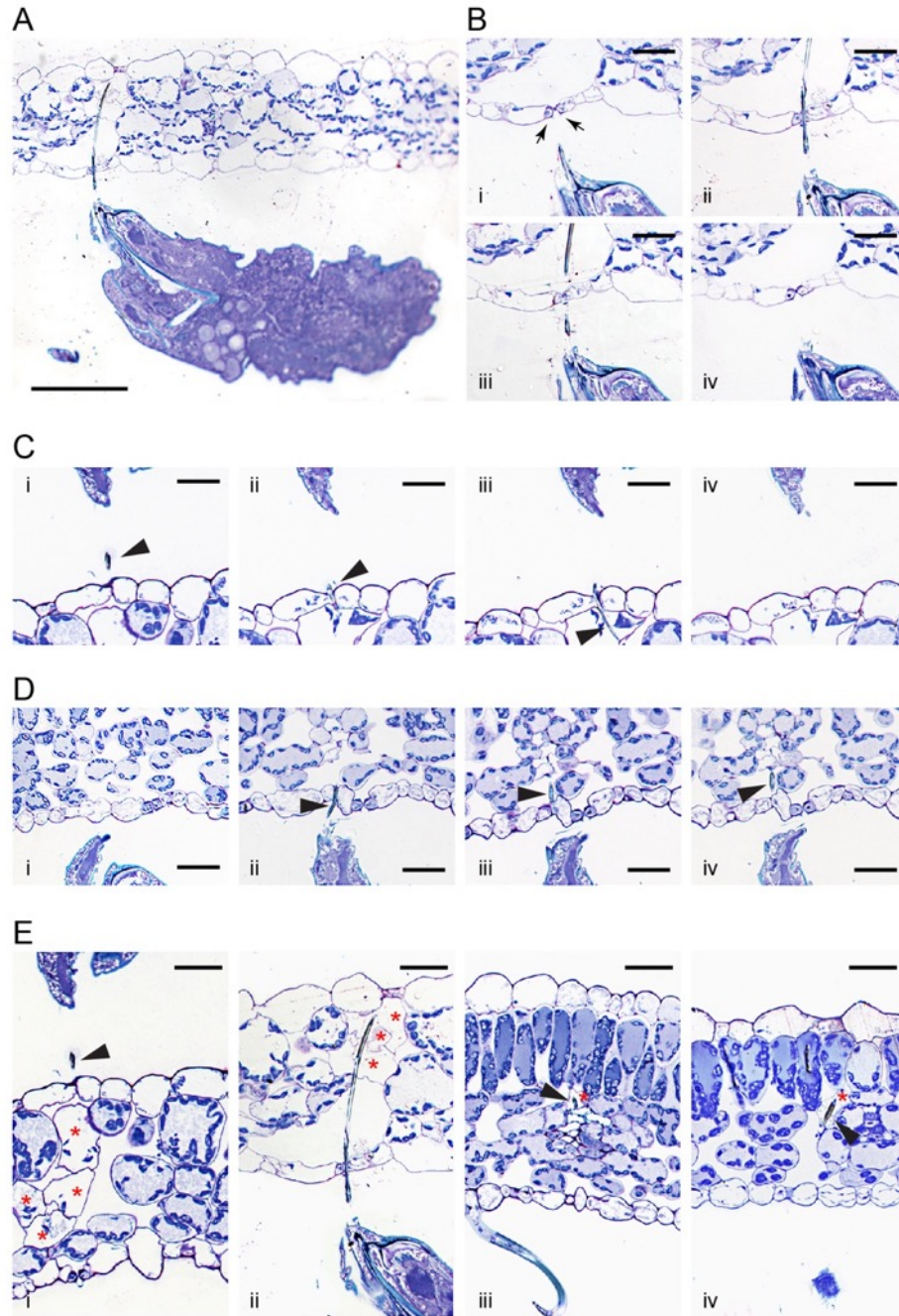


**Figure 2.5: Interface between *T. urticae* and plant tissue during feeding.** (A), A longitudinal cross section of mite feeding from the abaxial side of the *Arabidopsis* leaf. (B, C), Serial sections (1  $\mu\text{m}$  apart) of stylet penetration through epidermal cellular layers of *Arabidopsis* leaves while mites fed from the abaxial side (in B) and adaxial side (in C). Guard cells were labeled with arrows in (B). (D), *T. urticae* stylet penetration while feeding from the abaxial side of bean leaf. (E), Plant cell damage associated with spider mite feeding. Longitudinal cross sections of *Arabidopsis* (i and ii) and bean (iii and iv) leaves showing cells (marked with asterisks) that were in direct contact with mite stylet. Stylet is marked with arrowhead throughout. Scale bars: 100  $\mu\text{m}$  in (A), 25  $\mu\text{m}$  in (B–E).

quality was improved for the mite material and I could see the stylet in the leaf section (Appendix 3). However, the plant tissue was altered and plant cells were hardly distinguishable. Finally, when frozen tissue was embedded in epoxy resin and sectioned with the ultramicrotome, both plant and mite tissues were well preserved, allowing me to assess stylet penetration into plant tissue. Longitudinal serial sections of feeding mites, recovered with their stylets within leaf tissues, are shown in Figures 2.5A–E. These histological sections are oriented with the leaf adaxial (upper) epidermis toward the top and the mite's prosoma (anterior end) toward the left. The epidermal pavement cells, which lack chloroplasts, appear empty in cross sections of glutaraldehyde-fixed and toluidine blue-stained preparations. Interspersed among these cells are stomata, natural openings at the leaf epidermis. Stomata can be recognized on the longitudinal leaf cross sections by the presence of guard cells (marked with arrows in Figure 2.5B), which are smaller in size relative to the pavement cells, contain chloroplasts, stain blue in our preparations, and are positioned above the substomatal cavity. Cells within the mesophyll layer contain chloroplasts that can be seen as blue circles at the cellular periphery in our toluidine-blue stained leaf cross sections (Figure 2.5).

A low magnification view of a mite feeding on an *Arabidopsis* leaf from the abaxial epidermis is shown in Figure 2.5A. In this particular case, the stylet penetrates the epidermal cellular layer through the stomatal opening (see Figures 2.5Bi–iv). Micron-thick serial sections reveal stylet in two adjacent sections that is consistent with stylet's estimated diameter of 2  $\mu\text{m}$ . The stylet transverses the epidermis in between the two guard cells that remain intact (see Figures 2.5Bii, iii), indicating that the stylet uses a stomatal opening to reach the leaf mesophyll. An examination of additional independent feeding events demonstrates that mites do not always use stomata to insert their stylets into the leaf. Serial sections in Figure 2.5C show stylet penetration during spider mite feeding from the adaxial epidermis of an *Arabidopsis* leaf. The plane of sectioning is not parallel to the stylet, resulting in the presence of stylet segments (marked by arrowheads) in consecutive sections. Importantly, the stylet crosses the epidermis in between the two pavement cells (Figures 2.5Cii, iii). Similarly, stylet penetration into the bean leaf upon mite feeding from the abaxial epidermis is shown in serial sections, Figure 2.5D. In this instance, the penetration occurs between pavement cells that are adjacent to stomata,

indicating that mites do not have a preference for transversing the leaf epidermis by inserting their stylet through the stomatal opening. Thus, our histological analysis indicates that stylet penetration occurs either through the stomatal opening (between guard cells) or between the pavement epidermal cells, leaving the epidermal cells intact. This stylet penetration path is consistent with the observed lack of cell death and trypan blue staining in the epidermis.

Histological analysis of independent feeding events also allowed me to visualize for the first time, the appearance of cells that were direct targets of stylet penetration. While intact mesophyll cells have chloroplasts at the cell periphery that are stained dark with toluidine blue and a central vacuole that stains light blue, cells in contact with the stylet are either completely empty, or their cellular contents appeared condensed and partially removed (Figure 2.3E, see cells marked with asterisks). As a single trypan blue-stained mesophyll cell was the most frequently associated with mite feeding, sections shown in Figures 2.5Eiii, iv identify individual cells in which the stylet path terminated (labeled with the arrow head) and whose contents have been removed, resulting in empty plasmolysed cells.

In other sections, multiple cells that were on the stylet path showed extensive damage (Figures 2.5Ei, ii) correlating with the identification of multiple cells that were stained with trypan blue. A stylet that transversed the stomatal cavity (Figures 2.5A, B) penetrated cells toward the adaxial side of the leaf. These cells lacked chloroplasts and were collapsed (Figure 2.5Eii). In addition, Figure 2.5Ei shows damage to multiple mesophyll cells whose contents were still partially present but were coagulated. Therefore, mite stylet pierces the leaf epidermis in between cells without damaging them to reach mesophyll layer. The stylet either passes between two pavement cells, or through the stomatal opening created by the two guard cells.

Spider mite feeding results in the removal of the contents of a single or limited number of mesophyll cells that were on the stylet path. In some cases, the cell content can be seen, but is coagulated. The mesophyll cells surrounding damaged cells remained intact with unperturbed internal organization.

## 2.4 Discussion

### 2.4.1 Mechanism of *T. urticae* feeding

The reconstitution of complex relationships between mites and their hosts requires an understanding of mite feeding and its impact on plant integrity. In this study I identified several key features of *T. urticae* feeding: first, I showed that stylet penetrates the leaf either in between epidermis pavement cells or through a stomatal opening, without damaging the epidermal cellular layer (Figures 2.4, 2.5); second, mites feed from mesophyll cells without a preference for cell type within this layer (Figure 2.4 and Table 2.1); third, the similarity of mite feeding on bean (preferred host) and *Arabidopsis* (a non-preferred host for the strain used in this study) indicates that mite feeding pattern is not affected by the plant host preference (Figure 2.4 and Table 2.1); fourth, the duration of a single mite feeding event is longer than previously estimated, ranging from several minutes to more than half an hour (Figure 2.1 and Supplemental Movies); fifth, chlorotic spots that form on damaged leaves are not an immediate consequence of mite feeding (Figure 2.2). Finally, I initiated mapping of several gene expression domains in mite's prosoma that may be associated with salivary secretion.

The leaf epidermis, with its cuticular depositions, is one of the constitutive defenses developed by plants to deter pathogen infection and herbivory. However, stomatal openings disrupt epidermal confluence and are used by most microorganisms and some arthropod pests to access the inner leaf cellular layers (Melotto et al., 2008). Some Tetranychid and Tenuipalpidae mites exclusively target stomatal openings for stylet penetration, e.g., stomatal stylet penetration has been proposed for *Tetranychus lintearius*, which feeds on gorse, *Ulex europaeus* (Marriott et al., 2013) and was demonstrated for *Raoiella* mites on wide range of plant hosts (Beard et al., 2012). Exclusive utilization of stoma as an entry point for the stylet of these mites may arise due to the thick cuticle at the epidermis of host plants, which may present an impermeable physical barrier to stylet penetration. My analyses showed that *T. urticae* transverse the epidermis either through a junction between epidermal pavement cells or through stomata (Figure 2.5). Given the limited number of independent penetration events available for the histological analysis I cannot exclude the possibility that *T. urticae* sometimes

penetrate the epidermis by puncturing pavement cells, as proposed by Tanigoshi and Davis (1978), and Campbell et al. (1990). However, if that pattern occurs, it is rare (I did not encounter it in any of the 10 complete serial cross sections) and it does not result in disruption of the epidermal cells (I did not observe trypan-blue stained epidermal cells in the analysis of more than 600 independent feeding events (Figure 2.4 and Table 2.1)).

Mites exclusively feed from cells within the mesophyll parenchyma of either bean or *Arabidopsis* leaves (Table 2.1). Most frequently, the disturbed cells were adjacent to the epidermal layer of the leaf surface that mites fed from (Figure 2.4). However, such a pattern is not a reflection of the mite's inability to reach deep into the leaf tissue when feeding. The *T. urticae* stylet is estimated to be up to ~150  $\mu\text{m}$  in length (Avery and Briggs, 1968; Ekka, 1969; Sances et al., 1979). As leaf thickness ranges between 100 and 150  $\mu\text{m}$  (depending on species and part of the leaf blade), the mite stylet can completely transverse a leaf, allowing it to reach either the palisade or spongy mesophyll regardless of the leaf surface mites are on (see Figure 2.5A for example). Thus, my data suggest that mites have no preference for the mesophyll cell type, but apparently feed from the first parenchyma cell the stylet encounters. While *T. urticae* exclusively feeds from cells within the mesophyll parenchyma, the eriophyoid mites that are smaller in size and have short stylets only feed from the epidermal cells (Gibson, 1974; Krantz and Lindquist, 1979; Rancic et al., 2006; Nahrung and Waugh, 2012). This demonstrates that epidermal cells could be a source of nutrients as well. Thus, the exclusive feeding of *T. urticae* on cells within the mesophyll layer reflects mite's preference for this cell type. The basis for this preference is currently not known.

Mite feeding is not macroscopically visible (Figure 2.2). It causes limited damage to plant tissues and a feeding event usually results in the death of a single cell (Figure 4 and Table 2.1). Cells penetrated by the stylet collapse, with chloroplasts that are either completely removed or appear condensed, Figure 2.5. These changes are consistent with ultrastructural studies of plant damage caused by mite feeding that showed collapsed cells, devoid of any content, or those that contained condensed cellular debris (Tanigoshi and Davis, 1978; Campbell et al., 1990). Importantly, cells surrounding the dead cell remain alive with no apparent damage (Figure 2.5 and Campbell et al. 1990). In addition,

even though the formation of chlorotic spots has been used as a symptom of plant damage caused by mite feeding (Tanigoshi and Davis, 1978; Sances et al., 1979; Albrigo et al., 1981; Campbell et al., 1990; Park and Lee, 2002; Zhurov et al., 2014), they are not an immediate consequence of mite feeding.

Two possible ways were proposed to explain how mites ingest plant nutritive fluids: fluids either surface on the leaf epidermis and mites intake them directly using their buccal cavity (Alberti and Crooker, 1985; Nuzzaci and De Lillo, 1991a), or, mites use their stylet to suck the cell content in situ (Summers et al., 1973; Hislop and Jeppson, 1976; Andre and Remacle, 1984). If mites ingest the cell content from leaf surface, then it is unclear how mites can produce sufficient negative pressure to: (1) allow nutritive fluids to pass through the stylet holes that are created in the cell membrane and the cell wall, and are only few microns in diameter; (2) direct movement of nutritive fluids toward the epidermis, especially within the spongy mesophyll, which is greatly enriched in intracellular air space (Figure 2.3); and, (3) pass the nutritive fluid through the epidermis, which is otherwise non-permeable, to reach the surface. Moreover, contrary to what would be expected if fluid flowed from the damaged site to the leaf surface, I did not observe remains of cellular contents outside of disrupted cells nor in the apoplastic space leading toward the epidermis. I consider this mode of feeding improbable and favor the possibility that mites use their stylet to suck the nutritive fluid in situ. This possibility is consistent with the histological analysis showing stylets within cells whose content is either condensed or emptied (Figure 2.5) (the extremely high frequency of these observations while analyzing independent feeding events indicates that the stylet remains continuously protruded and inserted into the mesophyll cell during feeding).

However, if nutritive sap is sucked through the stylet, then some form of pre-oral digestion likely takes place within the feeding cell. Pre-oral digestion will facilitate consumption of cellular organelles whose size exceeds the stylet diameter (e.g., chloroplasts are several microns in diameter while the stylet tube is about 2  $\mu\text{m}$ ) and will reduce the viscosity of the cellular content. Digestive enzymes aiding the liquefaction of cellular content could originate from the mite's salivary secretions or from the plant cell itself. Predatory mites inject hydrolytic enzymes into their prey's body to liquefy its



content (Cohen, 1995). Thus, it is conceivable that phytophagous mites use a similar mechanism to liquefy the content of the plant cell that they feed on. Recently, serine proteases, deoxygenases and lipocalins were predicted to be part of the mite secretome (Villarroel et al., 2016), supporting the possibility that mites inject hydrolytic enzymes into the plant cell to facilitate nutrient acquisition. Alternatively, the tonoplast likely collapses upon stylet penetration, causing the release of vacuolar hydrolytic enzymes into the cytosol, leading to degradation of cellular structures in a manner similar to the vacuole-induced cell death associated with plant defenses against viruses and microbes (Hara-Nishimura and Hatsugai, 2011). The long duration of individual mite feeding events (Figure 2.1 and Supplemental Movies) supports the possibility of a complex process being required to prepare the cell contents for consumption.

#### 2.4.2 Mechanism of *T. urticae* Feeding: Comparison with other Cell-Content Feeding Herbivores and Implications for the Host Plant Defenses

Phytophagous Hemiptera and Acari are cell-content feeders that evolved stylets as part of their feeding apparatus to puncture cells they feed from. Among this group of herbivores, the mechanism of aphid feeding is the best understood (Will et al., 2013; Jaouannet et al., 2014). Both aphids and *T. urticae* use stylets to penetrate the epidermis between pavement cells and to reach feeding cells that are internal to the leaf tissue. However, despite being cell-content feeders, there are some important differences in feeding strategies of these herbivores. For example, aphids have an exclusive preference to feed from sieve element cells within the phloem. Aphids navigate their stylets through the leaf mesophyll and vascular bundle sheath apoplast and, guided by the cell chemical content, reach the phloem to insert the stylet into a sieve element cell (Hewer et al., 2011). Once in a sieve element cell, aphids use their stylet to suck the nutritive sap that is continuously replenished, keeping the feeding cell alive. In contrast, *T. urticae* feeds from mesophyll cells, without an apparent preference for the cell type (Table 2.1). In addition, mites feed by ingesting and emptying the content of the feeding cell, resulting in cell death. Thus, *T. urticae* feeding takes place in a different cellular context relative to aphids. A model depicting mite and aphid feeding is shown in Figure 2.4 and their anticipated consequences on induced plant defenses at feeding sites are discussed below.

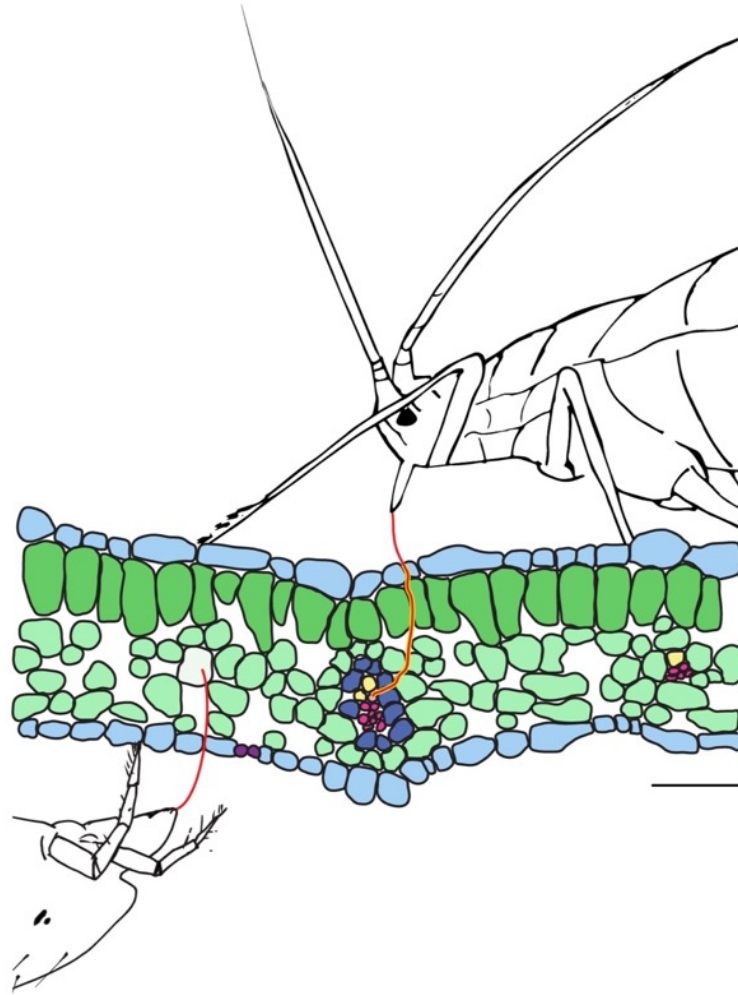
The duration of a single *T. urticae* feeding event is measured in minutes (Figure 2.1). During this time, I envision four processes: stylet penetration into the cell, pre-digestion of the cellular content, liquefaction of nutritive fluids and finally the consumption of nutrients. Thus, the feeding cell has limited time to respond to mite feeding. Early responses, including plasma membrane depolarization (measured in seconds; Mousavi et al., 2013), changes in ion fluxes (that occur within a minute; Felix et al., 1991) and release of signaling/defense compounds (e.g., reactive oxygen species; Miller et al., 2009) are expected to occur, but transcriptional reprogramming within the feeding cell is unlikely. Cell wall and membrane fragments generated as a result of stylet penetration, leakage of digested cell content, activation of mechano/turgor-sensitive channels, and potential presence of spider mite salivary secretions are among some of the potential damage- and herbivory-associated molecular patterns (DAMPs and HAPMs respectively) that can act as elicitors at the feeding site. These elicitors are expected to bind to the receptors at the surface of the intact cells surrounding the feeding cell and to trigger local and systemic defense responses, Figure 2.6B. Spider mite salivary secretions may also contain effectors, aimed at manipulating plant defenses, that have been discovered (Villaruel et al., 2016).

Salivary secretions and effectors have been critical for the evolution of the aphid feeding mechanism. Aphids feed for hours (and even days) from a single sieve element cell that remains alive (Tjallingii, 1995). Such prolonged feeding necessitates interference with host defenses that act locally at the feeding site, including: (1) secretion of salivary deposits that form a protective sheet around the stylet as it penetrates the plant tissue in search of the phloem, and, (2) salivary secretions delivered to the sieve element cell to prevent its occlusion and to keep it alive (Figure 2.6B; Tjallingii, 2006; Will et al., 2007). Interference with the host-induced transcriptional responses at the feeding site occurs in particular in companion cells that have tight symplastic connections with the enucleated sieve element cell. On the other hand, the importance of mite salivary secretions and the cellular processes that are potential targets of mite effectors are presently unknown. The existence of effectors has been monitored through their ability to modify host-induced defenses. Transcriptional changes associated with manipulated plant defenses identified so far indicate that only a subset of induced responses is attenuated (Kant et al., 2008;

Alba et al., 2014; Zhurov et al., 2014; Martel et al., 2015; Wybouw et al., 2015; Diaz-Riquelme et al., 2016). Such a pattern suggests that there is an interaction between the effectors and the intracellular components of the responding plant cells, evoking the internalization of effectors deposited in the apoplast at the feeding site. Even though the targets of mite effectors are not known, it is unlikely that they include interference with defense compounds that act locally, as mites move away from the feeding site. It is thus postulated that interference with a plant's ability to mount an effective systemic response will be of greater benefit to spider mite performance.

In summary, I have described the cellular pattern of spider mite feeding. I showed that mites feed from the content of a single mesophyll cell, resulting in its death. A model based on histological observations predicts the existence of both elicitor and effector molecules in the plant apoplast surrounding the feeding cell. The identification of mite effectors and determination of their interacting plant counterparts, as well as the identification of elicitors associated with mite feeding and their receptors, will ultimately allow mapping spatial and temporal events that are triggered by mite feeding.

A



B

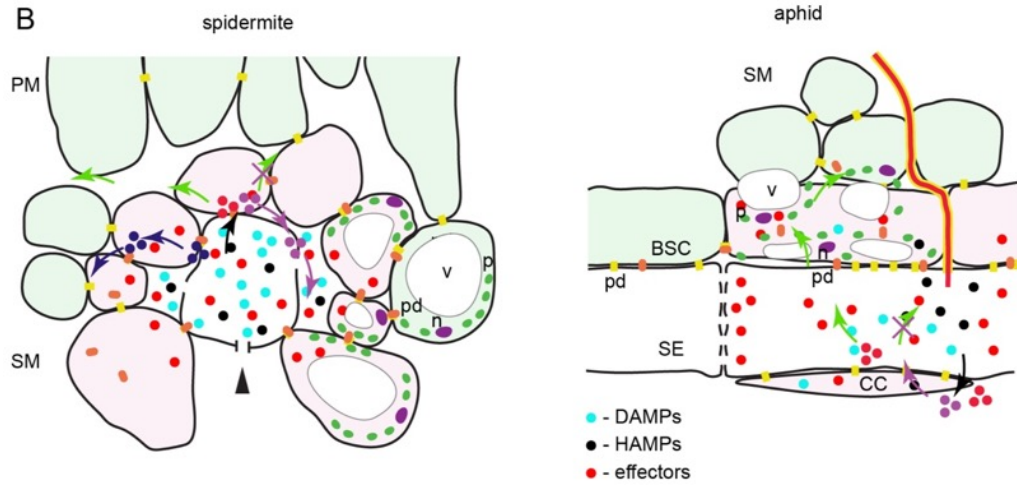


**Figure 2.6: Model of the interactions between the plant and the cell-content feeding herbivores—the two-spotted spider mite and the aphid.** (A), Schematic of leaf cross-section and feeding herbivores. Both *T. urticae* and aphid use stylets (red) to penetrate the leaf without disturbing epidermal cells. *T. urticae* feeds from the immediate cell in the mesophyll layer that stylet encounters, while aphid navigates its stylets through mesophyll apoplast to reach sieve element cell (SE). The schematic is drawn to scale; scale bar: 50  $\mu\text{m}$ . (B), Close-up diagrams of *T. urticae* and aphid feeding sites. On the left, *T. urticae* feeding results in a cell whose content has been removed. Stylet hole (marked with the arrowhead) is disturbing the unity of the plasma membrane and the cell wall. Damage- and Herbivore-Associated Molecular Patterns (DAMPs and HAMPs) are shown as blue and black dots, while mite effector molecules are shown in red. These molecules are expected within the damaged feeding cell and in the apoplast surrounding it, where they may diffuse. Cells that directly respond to DAMPs and HAMPs trigger local responses and are shown in pink. Model predicts that some *T. urticae* effectors (red dots) targeting the modulation of plant transcriptional response are internalized by these cells. Cells surrounding the feeding site and not directly exposed to DAMPs and HAMPs (light green) mount the systemic response. On the right, aphid stylet (red) is surrounded with a salivary sheath (yellow). It penetrates the sieve element cell (SE) where effectors are delivered. Effectors that modulate plant transcriptional reprogramming diffuse into adjacent companion (CC) and bundle sheath (BSC) cells that are symplastically connected with the enucleated sieve element cell. DAMPs and HAMPs also accumulate within the SE and diffuse into CC and BSC cells. PM, palisade mesophyll; SM, spongy mesophyll; pd, plasmodesmata. Schematic in (B) is not drawn to scale.

## 2.5 Reference

- Alba, J. M., Schimmel, B. C. J., Glas, J. J., Ataide, L. M. S., Pappas, M. L., Villarroel, C. A., et al. (2014). Spider mites suppress tomato defenses downstream of jasmonate and salicylate independently of hormonal crosstalk. *New Phytol.* 205, 828–840.
- Alberti, G., and Crooker, A. (1985). “Internal anatomy,” in *Spider mites: their biology, natural enemies and control.*, eds. W. Helle and M. W. Sabelis (Elsevier Ltd), 29–62.
- Alberti, G., and Kitajima, E. W. (2014). Anatomy and Fine Structure of Brevipalpus Mites (Tenuipalpidae) - Economically Important Plant-Virus Vectors. Stuttgart: Schweizerbart.
- Albrigo, L., Childers, C., and Syvertsen, J. (1981). Structural damage to citrus leaves from spider mite feeding. *Proc. Int. Soc. Citriculture.* 2, 649–652.
- Andre, H. M., and Remacle, C. (1984). Comparative and functional morphology of the gnathosoma of *Tetranychus urticae* (Acari: Tetranychidae). *Acarologia.* 25, 179–190.
- Avery, D. J., and Briggs, J. B. (1968). The aetiology and development of damage in young fruit trees infested with fruit tree red spider mite, *Panonychus ulmi* (Koch). *Ann. Appl. Biol.* 61, 277–288.
- Beard, J. J., Ochoa, R., Bauchan, G. R., Welbourn, W. C., Pooley, C., and Dowling, A. P. G. (2012). External mouthpart morphology in the Tenuipalpidae (Tetranychoida): *Raoiella* a case study. *Exp. Appl. Acarol.* 57, 227–255.
- Bray, D. F., Bagu, J., and Koegler, P. (1993). Comparison of hexamethyldisilazane (HMDS), Peldri II, and critical-point drying methods for scanning electron microscopy of biological specimens. *Microsc. Res. Tech.* 26, 489–495.
- Brusca, R. C., and Brusca, G. J. (2003). Invertebrates. Sunderland, MA: Sinauer Associates.
- Campbell, R. J., Grayson, R. L., and Marini, R. P. (1990). Surface and ultrastructural feeding injury to strawberry leaves by the twospotted spider mite. *HortScience.* 25, 948–951.
- Cohen, A. C. (1995). Extra-oral digestion in predaceous terrestrial arthropoda. *Annu. Rev. Entomol.* 40, 85–103.
- Díaz-Riquelme, J., Zhurov, V., Rioja, C., Pérez-Moreno, I., Torres-Pérez, R., Grimplet, J., et al. (2016). Comparative genome-wide transcriptome analysis of *Vitis vinifera* responses to adapted and non-adapted strains of two-spotted spider mite, *Tetranychus urticae*. *BMC Genomics.* 17, 74.

- Ekka, I. (1969). *The Rearing of the Two-Spotted Spider Mite (Tetranychus urticae Koch) on Artificial Diets*. Ph. D. McGill University.
- Felix, G., Grosskopf, D. G., Regenass, M., and Boller, T. (1991). Rapid changes of protein phosphorylation are involved in transduction of the elicitor signal in plant cells. *Proc. Natl. Acad. Sci.* 88, 8831–8834.
- Garzo, E., Bonani, J. P., Lopes, J. R. S., and Fereres, A. (2012). Morphological description of the mouthparts of the Asian citrus psyllid, *Diaphorina citri* Kuwayama (Hemiptera: Psyllidae). *Arthropod Struct. Dev.* 41, 79–86.
- Gibson, R. (1974). Studies on the feeding behaviour of the eriophyid mite *Abacarus hystrix*, a vector of grass viruses. *Ann. Appl. Biol.* 78, 213–217.
- Grbic, M., Leeuwen, T., Clark, R. M., Rombauts, S., Rouze, P., and Grbic, V. (2011). The genome of *Tetranychus urticae* reveals herbivorous pest adaptations. *Nature* 479, 487–492.
- Hara-Nishimura, I., and Hatsugai, N. (2011). The role of vacuole in plant cell death. *Cell Death Differ.* 18, 1298–1304.
- Hewer, A., Becker, A., and van Bel, A. J. E. (2011). An aphid's Odyssey - the cortical quest for the vascular bundle. *J. Exp. Biol.* 214, 3868–3879.
- Hislop, R. G., and Jeppson, L. R. (1976). Morphology of the mouthparts of Several species of phytophagous mites. *Ann. Entomol. Soc. Am.* 69, 1125–1135.
- Jaouannet, M., Rodriguez, P. A., Thorpe, P., Lenoir, C. J. G., MacLeod, R., Escudero-Martinez, C., et al. (2014). Plant immunity in plant–aphid interactions. *Front. Plant Sci.* 5, 663.
- Jeppson, L. R., Keifer, H. H., and Baker, E. (1975). *Mites injurious to economic plants*. Berkeley: University of California Press.
- Jiang, L., Rogers, S. L., and Crews, S. T. (2007). The Drosophila Dead end Arf-like3 GTPase controls vesicle trafficking during tracheal fusion cell morphogenesis. *Dev. Biol.* 311, 487–499.
- Jonckheere, W., Dermauw, W., Zhurov, V., Wybouw, N., Van den Bulcke, J., Villarroel, C. A., et al. (2016). The Salivary Protein Repertoire of the Polyphagous Spider Mite *Tetranychus urticae*: A Quest for Effectors. *Mol. Cell. Proteomics.* 15, 3594–3613.
- Kant, M. R., Sabelis, M. W., Haring, M. A., and Schuurink, R. C. (2008). Intraspecific variation in a generalist herbivore accounts for differential induction and impact of host plant defences. *Proc. R. Soc. B Biol. Sci.* 275, 443–452.

- Keogh, R. C., Deverall, B. J., and McLeod, S. (1980). Comparison of histological and physiological responses to *Phakopsora pachyrhizi* in resistant and susceptible soybean. *Trans. Br. Mycol. Soc.* 74, 329–333.
- Krantz, G. W., and Lindquist, E. E. (1979). Evolution of phytophagous mites (Acari). *Annu. Rev. Entomol.* 24, 121–158.
- Liesering, R. (1960). Beitrag zum phytopathologischen Wirkungsmechanismus von *Tetranychus urticae* (Koch) (Tetranychidae, Acari). *Z. Naturforsch.* 67, 524–542.
- Marriott, J., Florentine, S., and Raman, A. (2013). Effects of *Tetranychus lintearius* (Acari: Tetranychidae) on the structure and water potential in the foliage of the invasive *Ulex europaeus* (Fabaceae) in Australia. *Int. J. Acarol.* 39, 275–284.
- Martel, C., Zhurov, V., Navarro, M., Martinez, M., Cazaux, M., Auger, P., et al. (2015). Tomato whole genome transcriptional response to *Tetranychus urticae* identifies divergence of spider mite-induced responses between tomato and *Arabidopsis*. *Mol. Plant-Microbe Interact.* 28, 343–361.
- Melotto, M., Underwood, W., and He, S. Y. (2008). Role of stomata in plant innate immunity and foliar bacterial diseases. *Annu. Rev. Phytopathol.* 46, 101–122.
- Migeon, A., and Dorkeld, F. (2006–2017). Spider Mites Web: a comprehensive database for the Tetranychidae. Available online at: <http://www.montpellier.inra.fr/CBGP/spmweb>
- Miller, G., Schlauch, K., Tam, R., Cortes, D., Torres, M. A., Shulaev, V., et al. (2009). The plant NADPH oxidase RBOHD mediates rapid systemic signaling in response to diverse stimuli. *Sci. Signal.* 2, ra45.
- Mousavi, S. A., Chauvin, A., Pascaud, F., Kellenberger, S., and Farmer, E. E. (2013). Glutamate receptor-like genes mediate leaf-to-leaf wound signalling. *Nature.* 500, 422–426.
- Nahrung, H. F., and Waugh, R. (2012). Eriophyid mites on spotted gums: population and histological damage studies of an emerging pest. *Int. J. Acarol.* 38, 549–556.
- Nuzzacci, G., and Lillo, E. de (1991b). “Fine structure and functions of the mouthparts involved in the feeding mechanisms in *Tetranychus urticae* Koch (Tetranychoidae: Tetranychidae),” in *Modern Acarology: Proceedings of the VIII International Congress of Acarology*, eds F. Dusbabek and V. Bukva (The Hague: Academia Prague and SPB Academic), 301–303.
- Nuzzacci, G., and De Lillo, E. (1991a). “Fine structure and functions of the mouthparts involved in the feeding mechanisms in *Cenopalpus pulcher* (Canestrini and Fanzago) (Tetranychoidae: Tenuipalpidae),” in *The Acari: Reproduction, Development and Life-History Strategies*, eds R. Schuster and P. Murphy (Dordrecht: Springer Science + Business Media), 367–376.



- Park, Y.-L., and Lee, J.-H. (2002). Leaf cell and tissue damage of cucumber caused by twospotted spider mite (Acari: Tetranychidae). *J. Econ. Entomol.* 95, 952–7.
- Pointeau, S., Ameline, A., Laurans, F., Sallé, A., Rahbé, Y., Bankhead-Dronnet, S., et al. (2012). Exceptional plant penetration and feeding upon cortical parenchyma cells by the woolly poplar aphid. *J. Insect Physiol.* 58, 857–66.
- Rancic, D., Stevanovic, B., Petanović, R., Magud, B., Tosevski, I., and Gassmann, A. (2006). Anatomical injury induced by the eriophyid mite *aceria anthocoptes* on the leaves of *Cirsium arvense*. *Exp. Appl. Acarol.* 38, 243–253.
- Sances, F. V., Wyman, J. A., and Ting, I. P. (1979). Morphological responses of strawberry leaves to infestations of twospotted spider mite. *J. Econ. Entomol.* 72, 710–713.
- Summers, F., Gonzales, R., and Witt, R. (1973). The mouthparts of *Bryobia rubrioculus* (Sch.) (Acarina: Tetranychidae). *Proc. Entomol. Soc. Washingt.* 75, 96–11.
- Tanigoshi, L. K., and Davis, R. W. (1978). An Ultrastructural study of *Tetranychus mcdanieli* feeding injury to the Leaves of “Red Delicious” apple (Acari: Tetranychidae). *Int. J. Acarol.* 4, 47–51.
- Tjallingii, W. F. (1995). “Regulation of phloem sap feeding by aphids,” in *Regulatory Mechanisms in Insect Feeding*, eds R. Chapman and G. De Boer (New York, NY: Chapman and Hall), 190–209.
- Tjallingii, W. F. (2006). Salivary secretions by aphids interacting with proteins of phloem wound responses. *J. Exp. Bot.* 57, 739–745.
- Villarroel, C. A., Jonckheere, W., Alba, J. M., Glas, J. J., Dermauw, W., Haring, M. A., et al. (2016). Salivary proteins of spider mites suppress defenses in *Nicotiana benthamiana* and promote mite reproduction. *Plant J.* 86, 119–131.
- Will, T., Furch, A., and Zimmermann, M. (2013). How phloem-feeding insects face the challenge of phloem-located defenses. *Front. Plant Sci.* 4, 336.
- Will, T., Tjallingii, W. F., Thönnessen, A., and van Bel, A. J. E. (2007). Molecular sabotage of plant defense by aphid saliva. *Proc. Natl. Acad. Sci.* 104, 10536–10541.
- Wybouw, N., Dermauw, W., Tirry, L., Stevens, C., Grbic, M., and Feyereisen, R. (2014). A gene horizontally transferred from bacteria protects arthropods from host plant cyanide poisoning. *Elife.* 3,e02365.
- Wybouw, N., Zhurov, V., Martel, C., Bruinsma, K. A., Hendrickx, F., Grbić, V., et al. (2015). Adaptation of a polyphagous herbivore to a novel host plant extensively shapes the transcriptome of herbivore and host. *Mol. Ecol.* 24, 4647–4663.

Zhurov, V., Navarro, M., Bruinsma, K. A., Arbona, V., Santamaria, M. E., Cazaux, M., et al. (2014). Reciprocal responses in the interaction between *Arabidopsis* and the cell-content-feeding chelicerate herbivore spider mite. *Plant Physiol.* 164, 384–399.

## Chapter 3

### 3 RNA interference in the two-spotted spider mite *Tetranychus urticae* through soaking in solution of dsRNA.

#### 3.1 Introduction

The chelicerates represent the second largest group of terrestrial animals after insects (Brusca and Brusca, 2003) that include horseshoe crabs, scorpions, spiders, mites and ticks. They display a plethora of different lifestyles and contain economically important species for human health and agriculture. Mite species exhibit a large range of adaptations including herbivory, predation, parasitism, detritivory and symbiosis (Dunlop, 2010; Dunlop and Alberti, 2008). With almost 50,000 species described by the end of 20<sup>th</sup> century, and 0.5 to 1 million species estimated to exist, mites are one of the most diverse groups in the animal kingdom (Halliday et al., 2000). The two-spotted spider mite, *Tetranychus urticae* (Koch), is the first chelicerate whose complete genome was sequenced and annotated (Grbić et al., 2011). It is a compact genome of 90 Mbp (54% of which is protein coding sequence), with simple gene structure. *T. urticae* develops rapidly. It is easy to maintain in the laboratory and can be enriched in specific developmental stages. Because it is a major agricultural herbivorous pest, a strong research community supports the emergence of *T. urticae* as a versatile chelicerate model organism (Grbic et al., 2007). Most organisms whose genome has been sequenced in the last few years lack genetic tools available in established model systems (e.g. *Caenorhabditis elegans*, *Drosophila*, zebrafish and mouse) thus, it is critical to develop high throughput platforms using reverse genetics aimed at the functional characterization of unknown genes. Since its discovery, RNAi has been a useful tool to dissect gene function (Cullen and Arndt, 2005; Kuttenukeuler and Boutros, 2004; Zhai et al., 2009). However, RNAi delivery is often a cumbersome process requiring the injection of dsRNA into the body of small animals to initiate gene silencing. In such cases, RNAi experiments remain limited to the silencing of individual genes, with the notable exception of the high throughput screen of over 5,000 genes in *Tribolium* (Schmitt-Engel

et al., 2015). The streamlined dsRNA delivery methods results in relatively large assays. For example, a medium size screen (hundreds of genes) was performed in the coleopteran western corn rootworm *Diabrotica virgifera virgifera* based on an artificial diet laced with dsRNA (Baum et al., 2007). Also, dsRNA delivery by soaking was implemented in a high throughput reverse genetic platform for *C. elegans* (Maeda et al., 2001; Tabara et al., 1998). The genome of *T. urticae* contains genes encoding for the complete RNAi processing machinery including components of the RISC complex. It has already been shown that the maternal injection of either dsRNA or siRNA in *T. urticae* induces RNAi in embryos and causes developmental aberrations consistent with the loss-of-function phenotype of the target gene (Khila and Grbić, 2007). RNAi is thus a valid reverse genetic approach in *T. urticae*. However, compared to other arthropods, for example *Tribolium* and *Oncopeltus* (Bucher et al., 2002; Liu and Kaufman, 2005), injection of dsRNA in *T. urticae* females that are less than 0.5 mm in length remain challenging. More recently, Kwon et al., (2013), reported an alternative method for the oral administration of dsRNA via bean leaf discs floating on a dsRNA solution. Unfortunately, this protocol requires large quantities of dissolved dsRNA that must be replaced daily, making this method impractical for high throughput screens. To assess the potential of RNAi approaches in *T. urticae*, I developed a dsRNA delivery method in which mites are soaked in the solution containing dsRNA. In this study, I used the *T. urticae* target gene *Vacuolar-type H<sup>+</sup>-ATPase (VATPase)* encoding a protein that functions as a pump transferring protons across cellular membranes using the energy released by ATP hydrolysis (Finbow and Harrison, 1997). It has been previously used as a target for RNAi silencing in multiple arthropod system, e.g. the Western corn rootworm (*Diabrotica virgifera virgifera*), the pea aphid (*Acyrtosiphon pisum*), the red flour beetle (*Tribolium castaneum*), the tobacco hornworm (*Manduca sexta*), the whitefly (*Bemisia tabaci*) and the Colorado potato beetle (*Leptinotarsa decemlineata*) (Baum et al., 2007; Finbow and Harrison, 1997; Upadhyay et al., 2011; Whyard et al., 2009; Zhu et al., 2011). These studies established the essential role of *VATPase*, demonstrating that effective silencing of its expression leads to significant and measurable reduction of fitness across arthropod species. In addition, these studies showed that orally-delivered dsRNA against *VATPase* induces RNAi. Finally, *TuVATPase* has already been shown to

yield modest but significant mite mortality when silenced in *T. urticae* though the leaf floating method (Kwon et al., 2013).

Here I show that the application of dsRNA against *TuVATPase* by soaking resulted in the phenotypic change of mite body color correlated with gene downregulation and the reduction of mite fitness: survivorship and fecundity. However, these phenotypic changes occurred only in a subset of treated mite populations. The data suggested that variability in RNAi response were not due to the genetic background from heterogeneous mite population but were related to the intrinsic property of the soaking method. Overall, data gathered in this study show the potential towards the development of reverse genetic platforms applicable as high-throughput screens.

## 3.2 Materials and Methods

### 3.2.1 *T. urticae* rearing conditions

The stock population of *T. urticae* referred as London strain originated from the Vineland region in Ontario. The London population were maintained on California red kidney beans (*Phaseolus vulgaris* L., Stokes, Thorol, ON) grown in soil (PRO-MIX<sup>®</sup> BX MYCORRHIZAE<sup>™</sup>; Premier Tech, Rivière-du-Loup, QC), in a climate controlled chamber at light/dark photoperiod of 16/8 h, 26°C with relative humidity of 50%.

### 3.2.2 Preparation of developmentally synchronized mites

Adult female mites were allowed to lay eggs for 24 h on a fresh detached bean leaf at light/dark 16/8 h, 26°C, and 50% relative humidity (RH). After 24 h, the adult females were removed and 1-day-old eggs were allowed to develop until female mites became teleiochrysalis (7-8 days). Teleiochrysalis were collected and incubated at 18°C and 100% RH for 24 h, after which they were returned to 26°C and 50% RH environment. Adult female mites, emerged within 3 hours upon transfer to a 50% RH environment and were collected for experimentation.

### 3.2.3 dsRNA fragments

In this study 2 different dsRNA were used targeting the *TuVATPase* transcript to ensure the reproducibility and the specificity of the RNAi phenotype. Fragments corresponding to the region of *TuVATPase*, referred to as fragment A (an upstream fragment of 214 bp within the 3<sup>rd</sup> exon of the *TuVATPase* locus) and fragment B (a 416 bp fragment within the 4<sup>th</sup> exon) were chosen as templates for the preparation of dsRNA. In addition, a 382 bp intergenic fragment spanning the region 1690614-1690995 of the genomic scaffold 12 (Figure 3.1) was chosen as the template for the preparation of a negative control dsRNA, referred to as NC. A BLAST search against the *T. urticae* genome and transcriptome database confirmed that the 382 bp intergenic sequence is unique and not transcribed.

### 3.2.4 dsRNA preparation for *TuVATPase*

The nucleotide sequence of *TuVATPase* (tetur09g04140), and intergenic region (negative control (NC), genomic coordinates: scaffold 12, position 1690614 – 1690995) were obtained from the ORCAE database. Total RNA was extracted from the frozen mite females with the RNeasy Mini Kit (Qiagen, Valencia, CA) and cDNA was synthesized from 3 µg of the extracted total RNA with the SuperScript II cDNA Synthesis Kit (Thermo Fisher Scientific, Waltham, MA) and stored at -20°C. Fragments (A and B) of *TuVATPase* and a control sequence (NC) targeting a intergenic region were PCR amplified with primers shown in Table 3.1, using cDNA and genomic DNA as templates respectively, with Phusion DNA polymerase (NEB, New England Biolabs, UK). Amplified DNA fragments were purified with the Gel/PCR DNA Fragments Extraction Kit (Geneaid Biotech, New Taipei, Taiwan). Purified fragments were cloned in pLITMUS 38i vector (NEB, New England Biolabs, UK) containing T7 polymerase promoter sequence flanking multiple cloning sites to streamline dsRNA production. Inserts selected for the synthesis of dsRNA were re-sequenced to confirm their identity. RNA fragments were synthesized using 1 µg of DNA template with the TranscriptAid T7 High Yiled Transcription Kit (Thermo Fisher Scientific) in 1.5-ml centrifuge tubes, denaturated at 95°C for 5 min, followed by slow cool-down to room temperature to facilitate formation of dsRNA. dsRNA was purified by phenol-chloroform extraction

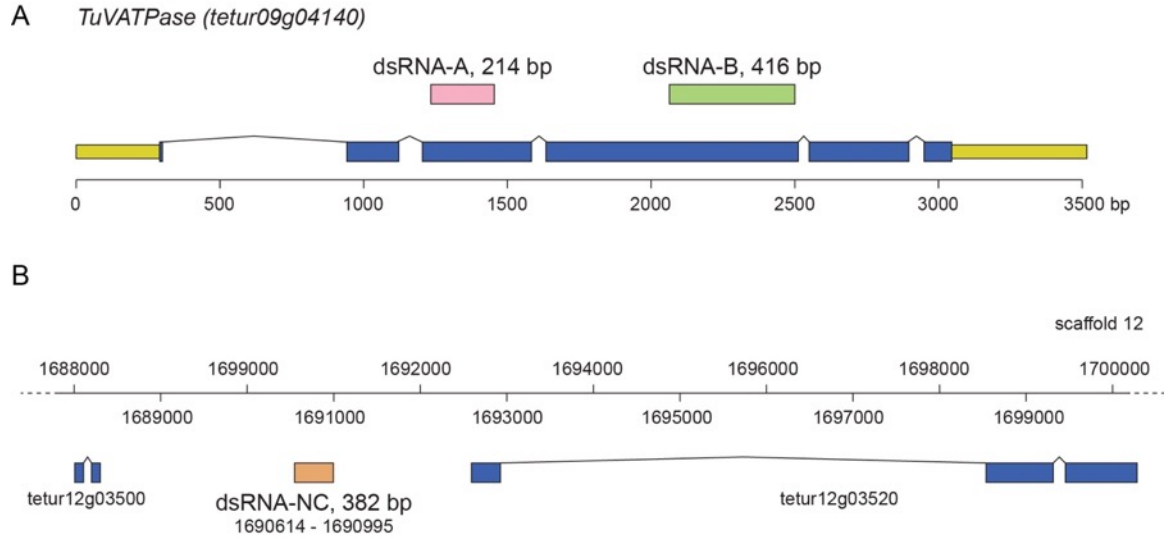


**Figure 3.1: Fragment used for the synthesis of dsRNAs.** Schematic of *TuVATPase* locus (A). DNA sequences used for the generation of dsRNA-*TuVATPase* are located in the 3<sup>rd</sup> exon, fragment A (214bp), and in the 4<sup>th</sup> exon, fragment B (416bp). UTR and coding sequences are shown in yellow and blue, respectively. Schematic of the part of scaffold 12 of *T. urticae* genome (B) depicting the location of the 382 bp fragment that was used to synthesized dsRNA-NC.

**Table 3.1: Primers used in this study.**

## Cloning primers

Primer names	Oligonucleotide sequence (5' to 3')	Fragment names (bp)
Tetur-VATP-F-A	CAGTTCTCCGAACCGGTA	A (214)
Tetur-VATP-R-A	CCACCGGTAATGTGACTACCA	
Tetur-VATP-F-B	CCGTGATATGGGTTACCATG	B (416)
Tetur-VATP-R-B	GAAGAGGTACGAAATCTGGG	
Tetur-sc12-F	GCCCTCTCCTGGTTGTAACTT	Control, NC (382)
Tetur-sc12-R	CGACCCCATCAGGCTATTGA	

## Spider mite RT-qPCR assay primers

Primer names	Oligonucleotide sequence (5' to 3')	Primer efficiency
RP49 (tetur18g03590) F	CTTCAAGCGGCA TCAGAGC	97.6%
RP49 (tetur18g03590) R	CGCA TCTGACCCTTGA	
VATPase qPCR F	GGGTACCATCACATTCCTCG	104.1%



followed by ethanol precipitation. dsRNA was dissolved in nuclease free water and quantified using NanoDrop (Thermo Fisher Scientific, Waltham, MA).

### 3.2.5 Soaking mites in solution of dsRNA

About 50 newly-emerged adult females were soaked in 50  $\mu\text{L}$  of dsRNA solution (160  $\text{ng}/\mu\text{L}$ ; 0.1% v/v Tween 20) respectively and incubated at 20°C for 24 hours according to Suzuki et al., 2017. After soaking, mites were transferred onto fresh bean leaf discs (10-mm diameter with 1 female per disc) placed on water-soaked cotton on the cup with a polyethylene lid with 4 venting holes each covered with a gas-permeable filter (0.45 micron pore size; Milliseal; Millipore, Billerica, MA), and incubated at light/dark 16/8 h, 26°C, and 50% RH. Survival of adult females were recorded over 10 days. The biological assays were conducted in 3 independent experimental runs. For RT-qPCR analysis, the adults were collected into 1.5-mL tube with at least 30 adults per tube at 5 days after 24 hours soaking. The collected samples were frozen in liquid nitrogen and stored at -80°C until RNA extraction. The collection and the RT-qPCR analysis were conducted in 3 independent experimental runs.

### 3.2.6 Analysis of RNAi efficiency in inbred lines

Newly-emerged adult females from thirteen inbred lines generated from the reference London population were soaked in 1.5-mL tube (60-80 adults per tube) with 50  $\mu\text{L}$  of dsRNA solution (160  $\text{ng}/\mu\text{L}$ ; 0.1% v/v Tween 20). Adult females soaked in the dsRNA solution were incubated at 20°C in a water bath for 24 hours. After soaking, mites were washed in 100  $\mu\text{L}$  of double distilled water and transferred onto a bean leaf that was placed on top of water-soaked cotton in a cup with a vented lid, and incubated at light/dark 16/8 h, 26°C, and 50% RH. After 5 days, mites with dark and normal body color were evaluated for mortality; surviving mites from each phenotypic group were separated and placed on new fresh bean leaves. After 3 additional days, the fecundity from each group was evaluated. Each experimental run was performed with 4 replicates and the reference London population was used as a positive control.

### 3.2.7 RT-qPCR

Mite total RNA was extracted with the RNAeasy Kit including a DNase treatment (Qiagen). Two micrograms of total RNA was reverse transcribed with the Maxima First Strand cDNA Synthesis Kit for RT-qPCR (Thermo Fisher Scientific). qPCR reactions were performed in 3 technical replicates for each sample with the Maxima SYBR Green/ROX qPCR Master Mix (Thermo Fisher Scientific). The RT-qPCR was performed on an Agilent Mx3005P qPCR instrument (Agilent Technologies, Santa Clara, CA). The reference gene was *RP49* (tetur18g03590) coding for a ribosomal protein. Primer sequences and amplification efficiencies (E) are listed in Table 3.1. Cycle Threshold (Ct) values from 3 technical replicates were averaged to calculate the Ct value of each independent experimental run. For plotting, expression value for each target gene (T) was normalized to the reference gene (R) and normalized relative quantity (NRQ) was calculated as follows:  $NRQ = (1+E_R)^{CtR}/(1+E_T)^{CtT}$ . NRQ values were then normalized to a mean of those control and treatments were analyzed with the Dunnett's test (function `glht`, R package `multcomp`) in the R 3.2.5 software (R Core Team 2016).

### 3.2.8 Data analysis of survival and fecundity

Survival curves were calculated with the Kaplan-Meier method (function `survfit`, R package `survival`) with comparisons performed based on the log-rank test (function `survdiff`, R package `survival`). Results for the fecundity are display as box-plots where central lines (second quartile, Q2) indicate the median of data, the distance between the box bottom (first quartile, Q1) and top (third quartile, Q3) indicate interquartile ranges (IQRs), and the whisker bottom and top indicate the minimum and maximum of data (except outliers that are outside the range between the lower ( $Q1-1.5 \times IQR$ ) and upper limits ( $Q3+1.5 \times IQR$ ) that are plotted as a white circle). Significant differences in the median developmental time and the median number of eggs laid between the control and other treatments were analyzed with the Wilcoxon-Mann-Whitney test (function `wilcox.exact`, R package `exactRankTests`). A significant difference in the proportion of color phenotype (normal or dark-body) was analyzed with the Fisher's exact test (Function `fisher.test`). For multiple comparisons based on the paired tests, the level of significance ( $\alpha$ ) was adjusted with the Bonferroni correction ( $\alpha/K$ , where  $K$  is the

number of pairs in the multiple comparison). Analysis was performed with the R 3.2.5 software (R Core Team 2016).

### 3.2.9 Data analysis of *TuVATPase* RNAi effect on inbred lines

RNAi was induced by soaking newly-emerged adult females. Number of alive and dead individuals, and phenotype (normal or dark-body) was assessed 5 days post soaking. Fecundity or surviving females was assessed over 3 days (days 5-8 after soaking). To build the heatmap, dead/alive and normal/dark-body counts were converted to proportion of total mites recovered after soaking procedure and hierarchical clustering analysis was performed based on Euclidian distance and with the average clustering method. Fecundity data were scaled to the 0-1 range and the heatmap was organized according to survival and phenotype clusters. The Wilcoxon-Mann-Whitney test was applied to analyze the differences in mortality and normalized fecundity between phenotype and treatment classes. *P*-values were adjusted for multiple testing with Bonferroni correction and  $K=9$ . Analysis was performed with the R 3.2.5 software (R Core Team 2016).

### 3.2.10 Imaging

All images were taken using a stereomicroscope Leica MZ FLIII (© Leica Microsystems, Wetzlar, Germany) fitted with the Canon EOS Rebel T5i camera (Canon, Japan).

## 3.3 Results

### 3.3.1 Induction of RNAi in soaked mites

To test the RNAi soaking method, newly-molted adults (Figure 3.2Ai) were synchronized and soaked in solution of dsRNA against *VATPase* and compared with the ones that were soaked in solution of dsRNA targeting the intergenic region, used as a negative control. The rationale for the fragment selection is stated in the methods section. Treated mites were divided in three phenotypic classes. One day post soaking, about 15% and 25% of mites displayed a white phenotype (Figure 3.2Aii), while the rest of the mites had the normal phenotype characterized by the two-spots on the back as shown in Figure 3.2Aiii. This white phenotype occurred after soaking adult females with either dsRNA-*TuVATPase*-B or dsRNA-NC respectively (Figure 3.2D), and resembled the phenotype of

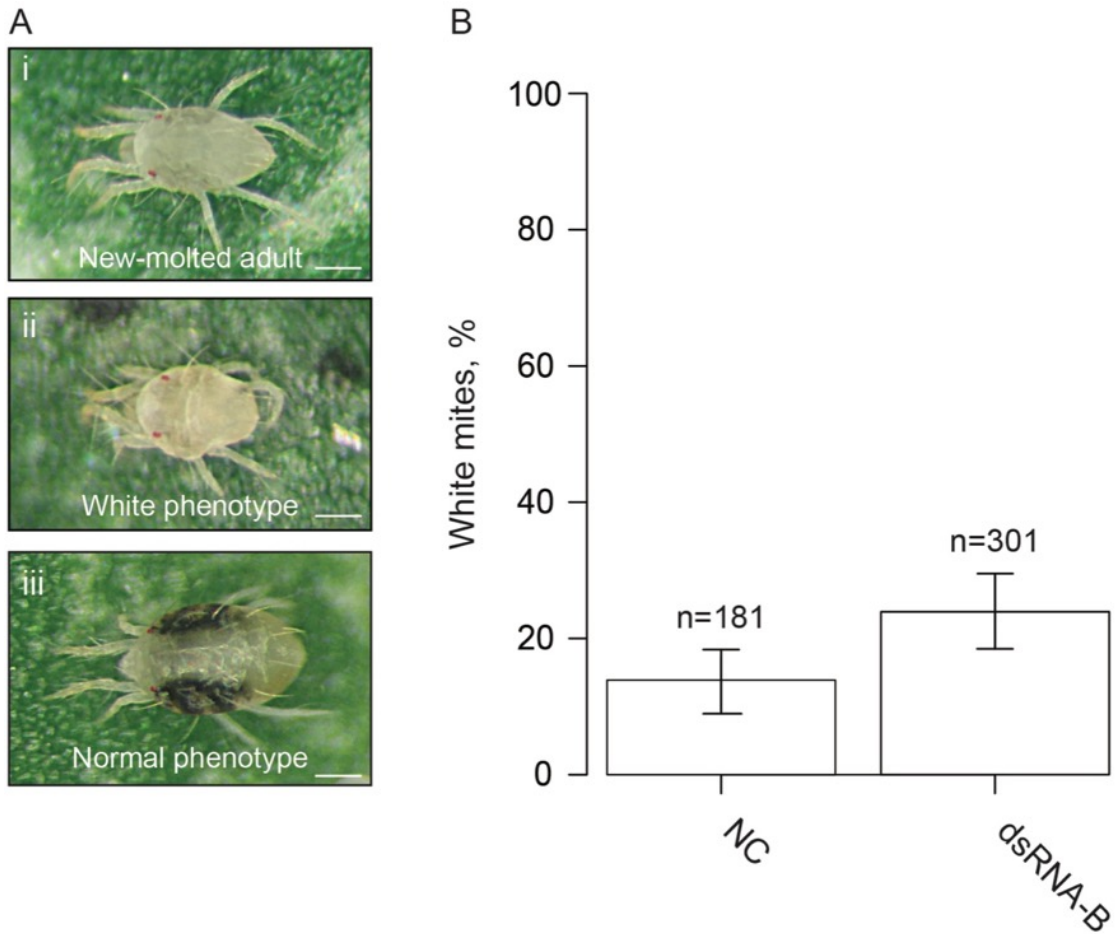


**Figure 3.2: White phenotype associated with soaking in solution of dsRNA.** Representative picture of a newly-molted adult (Ai) recovering on the leaf; a white phenotype (Aii) and a normal phenotype (Aiii). The bar graph represents the percentage of white mite when newly-molted adults were soaked in solution of dsRNA-NC and dsRNA-TuVATPase-B. (scale bar: 100  $\mu$ M).

of newly-molted adults. These mites do not feed and consequently they shrink and die. This phenotype was also observed when newly-molted adults were soaked in water, suggesting that such phenotype is a result of the stress from soaking rather than a response to dsRNA. Although these mites were not considered in the analysis in this study, it required an application of an increasing number of mites in order to keep the population size adequate.

About 5 days post-soaking, a change in body color could be observed as a portion of the mites turned dark (Figure 3.3Ai). The two distinctive spots visible in the back of the mite and characterizing a normal phenotype (Figure 3.3Bii) were not visible in mites with the dark phenotype (Figure 3.3Ai). Over 37% of the adults soaked in dsRNA-*TuVATPase-A* and 47% of adults soaked in dsRNA-*TuVATPase-B* displayed the dark-body phenotype. Mites that were soaked in the control dsRNA did not display such phenotype; instead all mites had a normal body coloration (Figure 3.3B). To test whether the dark-body phenotype correlates with RNAi responses, mites displaying dark and normal phenotypes were followed separately. Adult mites with normal body color phenotype (*normal* in Figure 3.4A and 3.4C) soaked in dsRNA-*TuVATPase-A* or dsRNA-*TuVATPase-B* had the same survivorship as mites soaked in the solution containing the control dsRNA-NC. Although mites with the dark-body phenotype (*dark* in Figure 3.4B and 3.4D) soaked with the dsRNA-*TuVATPase-A* fragment had a slightly lower survival than the control, the difference was not significant. However, mites with the dark-body phenotype soaked with the dsRNA-*TuVATPase-B* fragment had a significantly lower survival than the control (Figure 3.4D). The fecundity was significantly affected by mite soaking in solution containing the dsRNA-*TuVATPase* (Figure 3.5A) and was more prominently reduced in mites with dark than with normal body color.

To further confirm that the dark phenotype was associated with a RNAi response, I analyzed changes in target gene expression levels. I extracted RNA from dark and normal mites after 5 days post soaking and checked *TuVATPase* gene expression using RT-qPCR. The endogenous *TuVATPase* transcripts were significantly reduced in the dsRNA-*TuVATPase* treated mites. Moreover, the severity of the RNAi phenotypes correlated

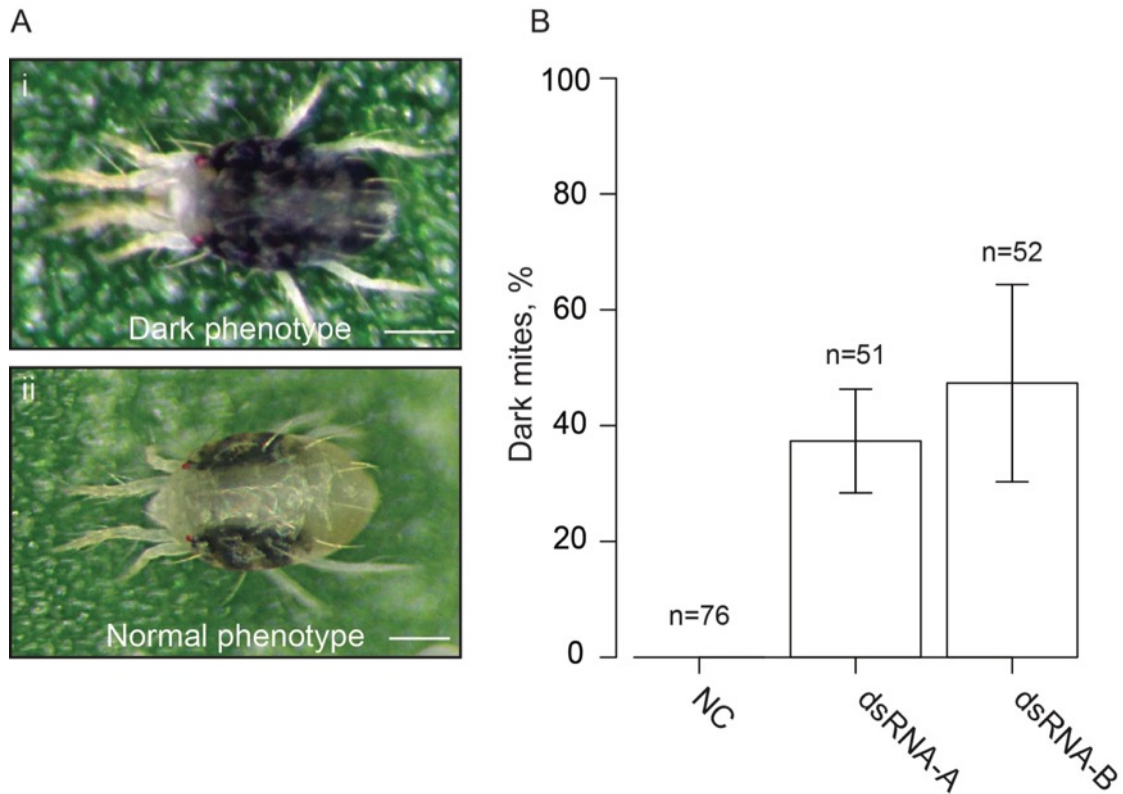


**Figure 3.3: Dark phenotype associated with RNAi response to dsRNA.** Dark-body (Ai) and normal phenotype (Aii) female mites and frequency of phenotypes observed after application of dsRNA-*TuVATPase-A*, dsRNA-*TuVATPase-B* or dsRNA-NC through soaking. The bar graph represents dark-body mite frequencies collected from 3 independent experimental runs (B). (Scale bars: 100 $\mu$ m).

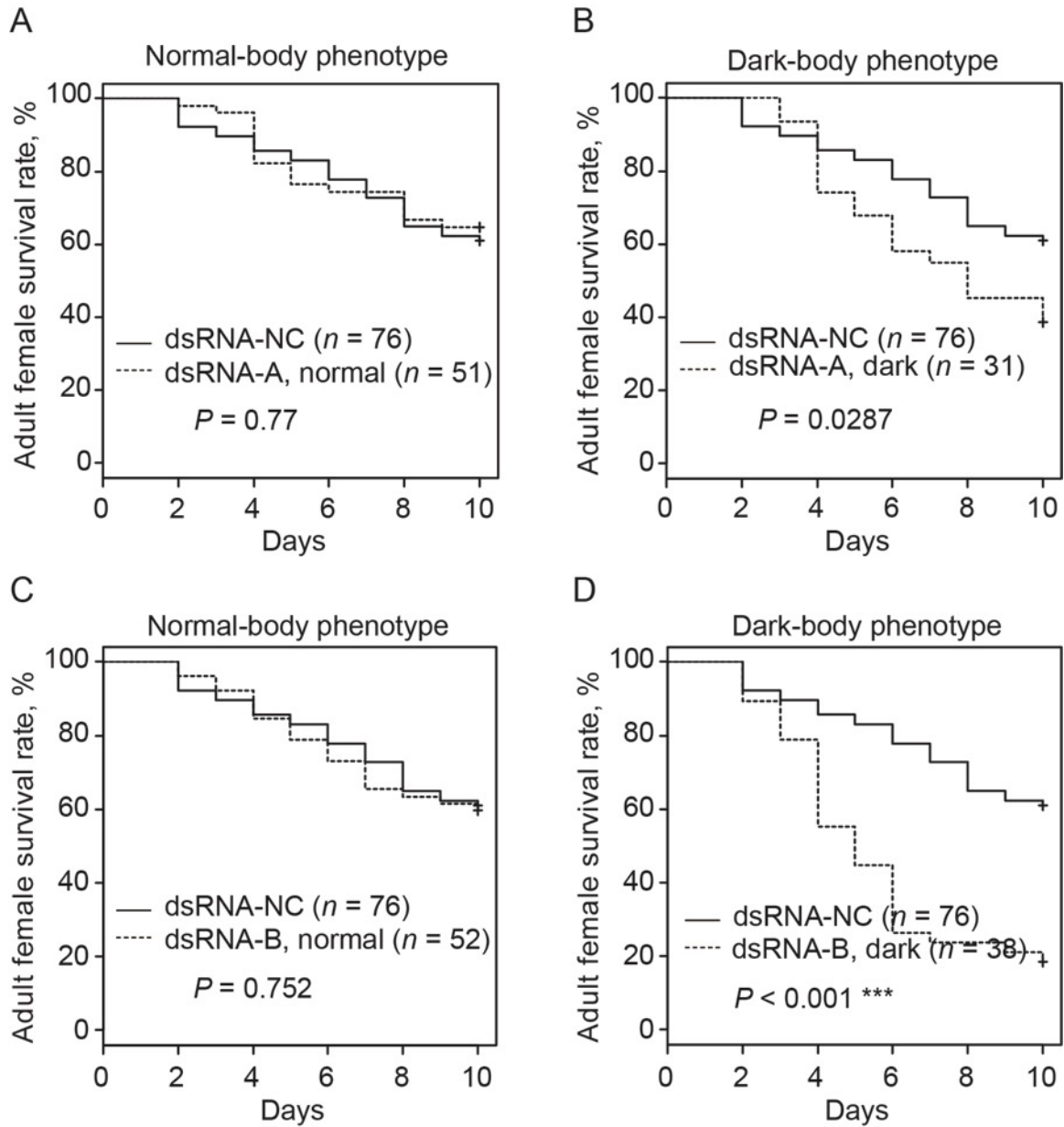


**Figure 3.4: Adult survivorship after soaking treatment in solution of dsRNA-*TuVATPase* separately for normal and dark-body mites.** Survivorship of adult female with normal phenotype (A) and dark phenotype (B) after treatment with dsRNA-*TuVATPase*-A (solid line) or dsRNA-NC (dashed line). Survivorship of adult female with normal phenotype (C) and dark phenotype (D) after treatment with dsRNA-*TuVATPase*-B (solid line) or dsRNA-NC (dashed line). Survival curves were plotted using Kaplan-Meier method and compared using the log-rank test with Bonferroni correction (no asterisk,  $P > 0.05$ ; \*\*\*,  $P < 0.001$ ).

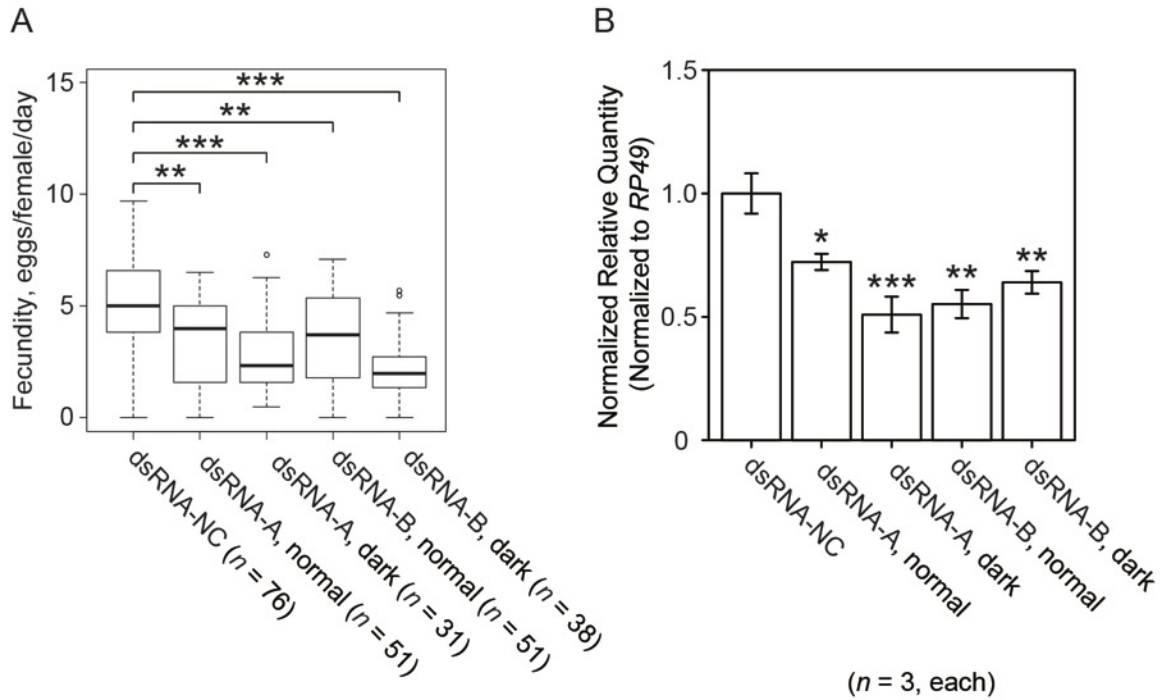


**Figure 3.5: Adult mite fecundity and *TuVATPase* gene expression after soaking treatment in solution of dsRNA-*TuVATPase*.** (A) Normal and dark-body mite fecundity after soaking in solution of dsRNA-*TuVATPase*-A, dsRNA-*TuVATPase*-B or dsRNA-NC. Data were collected from 3 independent experimental runs and were compared using Wilcoxon-Man-Whitney test with Bonferroni correction (\*\*,  $P < 0.01/4$ ; \*\*\*,  $P < 0.001/4$ ). (B) *TuVATPase* gene expression relative to the expression of *RP49* reference gene in normal and dark-body female mites. Data were represented as mean $\pm$ SE and analysed using Dunnett's test relative to dsRNA-NC treatment (\*, corrected  $P < 0.05$ ; \*\*,  $P < 0.01$ ; \*\*\*,  $P < 0.001$ ).



with the residual levels of the endogenous *TuVATPase* only in the treatment with one of the dsRNA fragments, the dsRNA-*TuVATPase-A* (Figure 3.5B). These results hinted that *TuVATPase*-dsRNA in soaking solution is 1) absorbed by the mite and 2) is able to trigger RNAi response resulting in the phenotypic change of mite body color correlated with reduced mite fitness.

### 3.3.2 Differential RNAi response in *T. urticae* inbred lines

Given that changes in body color occurred only in mites treated with dsRNA-*TuVATPase* and not when mites were soaked in the solution containing the control dsRNA-NC fragment, the observed phenotype is not a general response to dsRNA, but a specific response to the RNA interference with *TuVATPase* expression. These assays involved adults that were tightly synchronized in their development (within a 3 hours' interval) originating from the London mite population whose genetic variability is narrow. Nevertheless, the strong RNAi effects (characterized by dark-body color, significant increase of mortality and reduced fecundity) were observed only in a portion of treated mites. When mites were soaked in the solution of dsRNA-*TuVATPase*, around 50% of adults showed the strong RNAi effects despite well controlled age and uniform manipulations. This partial penetrance of the RNAi-induced phenotypes may be due to the biology of the mite or a heterogeneous genetic background in the London mite population. To test the genetic contribution to the observed variability of RNAi responses, I analyzed them in thirteen inbred lines (inbred lines were derived from the London population through 6 generations of mother-son matings. Given the high number of mites to be soaked, the thirteen inbred lines were divided into 8 batches with one or two inbred lines soaked at a time along with the London reference population, which was used as a positive control. For this assay only dsRNA-*TuVATPase-B* was used as RNAi response from fragment B was greater than the fragment A. For each inbred line, newly-emerged adult female mites were soaked in a solution containing either the dsRNA-*TuVATPase-B* or dsRNA-NC fragment. Mites with a normal or dark-body phenotype were then counted and the fitness (mortality and fecundity) of both classes was measured separately. When genotype/dsRNA combinations were clustered according to

Heatmap of scaled mite counts and normalized fecundity.

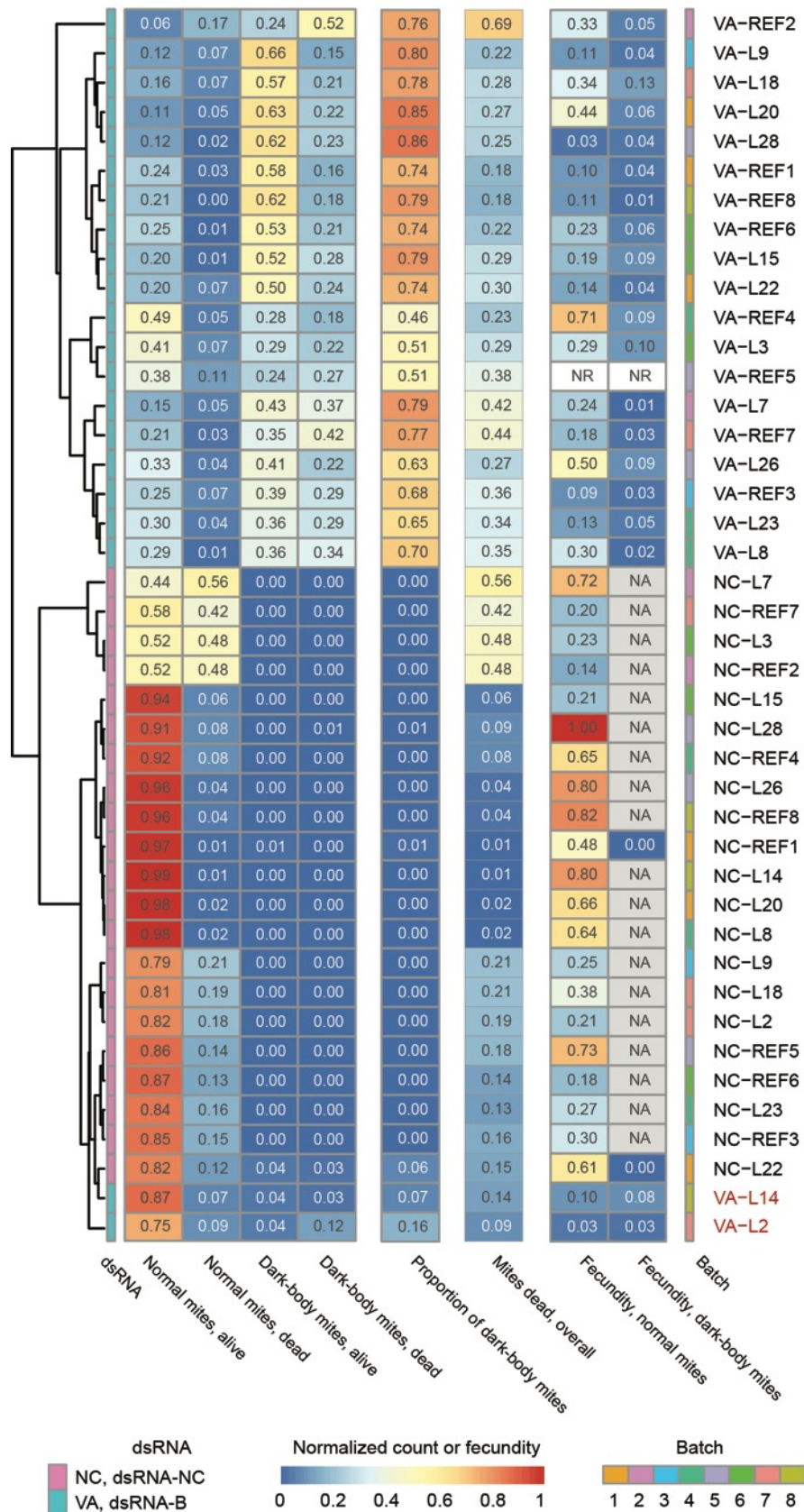


**Figure 3.6: RNAi response in soaked *T. urticae* inbred lines.** Experimental combinations of 14 mite group (13 inbred lines and the reference population) with 2 dsRNA (dsRNA-*TuVATPase-B* (label VA) and dsRNA-NC control (label NC) were classified using hierarchical average clustering and Euclidian distance based on normalized survivorship (dead/alive counts) and body color (proportion of dark mites). The mite/dsRNA combinations were tested in 8 experimental batches (indicated by colors at the right side of the panel) and analyzed together. Each run included a sample of the London reference population (label REF) and 1 or 2 inbred line samples (Label L). Normalized fecundity over 3 days and total proportion of dark mites are shown in the same order as dead/alive counts but were not taken in account for clustering. In most dsRNA-NC control treatments dark-body mites were not present and their fecundity could not be measured (not applicable, NA). Fecundity for VA-REF5 samples was not recorded (NR) due to technical issue. Data were collected from 4 independent experimental runs in 8 batches. All measurement are expressed as ratios relative to the total number of tested mites and represented accordingly to the heatmap color code (bottom). Data from 8 experimental batches was analyzed together and separated at the level of mite line type (REF and L), treatment (NC and VA), and phenotype (normal and dark-body) classes. As in most dsRNA-NC control treatments dark-body mites were not present their mortality and fecundity could not be measured (not applicable, NA). All *P*-values shown are corrected for multiple comparisons.

survivorship and body color, the highest-level clusters clearly portioned treatments with dsRNA-*TuVATPase*-B (top) and the control dsRNA-NC (bottom) (Figure 3.6). Within these 2 major groups, mite genotypes (London population and inbred lines) were intermixed and their performance values were similar, indicating that inbred lines reconstituted genetic variability existing in the London population. The RNAi response triggered by dsRNA-*TuVATPase*-B was characterized by dark mites that invariably had higher mortality (Figure 3.7) and lower fecundity (Figure 3.8) relative to control or normal mites within the same population, further strengthening the link between the silencing of the *TuVATPase* gene with the body color phenotype and performance parameters. However, mites with a normal body color treated with dsRNA-*TuVATPase*-B also displayed an effect of the RNAi, albeit at reduced level. The mortality of normal mites treated with dsRNA-*TuVATPase*-B is indistinguishable from the control population (Figure 3.7), however, their fecundity is significantly reduced (Figure 3.8). Thus, mite populations treated with the dsRNA-*TuVATPase*-B partition in 2 phenotypic classes (dark and normal body color) that differ in the quantitative severity of the RNAi effects. None of the dsRNA-*TuVATPase*-B treated population (either inbred lines or London reference population), displayed 100% of dark mites. Moreover, the percentage of dark mites was not significantly different between inbred lines and the reference London population (Figure 3.9), indicating that the high RNAi efficiency is not completely penetrant and that the variability is intrinsic to the treatment. Two inbred lines (L2 and L14) were peculiar outliers that clustered with the control dsRNA-NC treatments (Figure 3.10) displaying a low percentage of dark mites, 16% and 7% respectively. However, despite a normal color phenotype, these mite lines had similar mortality and fecundity as other inbred lines and London population, indicating that they respond to RNAi but seemingly lack the ability to display a dark-body phenotype.

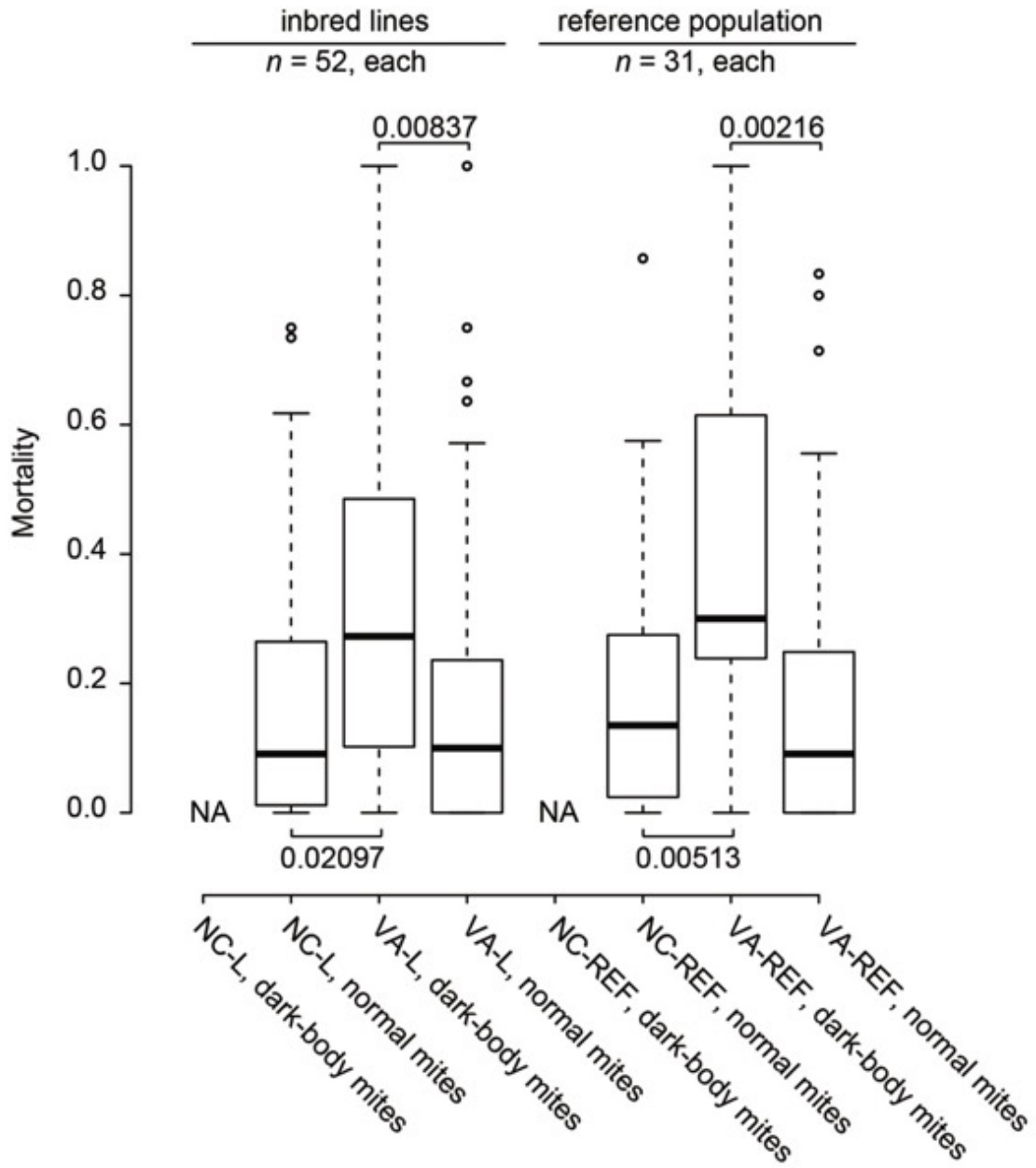


**Figure 3.7: Inbred line mortality after treatment with dsRNA-*TuVATPase*.** Normal and dark-body mite mortality (proportion of dead mites) in inbred lines (label L) and the reference population (label REF) treated with 2 dsRNA dsRNA-*TuVATPase*-B (label VA) and dsRNA-NC control (label NC).

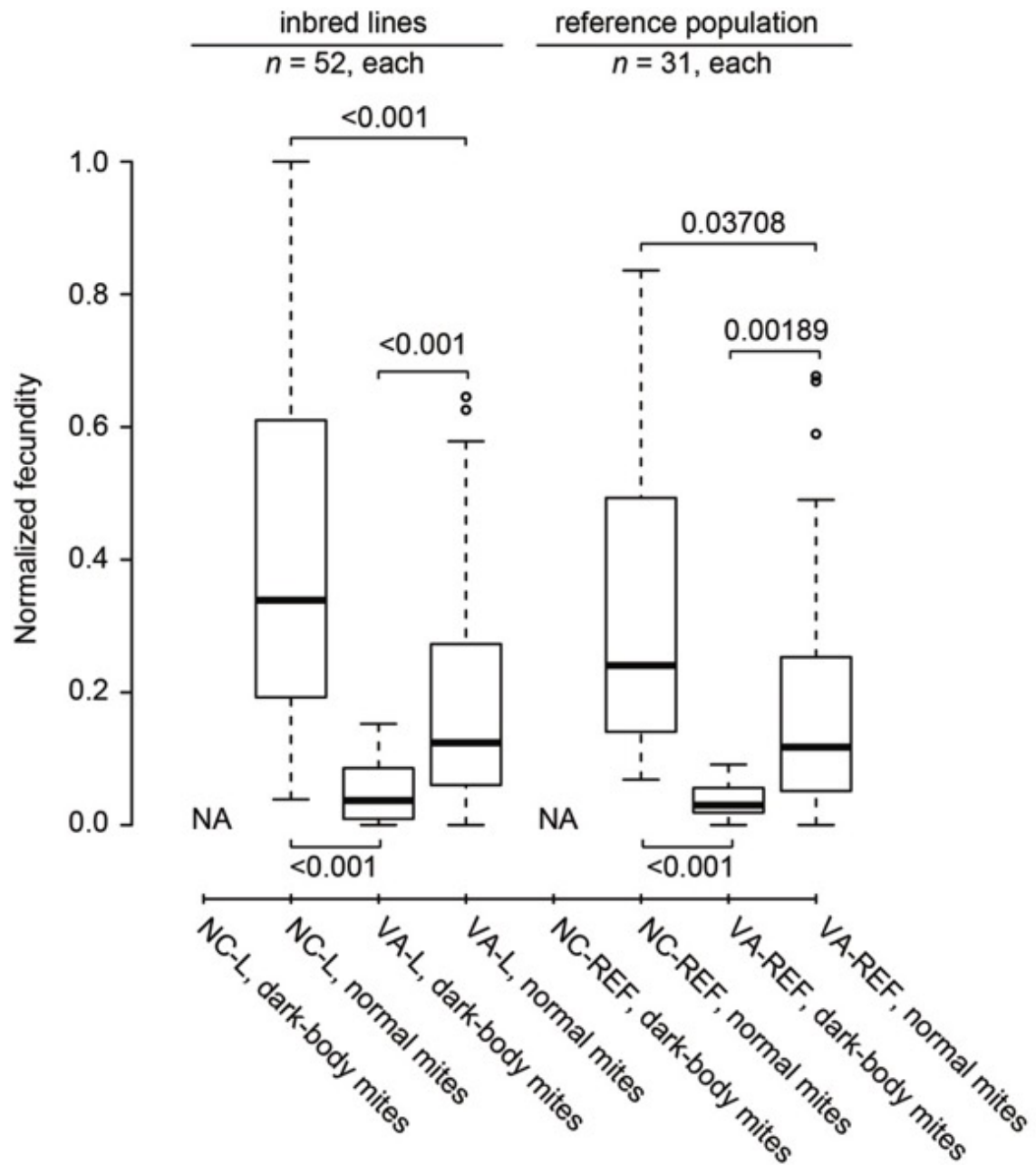


**Figure 3.8: Inbred line fecundity after treatment with dsRNA-*TuVATPase*.** Normal and dark body mite fecundity in inbred line and the reference population treated with dsRNA-*TuVATPase*-B (label VA) and dsRNA-NC control (label NC).

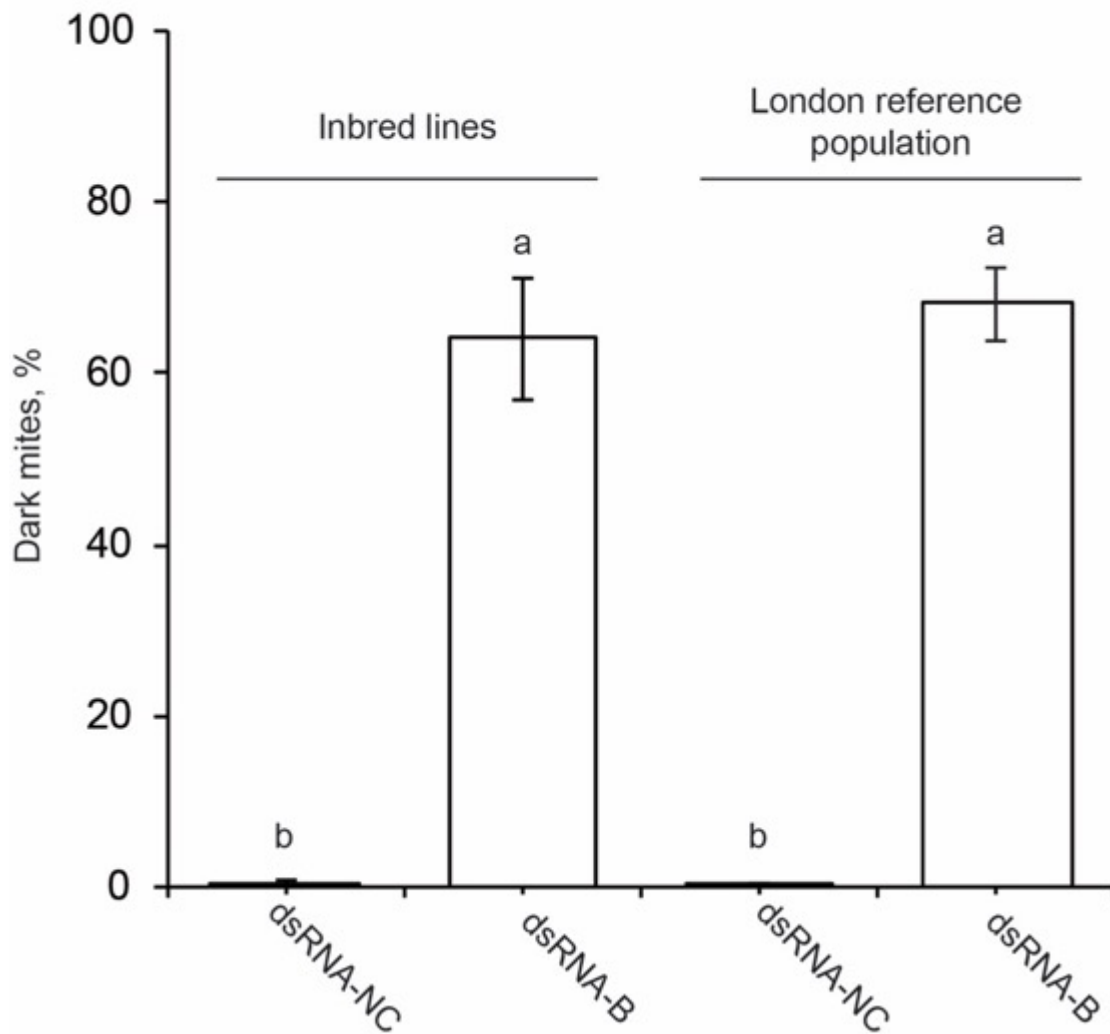


**Figure 3.9: Dark mite frequency in the inbred lines and London reference population after treatment with dsRNA.** Bar graph representing the percentage of dark phenotype from inbred lines and London reference population after treatment with dsRNA-NC and dsRNA-*TuVATPase-B*. Each bar represents the mean  $\pm$  SE from inbred lines (n=13) or London reference population (n=8) including 4 replicate from each line. Mean followed by the same letter are not significant different, (P=0.05).

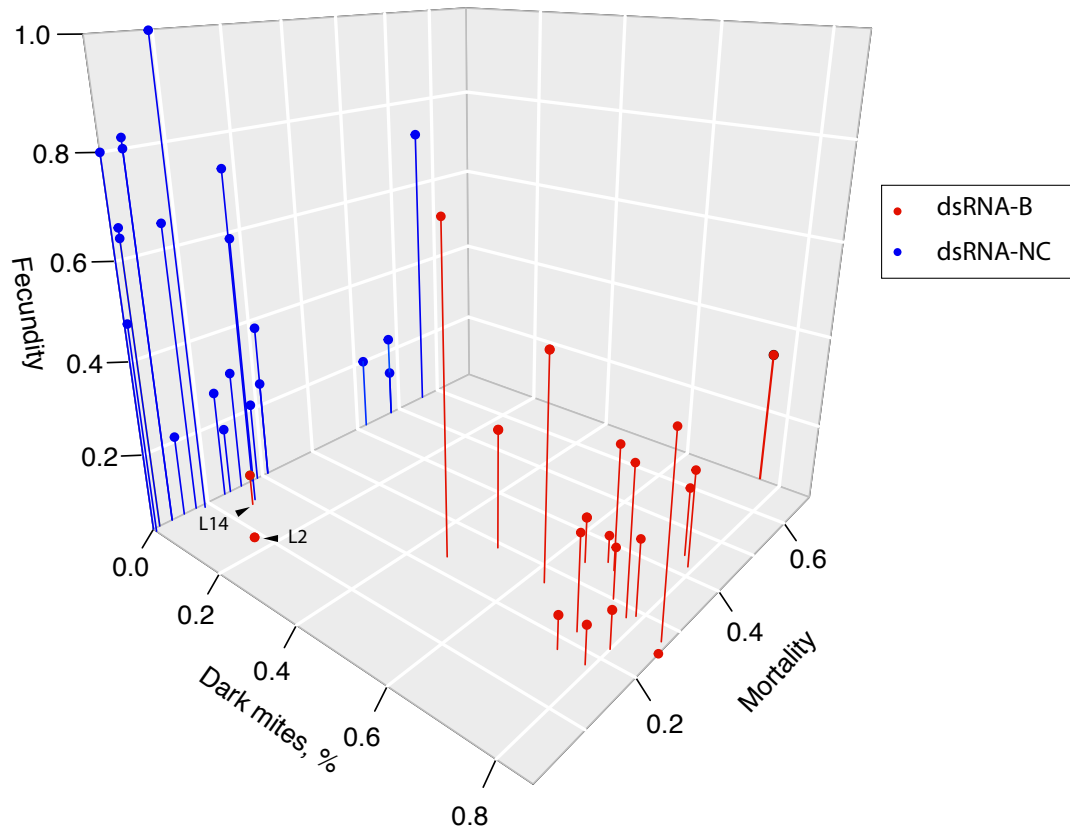


**Figure 3.10: Scatter 3D function displaying RNAi response parameter as a collection of points, plotted using three-dimensional Cartesian coordinates.** Scaled mite counts with the percentage of dark mites plotted on the x-axis and the mortality on the y-axis. Each bar represents normalized fecundity plotted on the z-axis. The red represents population treated with dsRNA-TuVATPase-B and the blue represents population treated with dsRNA-NC. Inbred lines L2 and L14 are shown with the black arrow.



### 3.4 Discussion

Even though *T. urticae* reverse genetics protocols describing the maternal injection and oral delivery of dsRNA have been published (Khila and Grbić, 2007; Kwon et al., 2013), they are not suitable for high throughput screens. The efficiency of the soaking method was compared to the floating leaf disc assay, with the same dsRNA-*TuVATPase* fragment at the same concentration as previously reported by Kwon et al., (2013). Several mite fitness parameters, adult survivorship, fecundity and the endogenous targeted transcript levels were measured to determine RNAi efficiency. Soaking adult *T. urticae* females in the solution of dsRNA-*TuVATPase* resulted in a reduction of mite survivorship, fecundity and target gene expression. Similar dsRNA-*TuVATPase* silencing phenotypes have been described across multiple experimental systems, e.g. whiteflies, western corn rootworms, western flower thrips, Colorado potato beetles, fruit flies, flour beetles, pea aphids, and tobacco hornworms (Badillo-Vargas et al., 2015; Baum et al., 2007; Finbow and Harrison, 1997; Thakur et al., 2014; Whyard et al., 2009; Zhu et al., 2011) confirming the essential role of the VATPase pump in proton transport across cellular membranes of eukaryotic organisms. However, in addition to these phenotypes, and unique to this study, the silencing of *TuVATPase* resulted in a dark-body phenotype (Figure 3.3Ai). The effect of dsRNA-*TuVATPase* on body pigmentation is not understood and may reflect distinctive features of mite physiology. It may also be a more general phenomenon that is only now observed in mites because they have semitransparent integument. In this study, the dark-body phenotype tightly correlated with dsRNA-*VATPase* treatment and high RNAi effectiveness (Figure 3.4 and 3.6). However, it could also be observed in aging mites in untreated mite population (note that adult mites used in our study were newly molted adult female). Thus, the dark-body phenotype is not specific to the disruption of the *TuVATPase* gene function, but may reflect mite body color change that associates with the stress that can be induced in multiple independent ways. Unlike the dark phenotype associated with dsRNA response, the white mites were not able to recover from the soaking treatment which can be due to the stress from immersion. After soaking, once newly-molted adults recover on the leaf, they start to feed and increase their body size by almost 1.5 time, with the two distinctive spots becoming apparent the following

day. In contrast to the dark mites that undergo the same recovering process until they turn dark about 4 to 5 days post soaking, the white mite seems not capable of feeding.

In this study, only a portion of mites treated with the dsRNA-*TuVATPase*-B fragment developed a dark body phenotype (Figure 3.3 and 3.6). The incomplete phenotypic penetrance is likely due to the differential ability to: 1) deliver dsRNA into a portion of the treated mites, or 2) to silence the target gene. In a previous study, dsRNA and siRNA designed to silence *Tu-DLL*, shown efficient RNA uptake with 50% and 60% of the total mites treated displaying downregulation, respectively. However, RNAi phenotype associated with truncated appendages was shown in only 33% of mite embryos that received the siRNA (Khila and Grbić, 2007). The partial RNAi efficiency was again observed in this study despite the homogeneity of mite genotype (inbred lines) and the tight synchronization of mite development in the experimental population (Figure 3.6). The instability of dsRNA due to the presence of nucleases has been shown to affect RNAi in several experimental systems (Garbutt et al., 2013; Kennedy et al., 2004; Wang et al., 2016). In addition, the sequence variability of gene regions targeted for interference and differential physiological backgrounds have been postulated as factors that affects RNAi efficiency (Chu et al., 2014). Further studies will be required to understand the source of partial and variable RNAi efficiency in spider mites.

This study further highlighted the ability of genetic component(s) to modulate RNAi-induced responses in mites. Two out of 13 inbred lines soaked in the solution containing dsRNA-*TuVATPase*-B did not develop the dark-body phenotype (Figure 3.9). However, the fecundity of these mites was significantly reduced relative to the dsRNA-NC treated controls (Figure 3.6 and 3.9), indicating effective RNAi despite the inability of these mites to develop a dark-body phenotype. The dark-body phenotype in dsRNA-*TuVATPase*-B responsive mite populations may be used as an easily scorable trait to compare factors such as RNA chemical modification, transfection reagents and carriers when optimizing dsRNA penetration into mites.

The analysis of the *T. urticae* genome sequence identified many genes that either belong to expanded known gene families or that are “orphan” genes, with no obvious

orthologues, often restricted to certain taxons (Grbić et al., 2011). Efficient reverse genetics platforms are urgently needed to study the biological and evolutionary role of these uncharacterized sequences. In this perspective, the soaking method presented here could be adapted for the application of dsRNA as a reverse-genetic tool for spider mites that will be an important asset for both fundamental and applied sciences. *T. urticae* is a pest with a staggering host range and one of the pest arthropod species that is most resistant to chemical pesticides (Migeon and Dorkeld, 2006; Whalon et al.). It is a prime model to study the evolution of host range, plant-herbivore interactions and mechanisms of xenobiotic resistance. RNAi itself, applied on fields or greenhouses, could prove to be a valuable and sustainable biotechnological approach for pest control (Kwon et al., 2016; Livak and Schmittgen, 2001; Upadhyay et al., 2011). For this approach, future investigations on design of dsRNA consisting of post-lethal sequences that are highly specific to the pest species and use of carriers for increasing stability of dsRNA will be needed.

### 3.5 Reference

- Badillo-Vargas, I. E., Rotenberg, D., Schneweis, B. A., and Whitfield, A. E. (2015). RNA interference tools for the western flower thrips, *Frankliniella occidentalis*. *J. Insect Physiol.* 76, 36–46.
- Baum, J. A., Bogaert, T., Clinton, W., Heck, G. R., Feldmann, P., Ilagan, O., et al. (2007). Control of coleopteran insect pests through RNA interference. *Nat Biotech* 25, 1322–1326.
- Brusca, R. C., and Brusca, G. J. (2003). Invertebrates. Sunderland, MA: Sinauer Associates.
- Bucher, G., Scholten, J., and Klingler, M. (2002). Parental RNAi in *Tribolium* (Coleoptera). *Curr. Biol.* 12, R85–R86.
- Chu, C.-C., Sun, W., Spencer, J. L., Pittendrigh, B. R., and Seufferheld, M. J. (2014). Differential effects of RNAi treatments on field populations of the western corn rootworm. *Pestic. Biochem. Physiol.* 110, 1–6.
- Cullen, L. M., and Arndt, G. M. (2005). Genome-wide screening for gene function using RNAi in mammalian cells. *Immunol Cell Biol* 83, 217–223.
- Dunlop, J. A. (2010). Geological history and phylogeny of Chelicerata. *Arthropod Struct. Dev.* 39, 124–142.
- Dunlop, J. A., and Alberti, G. (2008). The affinities of mites and ticks: A review. *J. Zool. Syst. Evol. Res.* 46, 1–18.
- Finbow, M. E., and Harrison, M. A. (1997). The vacuolar H<sup>+</sup>-ATPase: a universal proton pump of eukaryotes. *Biochem. J.*, 697–712.
- Garbutt, J. S., Bellés, X., Richards, E. H., and Reynolds, S. E. (2013). Persistence of double-stranded RNA in insect hemolymph as a potential determiner of RNA interference success: Evidence from *Manduca sexta* and *Blattella germanica*. *J. Insect Physiol.* 59, 171–178.
- Grbic, M., Khila, A., Lee, K.-Z., Bjelica, A., Grbic, V., Whistlecraft, J., et al. (2007). Mity model: *Tetranychus urticae*, a candidate for chelicerate model organism. *BioEssays.* 29, 489–496.
- Grbić, M., Van Leeuwen, T., Clark, R. M., Rombauts, S., Rouzé, P., Grbić, V., et al. (2011). The genome of *Tetranychus urticae* reveals herbivorous pest adaptations. *Nature.* 479, 487–492.
- Halliday, R., O'Connor, B., and Baker, A. (2000). “Global diversity of mites,” in *Nature and Human Society: The Quest for a Sustainable World*, eds. P. Raven and T. Williams (Washington DC: National Academy Press), 192–203.

- Kennedy, S., Wang, D., and Ruvkun, G. (2004). A conserved siRNA-degrading RNase negatively regulates RNA interference in *C. elegans*. *Nature*. 427, 645–649.
- Khila, A., and Grbić, M. (2007). Gene silencing in the spider mite *Tetranychus urticae*: dsRNA and siRNA parental silencing of the *Distal-less* gene. *Dev. Genes Evol.* 217, 241–251.
- Kuttenkeuler, D., and Boutros, M. (2004). Genome-wide RNAi as a route to gene function in *Drosophila*. *Brief. Funct. Genomics* 3, 168–176.
- Kwon, D. H., Park, J. H., Ashok, P. A., Lee, U., and Lee, S. H. (2016). Screening of target genes for RNAi in *Tetranychus urticae* and RNAi toxicity enhancement by chimeric genes. *Pestic. Biochem. Physiol.* 130, 1–7.
- Kwon, D. H., Park, J. H., and Lee, S. H. (2013). Screening of lethal genes for feeding RNAi by leaf disc-mediated systematic delivery of dsRNA in *Tetranychus urticae*. *Pestic. Biochem. Physiol.* 105, 69–75.
- Liu, P. Z., and Kaufman, T. C. (2005). *even-skipped* is not a pair-rule gene but has segmental and gap-like functions in *Oncopeltus fasciatus*, an intermediate germband insect. *Development* 132, 2081–2092.
- Livak, K. J., and Schmittgen, T. D. (2001). Analysis of relative gene expression data using real-time quantitative PCR and the  $2^{-\Delta\Delta CT}$  method. *Methods*. 25, 402–408.
- Maeda, I., Kohara, Y., Yamamoto, M., and Sugimoto, A. (2001). Large-scale analysis of gene function in *Caenorhabditis elegans* by high-throughput RNAi. *Curr. Biol.* 11, 171–176.
- Migeon, A., and Dorkeld, F. (2006-2014). Spider Mites Web: a comprehensive database for the Tetranychidae. Available online at: <http://www.montpellier.inra.fr/CBGP/spmweb>.
- Schmitt-Engel, C., Schultheis, D., Schwirz, J., Ströhlein, N., Troelenberg, N., Majumdar, U., et al. (2015). The iBeetle large-scale RNAi screen reveals gene functions for insect development and physiology. 6, 7822.
- Tabara, H., Grishok, A., and Mello, C. C. (1998). RNAi in *C. elegans*: Soaking in the Genome Sequence. *Science*. 282, 430–431.
- Thakur, N., Upadhyay, S. K., Verma, P. C., Chandrashekar, K., Tuli, R., and Singh, P. K. (2014). Enhanced whitefly resistance in transgenic tobacco plants expressing double stranded RNA of *v-ATPase A* Gene. *PLoS One*. 9, e87235.
- Upadhyay, S. K., Chandrashekar, K., Thakur, N., Verma, P. C., Borgio, J. F., Singh, P. K., et al. (2011). RNA interference for the control of whiteflies (*Bemisia tabaci*) by oral route. *J. Biosci.* 36, 153–161.

- Wang, K., Peng, Y., Pu, J., Fu, W., Wang, J., and Han, Z. (2016). Variation in RNAi efficacy among insect species is attributable to dsRNA degradation *in vivo*. *Insect Biochem. Mol. Biol.* 77, 1–9.
- Whalon, M. E., Mota-Sanchez, D., and Hollingworth, R. (2016). Arthropod Pesticide Resistance Database, Michigan State University. Available at: <http://www.pesticideresistance.org/index.php>.
- Whyard, S., Singh, A. D., and Wong, S. (2009). Ingested double-stranded RNAs can act as species-specific insecticides. *Insect Biochem Mol Biol.* 39, 824–842.
- Zhai, Z., Sooksa-nguan, T., and Vatamaniuk, O. K. (2009). Establishing RNA interference as a reverse-genetic approach for gene functional analysis in protoplasts. *Plant Physiol.* 149, 642–652.
- Zhu, F., Xu, J., Palli, R., Ferguson, J., and Palli, S. R. (2011). Ingested RNA interference for managing the populations of the Colorado potato beetle, *Leptinotarsa decemlineata*. *Pest Manag. Sci.* 67, 175–182.

## Chapter 4

### 4 Towards the establishment of an optimized method for gene silencing in the two-spotted spider mite *Tetranychus urticae*

#### 4.1 Introduction

RNA interference (RNAi) is an evolutionarily-conserved cellular process of gene silencing elicited by the presence of double-stranded RNA (dsRNA) (Fire et al., 1998; Meister and Tuschl, 2004; Mello and Conte, 2004). Induction of gene silencing can be triggered at the transcriptional level through the inhibition of endogenous gene translation (TGS) or at a post-transcriptional level through degradation of transcripts or interference with translation (PTGS; Hammond et al., 2000). This RNAi is a mechanism thought to have evolved to preserve the genome integrity against foreign DNA/RNA sequences (e.g. viruses; Ding and Voinnet, 2007) and transposition of transposons (Obbard et al., 2009). RNAi is based on complementarity between short RNAs and their targeted mRNAs, ultimately leading to either a cleavage of the target mRNA or prevention of its translation (Fire et al., 1998). Since its discovery in *C. elegans*, RNAi has been successfully used as a reverse genetic tool in model organisms for over a decade. More recently several studies have demonstrated the potential of RNAi as environmentally friendly control of plant pests through oral ingestion of dsRNA targeting vital genes, which results in death of the pest species (Baum et al., 2007; Whyard et al., 2009). Besides herbivorous insects, the chelicerate pests are also prominent herbivores that affect agricultural production. Among them, *Tetranychus urticae* is an extremely phytophagous pest that feeds on agricultural crops and ornamental plants with a global distribution. To date, *T. urticae* has been reported in 501 cases of resistance to pesticide including 94 active ingredients (Whalon et al., 2006-2017) making it one of the most resistant arthropod species, prompting development of new control methods. The *T. urticae* genome became available in 2011 and its analysis revealed that it encodes all elements required for a functional RNAi (Bensoussan and Grbić, 2017; Grbic et al., 2011). Recently, oral delivery of dsRNA through leaf disc has been reported. Application of dsRNA using this

method was successful to decrease gene expression of several lethal targets resulting in mortality in *T. urticae* (Kwon et al., 2013, 2016). Silencing of the proton pump *VATPase* and the *coatomer*  $\beta$  involved in vesicular trafficking from *trans* to *cis* Golgi and the endoplasmic reticulum induced 65% and 21% mite mortality, respectively. More recently, our group developed a soaking method consisting of an immersion of spider mites in a dsRNA-containing solution (Suzuki et al., 2017a). Using *VATPase* as a model target gene, I have shown that the soaking method induces a strong RNAi response characterized by a phenotypic change associated with gene downregulation and 80% mortality. However, these phenotypic changes occurred only in a subset of treated mite populations requiring the need for further optimization of dsRNA soaking delivery method. Moreover, due to its recent discovery, little is known about parameters required to achieve efficient RNAi in arthropod in general and *T. urticae* specifically. Our knowledge lies on studies from model insects like the red flour beetle (*Tribolium castaneum*), the Western corn rootworm (*Diabrotica vigifera vigifera* LeConte) and drosophila cell lines in which factors such as: dsRNA uptake, concentration, sequence position, length and tissue penetration have been shown critical for potent RNAi (Bolognesi et al., 2012; Miller et al., 2012; Ramadan et al., 2007).

The aim of my project was to further improve the soaking method developed previously, and investigate the parameters required to achieve a greater effectiveness of RNAi response in *T. urticae*. To further exploit the parameters needed for efficient RNAi, I first expanded the number of target genes that were so far limited to *TuVATPase*, by testing the application of dsRNA against *TuCOPB2*, the coatomer protein complex I (COPI) that is involved in important physiological process such as endosomal activities (Whitney et al., 1995), autophagy (Razi et al., 2009) and tube expansion in the silk gland (Wang et al., 2010). Moreover, silencing of the coatomer subunit has been shown to be lethal in the cotton bollworm *H. armigera* (Mao et al., 2015), the mosquito *Aedes Aegypti* (Zhou et al., 2011) and in *T. urticae* through application of dsRNA on leaf discs (Kwon et al., 2016) making *COPB2* a good candidate for the model target to be used for the improvement of the soaking method.



Herein, I show that application of dsRNA against *TuCOPB2* resulted in a phenotypic change in mite body color associated with the reduction of mite fitness: survivorship and fecundity. Moreover, I carried out *in situ* hybridization to localize the *TuCOPB2* transcript in the ovaries of the mite. Using the phenotypic changes associated with RNAi response to *TuVATpase* and *TuCOPB2* as a proxy, I demonstrated the possibility to use diets mixed with dsRNA to control for the dsRNA uptake and to enriched the number of mites responding to RNAi. In addition, using a dsRNA size series against *TuVATPase* and *TuCOPB2*, I established a minimum dsRNA size of 400 bp for efficient RNAi in *T. urticae*. Furthermore, I found that no additive effects existed when mixing 2 short dsRNA fragments together, suggesting that dsRNA cellular intake in *T. urticae* is potentially more efficient with long dsRNA fragments. Data collected in this study not only initiated the understanding of the RNAi mechanism in *T. urticae*, but also provided optimized RNAi design for an efficient reverse genetic screen in this chelicerate model.

## 4.2 Materials and Methods

### 4.2.1 *T. urticae* rearing conditions

The stock population of *T. urticae* referred to as London strain originated from the Vineland region in Ontario. The population was maintained on California red kidney beans (*Phaseolus vulgaris* L, stokes, Thorol, ON) grown in soil (PRO-MIX<sup>®</sup> BX MYCORRHIZAE<sup>™</sup>; Premier Tech, Rivière-du-Loup, QC), in a climate controlled chamber at light: dark photoperiod of 16/8 h, 26°C with relative humidity of 50%.

### 4.2.2 Preparation of developmentally synchronized mites

Adult female mites were allowed to lay eggs for 24 h on a fresh detached bean leaf at light/dark 16/8 h, 26°C, and 50% relative humidity (RH). After 24 h, the adult females were removed and 1-day-old eggs were allowed to develop into female teleiochrysalis (7-8 days). Teleiochrysalis were collected and incubated at 18°C and 100% RH for 24 h, after which they were returned to a 26°C and 50% RH environment. Adult female mites, emerged within 3 h upon transfer to a 50% RH environment and were collected for experimentation.

### 4.2.3 dsRNA fragments

Two different dsRNA fragments have been used to target the *TuCOPB2* (tetur24g00150) transcripts to ensure the reproducibility and the specificity of the RNAi phenotype. The fragment B of *TuVATPase* (tetur09g04140) was used for RNAi optimization experiments, since it was associated with the strongest RNAi response (Suzuki et al., 2017). Fragments corresponding to the region of *TuCOPB2*, referred to as fragments A (an upstream fragment of 308 bp overlapping the 4<sup>th</sup> and 5<sup>th</sup> exon of the *TuCOPB2* locus) and B (a 513 bp fragment within the 5<sup>th</sup> exon) were chosen as templates for the preparation of dsRNA. For RNAi optimization, a dsRNA fragment size of 600 bp overlapping the fragment A of *TuCOPB2* was synthesized and was used to generate six other nested dsRNA fragments of various lengths (Figure 4.1A). In the same way, the fragments corresponding to the region of *TuVATPase*, referred to as fragment B (a 416 bp fragment within the 4<sup>th</sup> exon of the *TuVATPase* locus) was chosen as template for the preparation of dsRNA (Figure 4.1B). For RNAi optimization, a dsRNA fragment size of 600 bp overlapping the fragment B of *TuVATPase* was produced and was used to generate six other dsRNA fragments of various lengths. Details of sizes and positions of these dsRNA fragment series is shown in Figure 4.1C. Briefly, a fragment size of 600 bp was used as template to generate six shorter dsRNA fragments of 100, 200 and 400 bps spanning the 3' and 5' ends for both 600 bp-fragments (see primers used in Table 1). In addition, the 600 bp was used as the longest dsRNA fragment. All fragments were used at the same concentration of 160 ng/ $\mu$ L in a volume of 50  $\mu$ L. The fragment B of both genes corresponds to the dsRNA sequence previously used by Kwon et al (2013), enabling direct comparison of method efficiency between the previous report and this study. In addition, a 382 bp intergenic fragment spanning the region 1690614-1690995 of the genomic scaffold has been chosen as the template for the preparation of a negative control dsRNA, referred to as NC. A BLAST search against the *T. urticae* genome and transcriptome database confirmed that the 382 bp intergenic sequence is unique and not transcribed (Figure 4.1D).

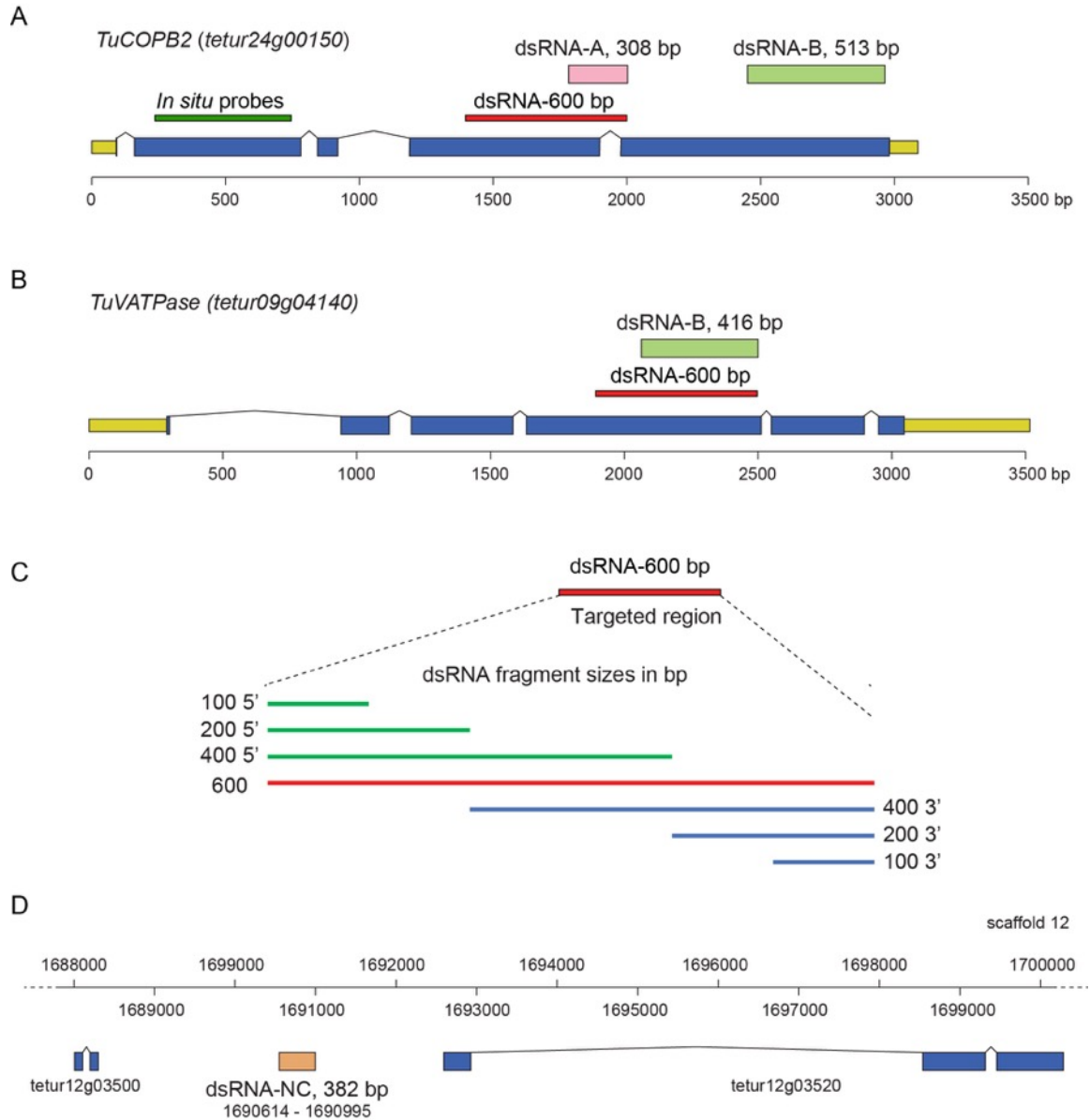


**Figure 4.1: Fragments used for synthesis of dsRNAs.** (A) Schematic of *TuCOPB2* locus. DNA sequences used for the generation of dsRNA-*TuCOPB2* are in the 4<sup>th</sup>, fragment A (308 bp), and in the 5<sup>th</sup> exon, fragment B (513 bp). The dsRNA of 600 bp overlapping the targeted sequence of dsRNA-A (in red line) was used to generate dsRNA series. The green line represents the targeted region for *in situ* hybridization probes (B) Schematic of *TuVATPase* locus with the DNA sequence used to generate dsRNA-*TuVATPase*-B (416 bp) corresponding to the 4<sup>th</sup> exon. The dsRNA of 600 bp overlapping the targeted sequence of dsRNA-B (in red line) was used to generate dsRNA series. (C) Detailed schematic of the 7 dsRNA fragment series of 100, 200, 400 bp spanning the 5' or 3' ends of the 600 bp dsRNA fragment. UTR and coding sequence are shown in yellow and blue, respectively. (D) Schematic of the part of scaffold 12 of *T. urticae* genome depicting the location of the 382 bp fragment that was used to synthesize dsRNA-NC.

**Table 4.1: Primers used in this study.** (Primer name, Function, Sequence, Product size, ISH: *in situ* hybridization)

Primer name/Function	Oligonucleotide sequence (5' to 3')	Product size
F_COPB2_dsRNA-A	<u>T7-TGGTCGGACAATGGAGATT</u>	308 bp
R_COPB2_dsRNA-A	<u>T7-TCAGGTGGAGTATAAACGGCT</u>	
F_COPB2_dsRNA-B	<u>T7-TTCGGGAATCTACAACGTTGC</u>	513 bp
R_COPB2_dsRNA-B	<u>T7-TCAGGTGGAGTATAAACGGCT</u>	
F_VATPase_dsRNA-B	<u>T7-CCGTGATATGGGTACCATG</u>	416 bp
R_VATPase_dsRNA-B	<u>T7-GAAGAGGTACGAAATCTGGG</u>	
F_COPB2_ISH_Sense	<u>T7-GTGAGGTTCTGTTTCGGTGT</u>	577 bp
R_COPB2_ISH	<u>TTCAATTCTTCCGGATCGAC</u>	
F_COPB2_ISH_Antisense	<u>GTGAGGTTCTGTTTCGGTGT</u>	577 bp
R_COPB2_ISH_Antisense	<u>T7-TTCAATTCTTCCGGATCGAC</u>	
F_COPB2_dsRNA_100_5'	<u>T7-AGTTTGTGGTGACGGAGAAT</u>	~100 bp
R_COPB2_dsRNA_100_5'	<u>T7-TGAGTCTAGGGCCCAAACAA</u>	
F_COPB2_dsRNA_200_5'	<u>T7-AGTTTGTGGTGACGGAGAAT</u>	~200 bp
R_COPB2_dsRNA_200_5'	<u>T7-TGCTTCTGGTTTGAATGACGT</u>	
F_COPB2_dsRNA_400_5'	<u>T7-AGTTTGTGGTGACGGAGAAT</u>	~400 bp
R_COPB2_dsRNA_400_5'	<u>T7-GCTTTGGCAACGTTATCAGG</u>	
F_COPB2_dsRNA_100_3'	<u>T7-GCTCGGTCAATAGACTCAATTATTTT</u>	~100 bp
R_COPB2_dsRNA_100_3'	<u>T7-TTTTCCTTCCGGCATGTATCC</u>	
F_COPB2_dsRNA_200_3'	<u>T7-ACGGAATTATTGATGCATTTCG</u>	~200 bp
R_COPB2_dsRNA_200_3'	<u>T7-TTTTCCTTCCGGCATGTATCC</u>	
F_COPB2_dsRNA_400_3'	<u>T7-CCGTGATATGGGTACCATG</u>	~400 bp
R_COPB2_dsRNA_400_3'	<u>T7-TTTTCCTTCCGGCATGTATCC</u>	
F_COPB2_dsRNA_600	<u>T7-AGTTTGTGGTGACGGAGAAT</u>	~600 bp
R_COPB2_dsRNA_600	<u>T7-TTTTCCTTCCGGCATGTATCC</u>	
F_VATPase_dsRNA_100_5'	<u>T7-TCCAACAGTGATGTTATTGTTTACG</u>	~100 bp
R_VATPase_dsRNA_100_5'	<u>T7-TAATTGATTCAGTAACTCCATTG</u>	
F_VATPase_dsRNA_200_5'	<u>T7-TCCAACAGTGATGTTATTGTTTACG</u>	~200 bp
R_VATPase_dsRNA_200_5'	<u>T7-ACGGAATATTTCAGATAATGTG</u>	
F_VATPase_dsRNA_400_5'	<u>T7-TCCAACAGTGATGTTATTGTTTACG</u>	~400 bp
R_VATPase_dsRNA_400_5'	<u>T7-ACACTTCTCTCTTTCTGGATTAC</u>	
F_VATPase_dsRNA_100_3'	<u>T7-ACATTTTCCATCCATTAATTGG</u>	~100 bp
R_VATPase_dsRNA_100_3'	<u>T7-TTTTCCTTCCGGCATGTATCC</u>	
F_VATPase_dsRNA_200_3'	<u>T7-TCACCACCCGGTGGTGAATTC</u>	~200 bp
R_VATPase_dsRNA_200_3'	<u>T7-TTTTCCTTCCGGCATGTATCC</u>	
F_VATPase_dsRNA_400_3'	<u>T7-CCGTGATATGGGTACCATG</u>	~400 bp
R_VATPase_dsRNA_400_3'	<u>T7-TTTTCCTTCCGGCATGTATCC</u>	
F_VATPase_dsRNA_600	<u>T7-TCCAACAGTGATGTTATTGTTTACG</u>	~600 bp
R_VATPase_dsRNA_600	<u>T7-GAAGAGGTACGAAATCTGGG</u>	
T7 promoter sequence	<u>TAATACGACTCACTATAGGG</u>	

#### 4.2.4 dsRNA synthesis

Template preparation for dsRNA fragments *TuCOPB2*, *TuVATPase* and dsRNA fragment series for RNAi optimization was achieved with polymerase chain reaction amplification using specifically designed oligonucleotide primers containing the T7 RNA polymerase promoters at their 5'-ends to produce PCR-fragments that could be directly used for *in vitro* transcription, omitting cloning preparation steps.

First, total RNA was extracted from the frozen mite females with the RNeasy Mini Kit (Qiagen, Valencia, CA) and cDNA was synthesized from 3 µg of the extracted total RNA with the SuperScript II cDNA Synthesis Kit (Thermo Fisher Scientific, Waltham, MA) and used as a template (Figure 4.2A). Template preparation for the control sequence (dsRNA-NC) targeting an intergenic region was performed by PCR using genomic DNA. Template preparation for dsRNA *TuCOPB2*-A and -B, *TuVATPase*-B, dsRNA-NC and all seven dsRNA fragments of different sizes of *TuCOPB2* and *TuVATPase* was performed by PCR using template gene specific forward and reverse primers (Table 4.1) with a minimal T7 promoter sequence at their 5' ends (Figure 4.2B). For the dsRNA fragment size series, one forward primer at the 5' ends of the 600 bp fragment and specific reverse primers was used to generate the three short fragments spanning at the 5' end (400 5', 200 5' 100 5'). In the same way one reverse primer at the 3' ends of the 600 bp fragment and specific forward primer was used to generate three short fragments spanning at the 3' end (400 3', 200 3' 100 3').

Amplified DNA fragments were purified with the Gel/PCR DNA Fragments Extraction Kit (Geneaid Biotech, New Taipei, Taiwan). Purified fragments were sequenced to confirm their identity. dsRNA fragments were synthesized using 1 µg of DNA template with the TranscriptAid T7 High Yiled Transcription Kit (Thermo Fisher Scientific) in 1.5-ml centrifuge tubes. dsRNA was treated with DNase I for 30 min (Thermo Fisher Scientific), was denaturated at 95°C for 5 min, and were allowed a slow cool-down to room temperature to facilitate formation of dsRNA. dsRNA was purified by phenol-chloroform extraction followed by ethanol precipitation. dsRNA was dissolved in nuclease free water and quantified using the NanoDrop (Thermo Fisher Scientific, Waltham, MA).

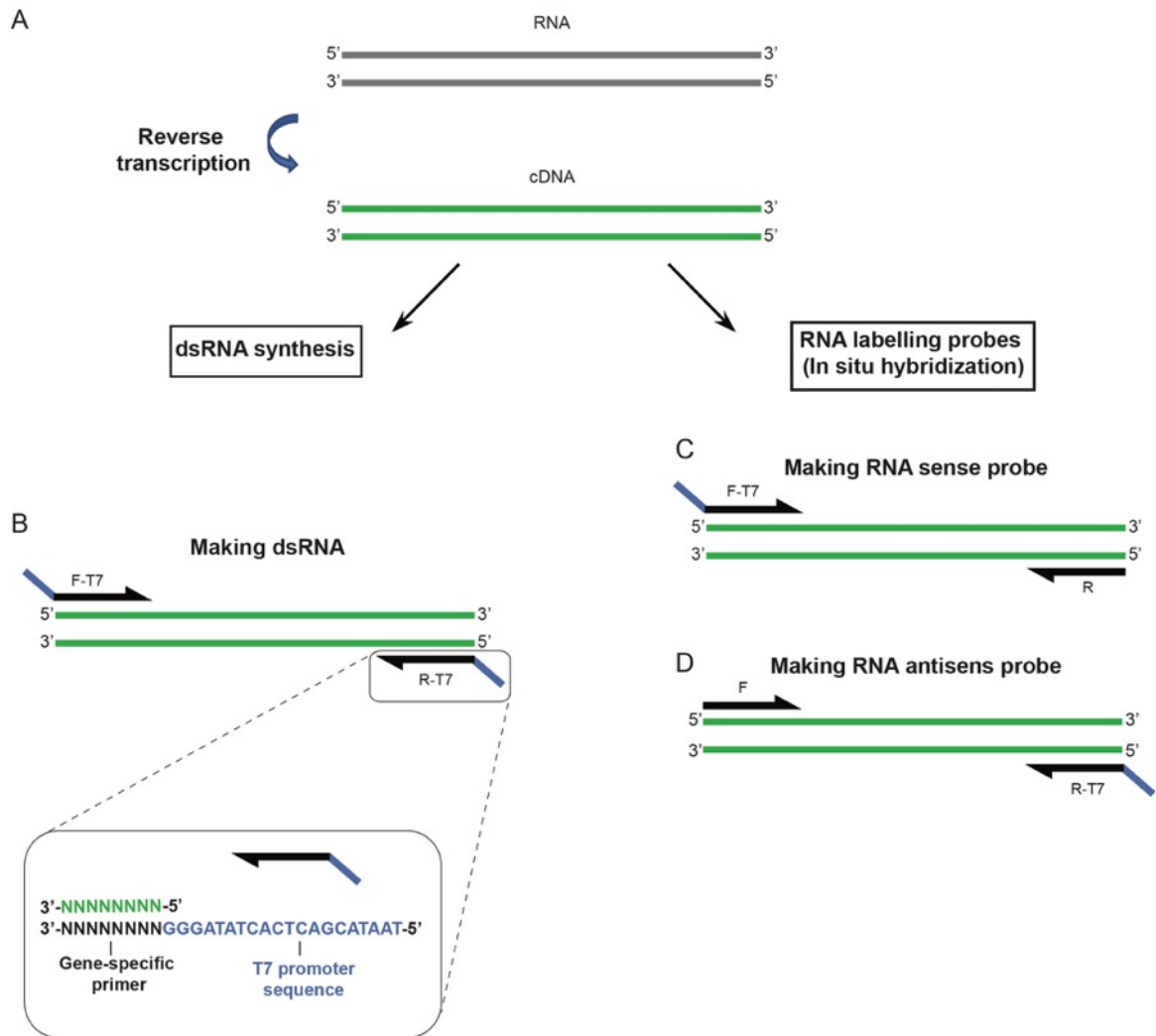


**Figure 4.2: Schematic of the template preparation for dsRNA synthesis and mRNA DIG-labeled probes using the PCR method.** (A) Total mRNA reverse transcribed and used as a template for downstream dsRNA synthesis or RNA labeling probes. (B) Schematic of PCR amplification using specific gene primer forward and reverse (black arrow; F: Forward; R: Reverse) tailed with the minimal T7 promoter sequence at the 5' end of each primers. (C) Schematic of template generation for RNA sense probe using a forward gene specific primer tailed with T7 and a reverse primer. (D) Template preparation for RNA antisense probe using the same forward primer as the sense probe without T7 promoter and the same reverse primer were used with the T7 promoter sequence.

#### 4.2.5 Localization of *COPB2* mRNA expression pattern using whole mount *in situ* hybridization

Whole-mount *in situ* hybridization in *T. urticae* was performed as described by Dearden *et al.*, 2000 with some modification as per Jonckheere *et al.*, (2016). Total RNA was extracted from *T. urticae* adult females as described above. PCR reactions using primers F-T7 with R (Figure 4.2C and Table 4.1), was used to generate the sense template and primers using F and R-T7 (Figure 4.2D and Table 4.1) was used to generate antisense templates for *in vitro* transcription. For generating the sense probe, a set of primers with only the forward primer containing the T7 promoter was used (Figure 4.2C). For the antisense probe, only the set of primers with the reverse primer containing the R7 promoter was used (Figure 4.2D). Depending on the primer combination, sense and antisense probes labeled with digoxigenin (DIG) were generated using T7 polymerase (Roche, Anderlecht, Belgium) and DIG-UTPs (Roche) in the *in vitro* labeling reaction. The probes are then purified using SigmaSpin Sequencing Reaction Clean-Up Columns (Sigma) and mixed in 1:1 volume of hybridization buffer (50% formamide (Sigma), 4× SSC (Sigma), 1× Denhardt's solution (Sigma), 250 µg/mL heparin (sodium salt, Sigma), 0.1% Tween-20 (Sigma), 5% dextran sulfate (sodium salt, Sigma), and stored at – 20°C. *T. urticae* adults were fixed overnight in a solution containing PTw (PBS with 0.1% Tween-20) mixed with 4% formaldehyde and heptane in 1:1 volume ratio. Mites were washed with cold methanol at – 20 °C following by multiple washes with methanol at room temperature. Mites were gradually rehydrated in PTw, followed by a brief sonication in a sonic cleansing bath and re-fixed with 4% formaldehyde in PTw. Mites were subsequently washed 3 times in PTw and pre-hybridized in hybridization buffer at 52 °C for 1 hour. Buffer was then replaced with probe (1µL in 200 µL hybridization buffer) and mites were incubated overnight at 52 °C. Afterwards, mites were washed six times with wash buffer (50% formamide, 2× SSC, 0.1% tween-20) every 10-15 minutes at 52°C. Mites were then washed in a blocking solution composed of PBTw (PTw with 0.1% BSA, Sigma) 2 times and incubated at RT for 2 hours with a 1:1000 dilution of anti-digoxigenin antibodies conjugated with (AP) alkaline phosphatase enzyme (Fab fragments, Roche) in PBTw. Mites were then washed in PTw and placed on a 9-cavity

Pyrex pressed plate (Pyrex, USA) in the dark with AP buffer (100 mM Tris pH 9.5, 100 mM NaCl, 1M MgCl<sub>2</sub>, 0.1% Tween-20) mixed with 4.5 µL/mL of nitro blue tetrazolium (NBT, Sigma) and 3.5 µL of bromo-chloro-indolyl-phosphate (BCIP, Sigma) until purple staining was visible. Mites were washed in 100% methanol to reduce the background and were mounted in 50% glycerol in PTw for observation in the light microscope.

#### 4.2.6 Soaking mite in a solution of dsRNA

About 50 newly-emerged adult females were soaked in 50 µL of dsRNA solution (160 ng/µL; 0.1% v/v Tween 20) respectively and incubated at 20°C in a water bath for 24 hours according to Suzuki et al. (2017). After soaking, mites were transferred onto bean leaf discs (10-mm diameter with 1 female per disc) placed on water-soaked cotton on the cup with a polyethylene lid with 4 venting holes each covered with a gas-permeable filter (0.45-micron pore size; Milliseal; Millipore, Billerica, MA), and incubated at light/dark 16/8 h, 26°C, and 50% RH. Survival of adult females was recorded over 10 days. The biological assays were conducted in 3 independent experimental runs. For RT-qPCR analysis, the adults were collected into 1.5-mL tube with at least 30 adults per tube at 5 days after 24 hours soaking. The collected samples were frozen in liquid nitrogen and stored at -80°C until RNA extraction. The collection and the RT-qPCR analysis were conducted in 3 independent experimental runs.

#### 4.2.7 Data analysis of survival and fecundity

Survival curves were calculated with the Kaplan-Meier method (function `survfit`, R package `survival`) with comparisons performed based on the log-rank test (function `survdiff`, R package `survival`). Results for the fecundity are displayed as box-plots where central lines (second quartile, Q2) indicate the median of data, the distance between the box bottom (first quartile, Q1) and top (third quartile, Q3) indicate interquartile ranges (IQRs), and the whisker bottom and top indicate the minimum and maximum of data (except outliers that are outside the range between the lower (Q1-1.5× IQR) and upper limits (Q3=1.5×IQR) that are plotted as a white circle). Significant differences in the median number of eggs laid between the control and other treatments were analyzed with the Wilcoxon-Mann-Whitney test (function `wilcox.exact`, R package `exactRankTests`). A



significant difference in the proportion of color phenotype (normal or dark-body) was analyzed with the Fisher's exact test (Function `fisher.test`). For multiple comparisons based on the paired tests, the level of significance ( $\alpha$ ) was adjusted with the Bonferroni correction ( $\alpha/K$ , where  $K$  is the number of pairs in the multiple comparison). Analysis was performed with the R 3.2.5 software (R Core Team 2016).

#### 4.2.8 Analysis of dsRNA uptake

To test the correlation between dsRNA uptake and RNAi response, newly-emerged adult females from the reference London population were soaked in a 1.5-mL tube (60-80 adults per tube) with 50  $\mu$ L of dsRNA solution (160 ng/ $\mu$ L; 0.1% v/v Tween 20) mixed with 6% of blue food dye (erioglaucine; McCormick, Sparks Glencoe, MD). Adult females soaked in the dsRNA solution were incubated at 20°C in a water bath for 24 hours. After soaking, mites were washed in 100  $\mu$ L of double distilled water and separated according to their color (blue or transparent) onto a bean leaf that was placed on top of water-soaked cotton in a cup with vented lid, and incubated at light/dark 16/8 h, 26°C, and 50% RH. After 2 days, the body color associated with RNAi responses to either dsRNA against *TuVATPase* or *TuCOPB2* were counted and frequencies calculated. A Mann-Whitney *U*-test was run to check the differences between phenotype and treatment. Analysis was performed with the R 3.2.5 software (R Core Team 2016). Differences were considered significant with a 5% significance level ( $P < 0.05$ ). Each experimental run was performed in 3 independent replicates.

#### 4.2.9 Analysis of RNAi efficiency using various dsRNA fragment lengths

Newly-emerged adult females from the reference London population were soaked in 1.5-mL tubes (60-80 adults per tube) with 50  $\mu$ L of dsRNA solution (160 ng/ $\mu$ L; 0.1% v/v Tween 20) after 6 hours of starvation. Adult females soaked in the dsRNA solution were incubated at 20°C in a water bath for 24 hours. After soaking, mites were washed in 100  $\mu$ L of double distilled water and transferred onto a bean leaf that was placed on top of water-soaked cotton in a cup with vented lid, and incubated at light/dark 16/8 h, 26°C, and 50% RH. After 2 days, mites with dark, red and normal body color were counted.

Each experimental run was performed in 3 independent replicates. A significant difference in the proportion of color phenotype (normal, dark, or red-body) was analyzed with the Fisher's exact test (Function `fisher.test`). For multiple comparisons, one-way ANOVA (Tukey HSD) tests were performed. Analysis was performed with the R 3.2.5 software (R Core Team 2016).

#### 4.2.10 dsRNA-*TuVATPase* mix

The two fragments of 200 bp spanning the 5' and 3' ends of the *TuVATPase* gene were used separately and mixed together to a final volume of 50  $\mu$ L at a concentration of 160 ng/ $\mu$ L. In parallel the fragment of 400 bp spanning the 5' end of *TuVATPase* was used as the reference.

#### 4.2.11 Imaging

All images were taken using a stereomicroscope Leica MZ FLIII (© Leica Microsystems, Wetzlar, Germany) fitted with the Canon EOS Rebel T5i camera (Canon, Japan).

### 4.3 Results

#### 4.3.1 Induction of RNAi in dsRNA *TuCOPB2* soaked mites

When soaked in a solution of dsRNA-*TuCOPB2* of either fragment A or B, I observed that a portion of adult mites developed a pale-red phenotype with a smaller body size compared to the mites that have been soaked in solution containing dsRNA-NC (Figure 4.3A). About 51% of the adults soaked in dsRNA-*TuCOPB2*-A and 62% of mites treated with dsRNA-*TuCOPB2*-B developed the red-body color (Figure 4.3B). However, this red phenotype was not present in the mites treated with dsRNA-NC. To test the potential correlation between the red phenotype and RNAi response, I followed mites separately according to their body color. I checked the survivorship of mites separated in groups based on their size and body color that were treated with either dsRNA-*TuCOPB2*-A or -B (Figure 4.4A and 4.4C). Mites with normal body color had survivorship as mites treated with dsRNA-NC. However, the red mites treated with dsRNA-*TuCOPB2*-A or -B (Figure 4.4B and 4.4D) presented a significantly lower survivorship compared to the

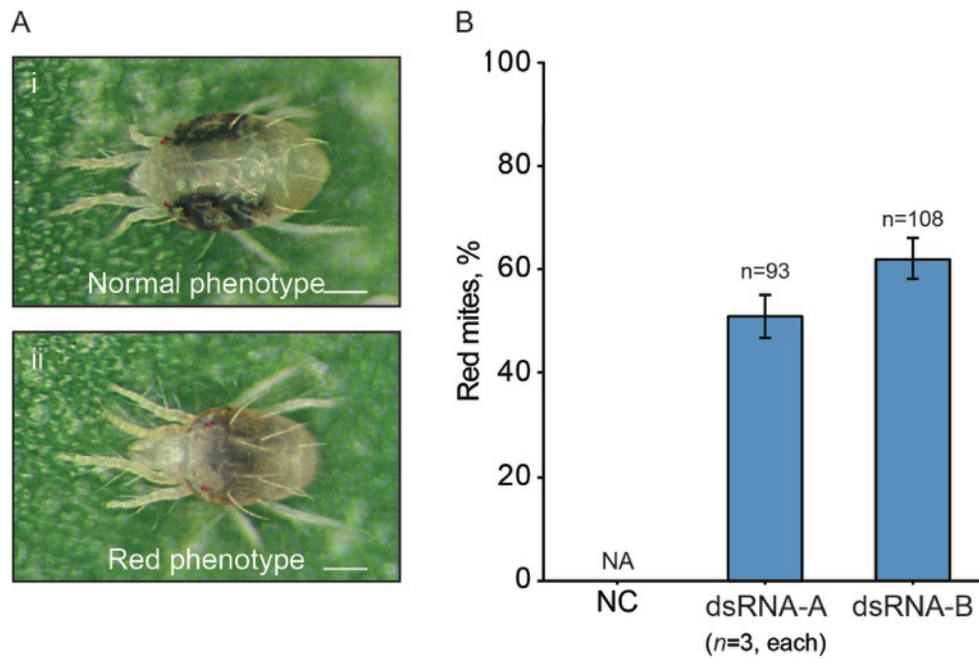


**Figure 4.3: Mite phenotype associated with RNAi response to dsRNA-*TuCOPB2*.** Normal phenotype (Ai) and red-body (Aii) female mites and frequency of phenotypes observed after application of dsRNA-*TuCOPB2*-A, dsRNA-*TuCOPB2*-B or dsRNA-NC through soaking (B). The bar graph represents red-body mite frequencies collected from 3 independent experimental runs. (Scale bars: 100  $\mu$ m).

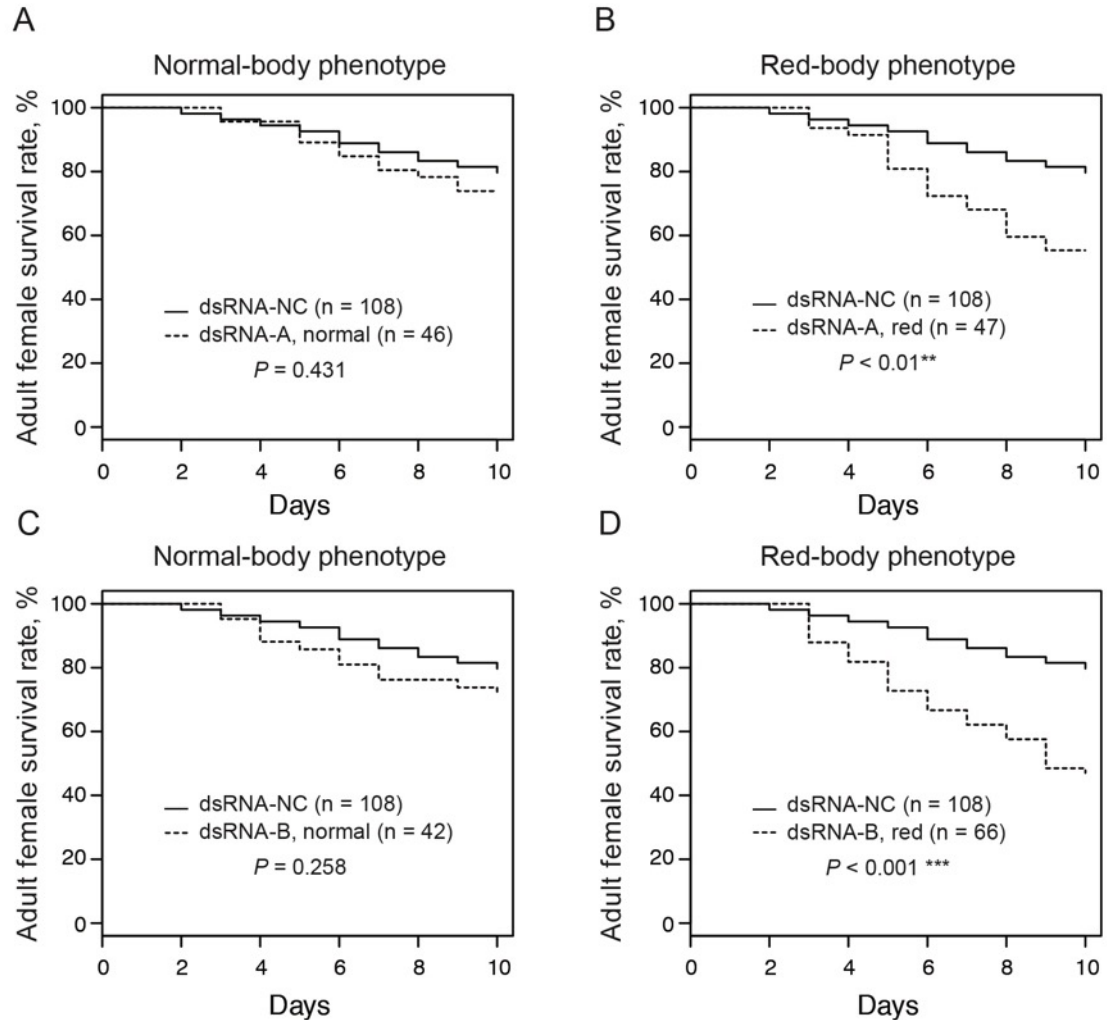


**Figure 4.4: Adult survivorship after soaking treatment in solution of dsRNA-*TuVATPase* separately for normal and dark-body mites.** Survivorship of adult female with normal phenotype (A) and dark phenotype (B) after treatment with dsRNA-*TuVATPase*-A (solid line) or dsRNA-NC (dashed line). Survivorship of adult female with normal phenotype (C) and dark phenotype (D) after treatment with dsRNA-*TuVATPase*-B (solid line) or dsRNA-NC (dashed line). Survival curves were plotted using Kaplan-Meier method and compared using the log-rank test with Bonferroni correction (no asterisk,  $P > 0.05$ ;  $***$ ,  $P < 0.001$ ).

control (dsRNA-NC). Similarly, the fecundity of normal mites treated with dsRNA-*TuCOPB2* was not impaired compared to the control, showing a similar oviposition rate of about 5 eggs per female per day (Figure 4.5). However, the fecundity of mites with red body color were drastically affected, displaying a significantly lower fecundity compared to the control with a reduction of 90% and 96% oviposition rate when treated with dsRNA-*TuCOPB2*-A and dsRNA-*TuCOPB2*-B respectively (Figure 4.5).

#### 4.3.2 Whole mount *in situ* hybridization

To examine the spatial expression pattern of *COPB2*, a whole mount *in situ* hybridization on *T. urticae* adults was carried out. A strong signal was detected in the medioventral part of the mite, on the body surface, posterior to the central nervous mass (Figure 4.6B). This pattern likely corresponds to the reproductive system of *T. urticae* female including ovaries and oviduct as shown in Figure 4.6A-C. The organs composing the reproductive system fill the ventral body cavity, extending from the anal region forward to the central nervous mass. No signal was detected when using the sense probe. Moreover, when off target effect was checked, no significant sequence match other than *COPB2* was found when the sequence used to generate the antisense probe was BLAST against *T. urticae* coding sequence, indicating that the expression pattern is specific to *COPB2*.

#### 4.3.3 Testing the uniformity of the dsRNA uptake

As previously shown with the treatment of dsRNA-*TuVATPase* (Suzuki et al., 2017) and in this study using the dsRNA-*TuCOPB2*, only a portion of dsRNA-treated mites displayed RNAi. This low RNAi penetration was postulated to be the consequence of the intrinsic property of the delivery method, mite manipulation, or mite physiology. In order to improve dsRNA delivery, non-toxic food dyes were tested in a soaking solution with mites, at different concentrations, to assess their potential to be a visual tracer of dsRNA intake. I found that 6% blue food dye was the optimum concentration that could be visualized through the transparent integument of the mite, accumulating in the midgut. Next, I examined the capacity of the blue dye to be used as a

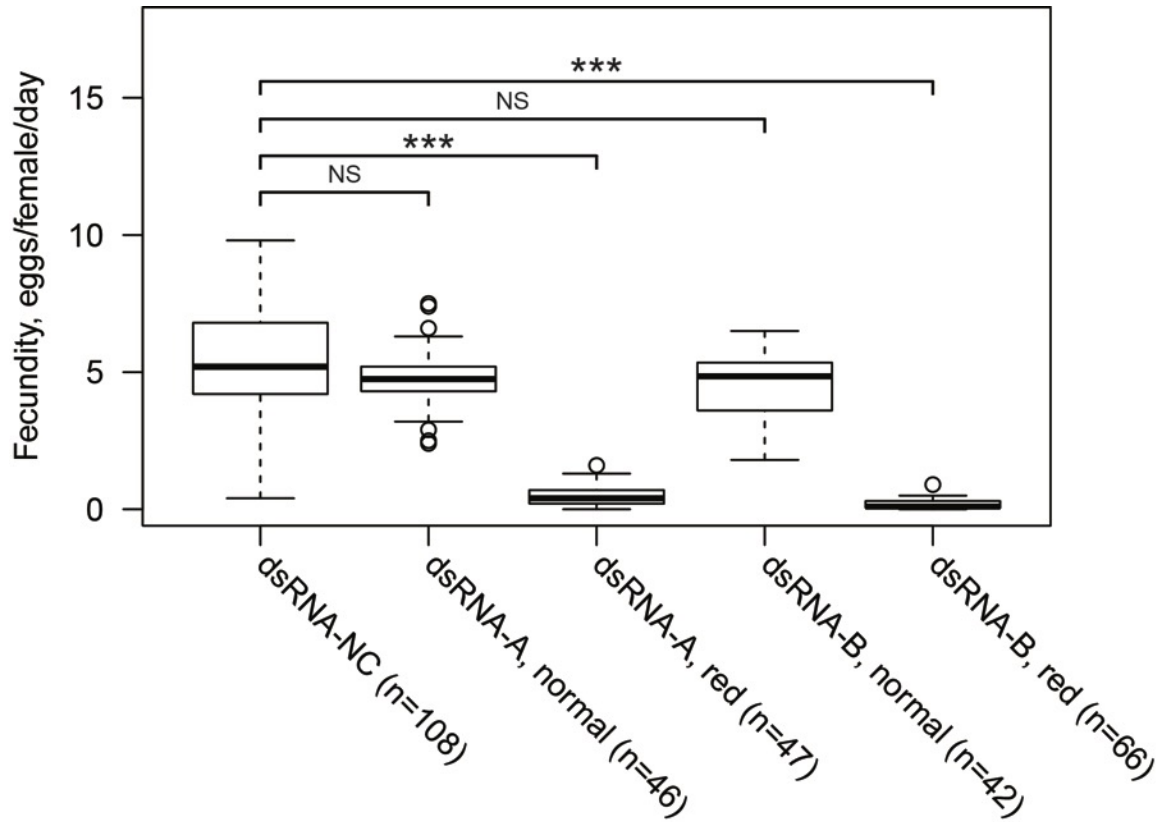


**Figure 4.5: Adult mite fecundity after soaking treatment in solution of dsRNA-*TuCOPB2*.** Normal and red-body mite fecundity after soaking in solution of dsRNA-*TuVATPase-A*, dsRNA-*TuVATPase-B* or dsRNA-NC. Data were collected from 3 independent experimental runs and were compared using Wilcoxon-Man-Whitney test with Bonferroni correction (no asterisk: NS, Not significant,  $P > 0.05$ ; \*\*\*,  $P < 0.001$ ).

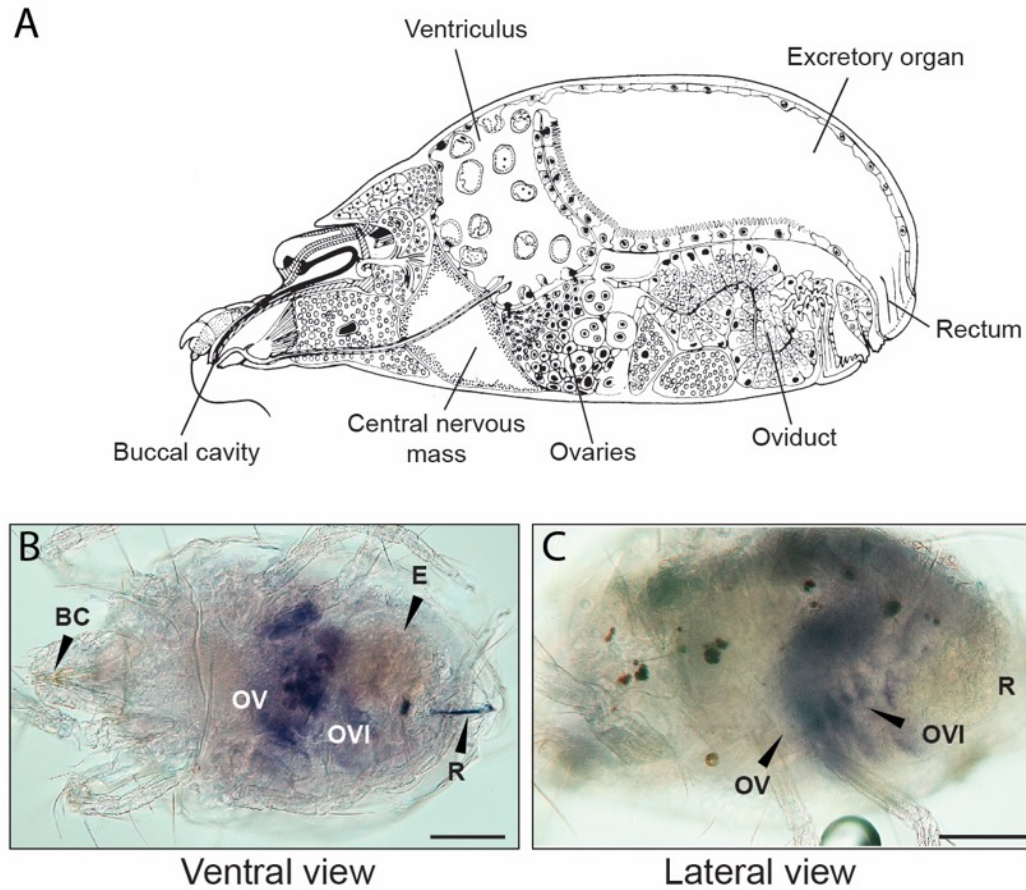


**Figure 4.6: Whole-mount in situ hybridization of *COPB2* gene expression pattern in *T. urticae* female.** (A) Schematic representation of a sagittal section of a female *T. urticae* (Adapted from Alberti and Crooker (1985), with the permission of Elsevier)). (B) Ventral and lateral (C) view of adult mite female showing *COPB2* expression pattern localized in the ovary within the oocyte and part of the oviduct. BC: buccal cavity; OV: Ovary; OVI: Oviduct; R: Rectum; E: eggs in formation. Scale bar represents 100 μm.

marker of dsRNA uptake, with the hypothesis that when mites were soaked in dsRNA mixed with the blue dye, only mites with accumulated blue dye in their midgut would respond to RNAi. A lack of the blue dye in the midgut would indicate insufficient or no dsRNA uptake. I used the phenotypic change in body color associated with RNAi responses to dsRNA-*TuVATPase* and dsRNA-*TuCOPB2* as a visual cue to test the correlation between accumulation of blue dye in the mite gut and RNAi response. When mites were treated with dsRNA-*TuVATPase*-B or dsRNA-*TuCOPB2*-B mixed with blue dye, around 94% and 95% of the mites with a blue gut presented a dark-body and a red-body phenotype respectively (Figure 4.7). However, mites without visible blue accumulation in the gut showed a significantly lower frequency of change in body color normally associated with RNAi response in mites treated with dsRNA-*TuVATPase*-B or dsRNA-*TuCOPB2*-B (Figure 4.7B, C). Consequently, the blue dye could be used as a dsRNA tracer in future experiments.

#### 4.3.4 The effect of dsRNA size on RNAi efficiency

To test the relationship between dsRNA size and its position relative to the targeted transcript on RNAi efficiency, a dsRNA size series was designed against *TuVATPase* (Figure 4.8A and 4.8B) and *TuCOPB2* (Figure 4.9A and 4.9B). In these assays, seven nested dsRNA fragments of different sizes were generated (600, 100, 200 and 400 bps in length). These fragments are overlapping at either the 5' or the 3' end.

When mites were treated with the fragment size series from 100, to 600 bp against dsRNA-*TuVATPase*, a positive correlation between the increase of the dsRNA fragment length and the increase of the frequency of dark mites was observed (Figure 4.8C). The 100 bp dsRNA fragments from either the 5' or 3' ends, yielded only a small portion of dark mites, 1.7 and 2.3 % respectively, of the total population treated. This proportion slightly increased when the 200 bp fragment was used. It resulted in 15.8 and 17.5% of dark mites from the 5' and 3' ends, respectively. The two dsRNA fragments of 400 bp targeting either the 5' or 3' ends of *TuVATPase* showed high RNAi efficiency with 54 and 45 % of black mites respectively. When mites were soaked with dsRNA-*TuVATPase* of 600 bp, RNAi response was the strongest showing about 65 % of dark-body mites. The same correlation between the length of the dsRNA fragment size and the RNAi efficiency



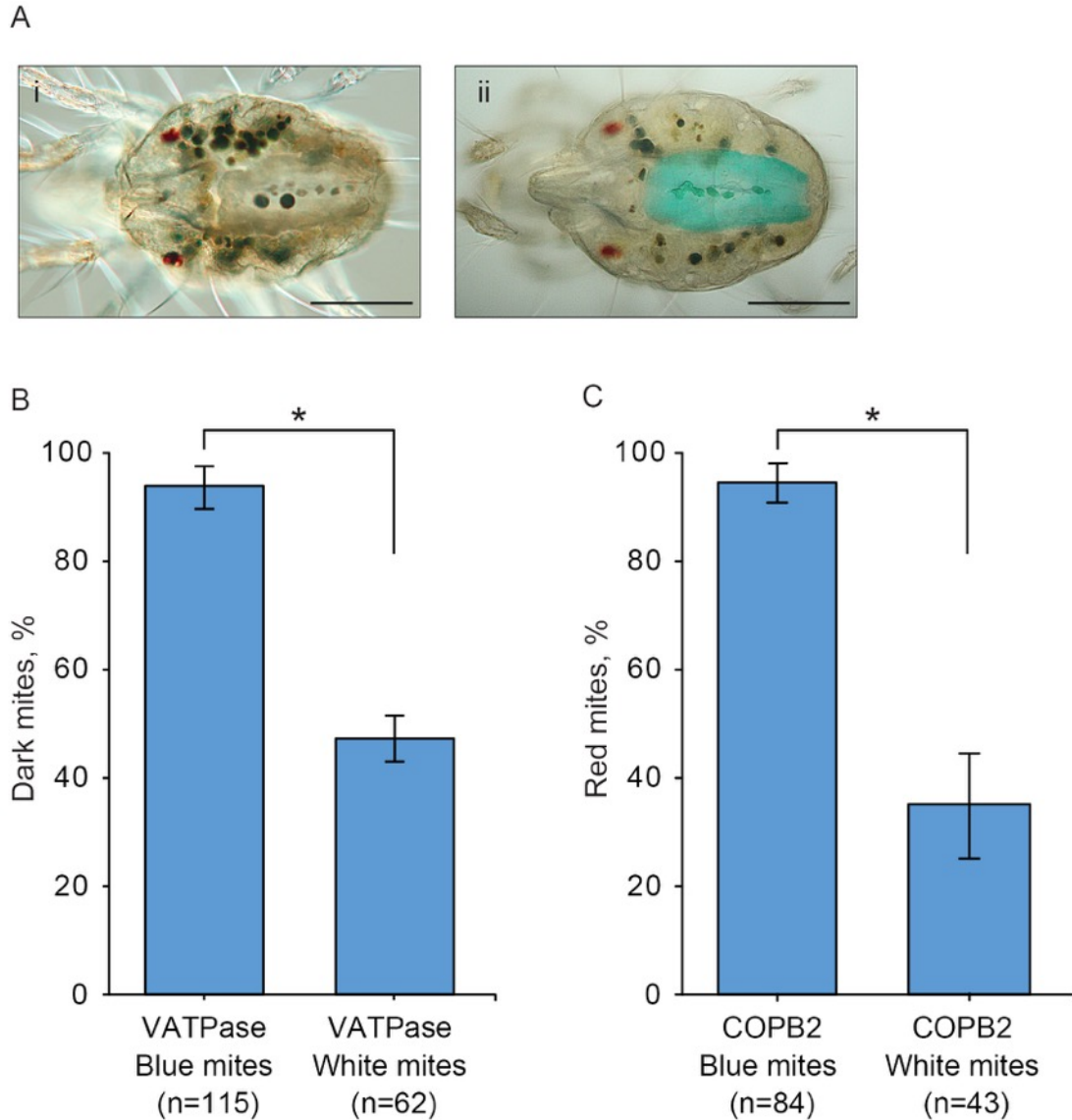


**Figure 4.7: Correlation between blue mite and RNAi response after soaking for 24 hours in solution containing dsRNA with blue dye.** Representative pictures showing absence (Ai) or accumulation (Aii) of tracer dyes in adult female midgut after soaking 24 hours in solution of dsRNA and 6% blue dye. RNAi response after soaking treatment in solution of dsRNA-*TuVATPase-B* separately for white mite; no blue accumulation and blue mites (B). RNAi response after soaking treatment in solution of dsRNA-*TuCOPB2-B* separately for white mite and blue mites (C). Data were collected from 3 independent experimental runs and were compared using Mann-Whitney *U*-test (\*,  $P < 0.05$ ); (scale bars: 250  $\mu$ m).

was observed with *TuCOPB2* (Figure 4.9). Only 5.4 and 3.13% of the red phenotype was observed when mites were soaked in the solution of 100 bp dsRNA fragments from the 5' and 3' ends respectively (Figure 4.9C). When treated with the fragment size of 200 bp, 19 and 13 % from the 5' and 3' ends respectively, developed the red phenotype. When mites were soaked with the 400 bp from the 5' ends, a significant increase of red phenotype was observed compared to the 200 bp 5' fragments but not with the 400 bp 3' fragments. As expected, the 600 bp dsRNA fragment yielded the strongest RNAi phenotype with 71% of the mites displaying a red-body phenotype. Similar to the treatment with *TuVATPase*, RNAi efficiency of two dsRNA fragments of 400 bp targeting either the 5' or 3' ends of *TuCOPB2* were not significant compared to the 600 bp dsRNA fragment suggesting that there is a threshold of dsRNA size: dsRNA  $\geq$  400 bp is required for the RNAi effectiveness. Also, there was no significant differences between dsRNA fragments targeting *TuVATPase* and *TuCOPB2*, indicating that correlation between dsRNA fragment size and RNAi responsiveness is a systematic feature of gene silencing in *T. urticae*. Interestingly, no significant differences were observed between fragments of the same length targeting the 5' or the 3' end of the 600 bp coding sequence for either *TuVATPase* or *TuCOPB2*. This indicates a negligible effect of the position of dsRNA within the target transcript, albeit within the coding region. From these series of experiment, a size-activity relationship was established: significant body-color changes frequency associated with RNAi response was measured with dsRNA sequence length equal or longer than 400 bp. These results suggest that a size cut-off of approximately 400 bp for a dsRNA is required to achieve significant effect against *T. urticae*.

### **Mixed *VATPase* dsRNA fragments**

To test whether the low RNAi efficiency caused by shorter dsRNA fragments was due to the low degree of sequence coverage, I used the combination of two short dsRNA fragments of 200 bp each (200 bp 5' and 200 bp 3'), to test whether they could reconstitute the RNAi effects observed when the dsRNA fragment of 400 bp (400 bp 5') was used. Interestingly, when both short fragments of 200 bp were combined (200 bp 5' and 200 bp 3'), the frequency of dark mites was similar to the one observed with the fragments of 200 bp 5' or 200 bp 3' alone with about 20% of the mites dark (Figure 10). As expected, the 400 bp

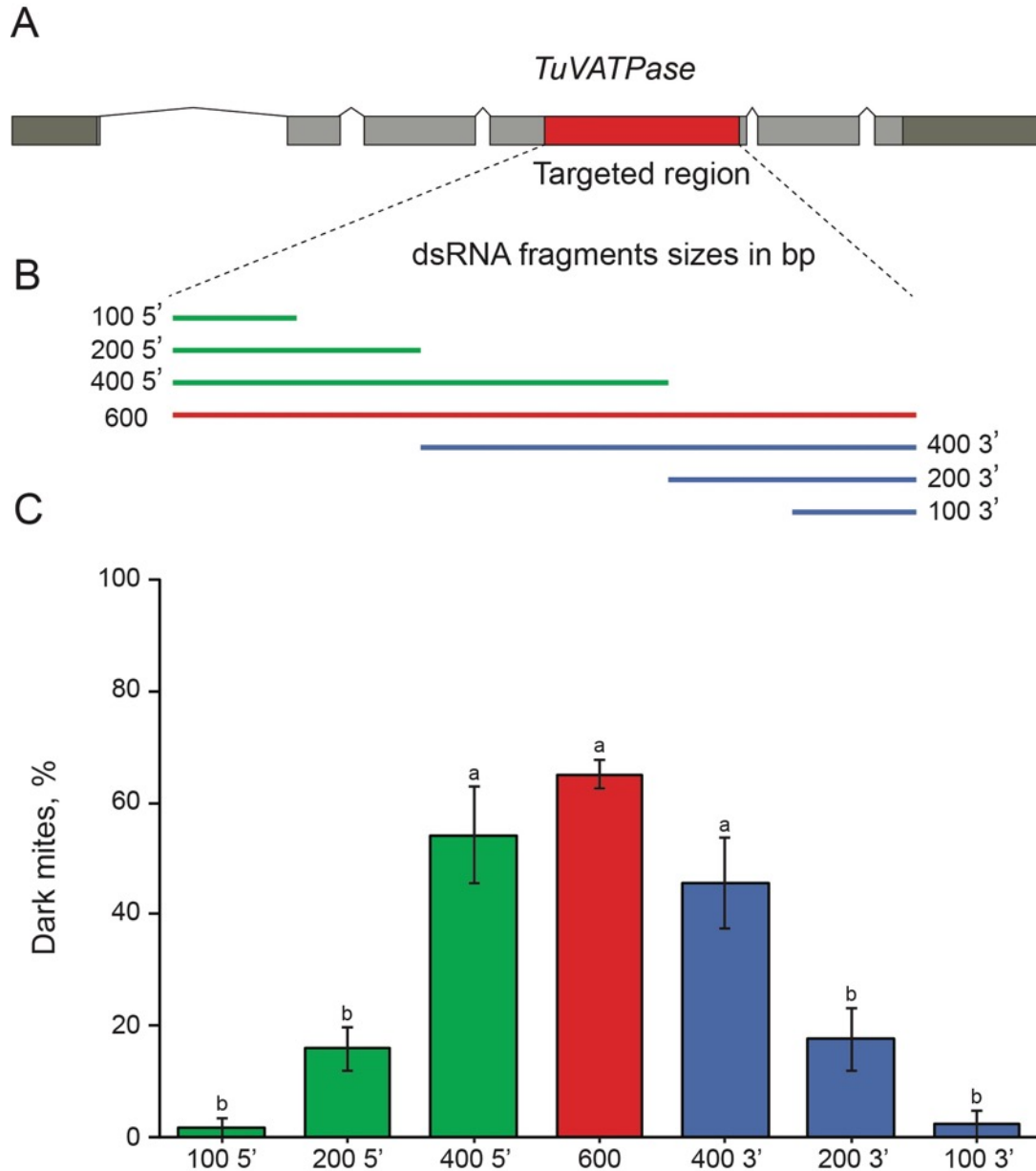


**Figure 4.8: The effect of dsRNA-*TuVATPase* sequence sizes and variability of gene regions targeted on RNAi efficiency.** Schematic representation of *TuVATPase* gene and location of the targeted region (A) represented by a red box. Schematic of dsRNA sequence sizes and position relative to the 3' end (solid green line) or 5' end (solid blue line) of the targeted region including the longest fragment of 600 bp (red solid line) (B). Frequency of dark-body mites after treatment with dsRNA-*TuVATPase*. Statistical analysis was performed using one-way ANOVA (Tukey HSD test). Means with the same letter are not significantly different from each other. (bars = mean  $\pm$  SE; \*,  $P < 0.05$ ).

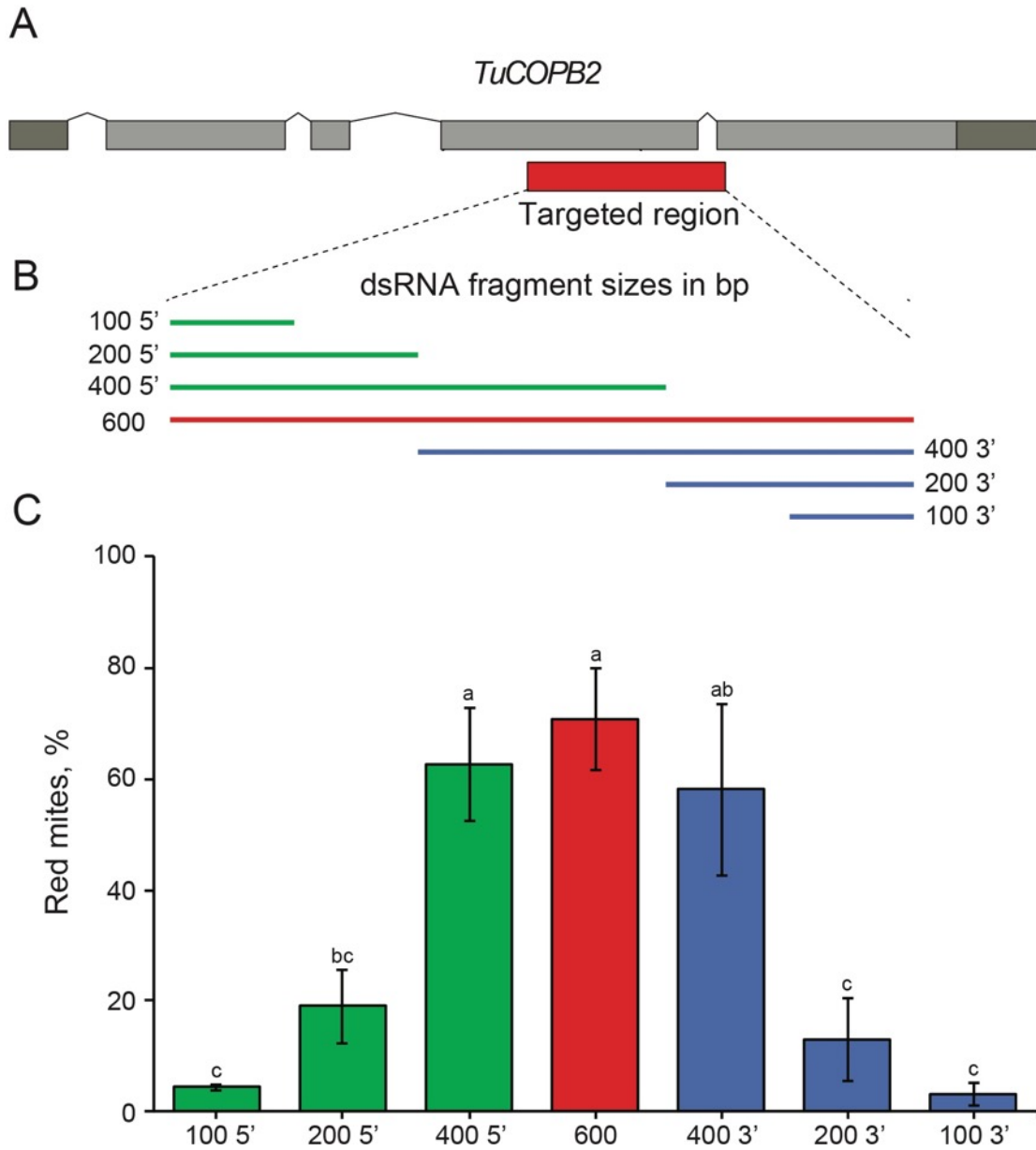


**Figure 4.9: The effect of dsRNA-*TuCOPB2* sequence sizes and variability of gene regions targeted on RNAi efficiency.** Schematic representation of *TuCOPB2* gene and location of the targeted region (A) represented by a red box. Schematic of dsRNA sequence sizes and position relative to the 3' end (solid green line) or 5' end (solid blue line) of the targeted region including the longest fragment of 600 bp (red solid line) (B). Frequency of red-body mites after treatment with dsRNA-*COPB2*. Statistical analysis was performed using one-way ANOVA (Tukey HSD test). Means with the same letter are not significantly different from each other. (bars = mean  $\pm$  SE; \*,  $P < 0.05$ ).

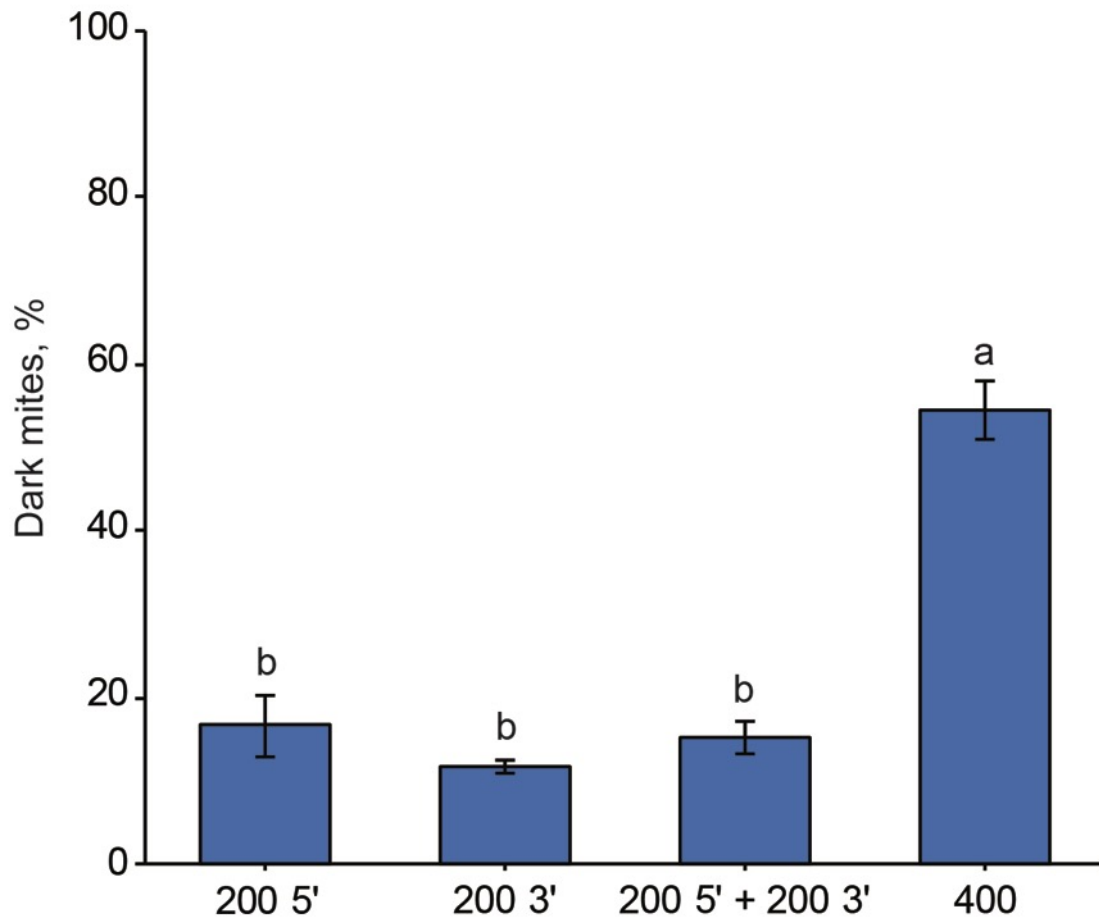


**Figure 4.10: The effect of mixed dsRNA-*TuVATPase* fragments on RNAi efficiency.** Bar graph are representing the frequency of dark mites from 3 independent replicates after soaking adult female in solution of dsRNA. Statistical analysis was performed using one-way ANOVA (Tukey HSD test). Means with the same letter are not significantly different from each other. (bars = mean  $\pm$  SE; \*,  $P < 0.05$ ).

fragment yielded the highest % of dark mites (about 58%), a significantly higher proportion than when dsRNA of 200 bp was used either as a mix (200 5' and 200 3') or individually. Therefore, the combination of the two short dsRNA fragments did not have an additive effect when compared to the 400 bp dsRNA fragment, suggesting that the absence of sequence diversity is not the cause of the ineffective RNAi response. Rather, it appears that the *T. urticae* RNAi machinery requires longer dsRNA fragments for its appropriate processing into a population of siRNAs.

## 4.4 Discussion

### 4.4.1 Induction of RNAi in dsRNA *TuCOPB2* soaked mites

In this study, soaking mites in a solution of dsRNA-*TuCOPB2* induced a change in body color correlated with an increase of mortality and a decrease of fecundity. Although, reduction of mite fitness seems to be correlated with application of dsRNA-*TuCOPB2*, the downregulation of *TuCOPB2* transcript must be confirmed by RT-qPCR. Unlike the treatment with dsRNA-*TuVATPase* displaying a dark phenotype in a subset of mites (Suzuki et al., 2017b), RNAi response to *COPB2* yielded red and small sized mites (Figure 4.2Ai and 4.2Aii). Interestingly, this phenotype was not observed in the treatment with dsRNA control (dsRNA-NC), dsRNA-*TuVATPase* nor in the rearing colony. However, similar to the treatments with dsRNA-*TuVATPase*, only a portion of the mites responded to dsRNA-*TuCOPB2* (51% with the fragment A and 62 % with the fragment B (Figure 4.3B)) supporting the hypothesis that RNAi phenotype penetration is limited to a fraction of mites due to the intrinsic property of the delivery method. Similarly to phenotypic change observed upon the application of dsRNA-*TuVATPase*, red body phenotype/reduced body size was not reported in study that delivered dsRNA-*TuCOPB2*-B through the floating leaf disk assay (Kwon et al., 2013). Even though delivery of dsRNA via soaking has been shown to have greater efficiency relative to the floating leaf disk assay when *TuVATPase* was targeted, that did not seem to be the case with dsRNA-*TuCOPB2* fragment: Kwon et al., (2013) reported mortality of 65,4 % of treated mites 5 days post feeding, while with the soaking method I recorded the mortality of 53% after 10 days of treatment. Rather, the difference may be in the ability of dsRNA delivered by soaking to reach tissues outside of the mite gut, especially because the *in situ* localization

of *COPB2* transcript is found in mite reproductive tissues rather than in the gut. Furthermore, when soaking treatments with dsRNA targeting *TuVATPase-B* and *TuCOPB2-B* are compared, mite fitness parameters were different. The mortality was higher with dsRNA treatment against *TuVATPase-B* (reaching about 80% compared to 53% with *TuCOPB2-B*), however the fecundity was much lower in dsRNA *TuCOPB2-B* treated mites than when *TuVATPase* was targeted (with about 0.5 eggs per female per day and 2.5 eggs per female per day, respectively). Whole-mount *in situ* hybridization revealed transcript accumulation of *TuCOPB2* in mite ovaries and the oviducts (Figure 4.6). These organs are essential for eggs development and maturation (Beament, 1951). Thereby disruption of vesicular trafficking function within these tissues is expected to impair egg formation and/or oviposition rates. However, despite detection of a strong localization signal of *COPB2* transcript in mite reproductive tissues, I cannot exclude the possibility that this gene is also expressed at the lower level in the gut. In the yellow fever mosquitoes *Aedes aegypti*, downregulation of the *COPI* subunit has been shown to disturb integrity of midgut epithelial cells (Zhou et al., 2011), ovaries follicular development and eggshell formation (Isoe et al., 2011). Interestingly, in the silkworm *Bombix mori*, suppression of *COPI* expression disrupted tube expansion of the posterior silk gland involved in fibroin secretion for silk formation. These studies highlight the wide spectrum of potential processes that *COPI* may participate in and its potential to be used as a biocontrol.

#### 4.4.2 Optimization of dsRNA soaking method and RNAi design

Although RNAi has become a valuable tool for reverse genetic studies in non-model organisms, parameters that associate with the successful RNAi may differ between living systems and need to be investigated. Until now, an obstacle towards RNAi optimization in *T. urticae* was the lack of a trackable phenotype that can be used as a proxy for the effectiveness of RNAi. Herein, I established two model targets, *TuVATPase* and *TuCOPB2*, whose silencing leads to easily scored phenotypes. Using these phenotypes to score effects of several experimental parameters I demonstrated a method to control for the dsRNA uptake. The food blue dye mixed with dsRNA-*TuVATPase-B* and dsRNA-*TuCOPB2-B* can be used to preselect treated mites that absorbed higher concentration of

dsRNA/blue dye solution. Such preselection increased the frequency of RNAi responses from 47% to 94% and 62% to 95% for dsRNA-*TuVATPase-B* and dsRNA-*TuCOPB2-B*, respectively (Figure 4.7). Moreover, this method allows a more accurate estimation of gene knockdown measurements as it allows a preselection of individuals that ingested the dye with dsRNA are selected. Bilgi et al., (2017) reported the use of the neutral red dye that was mixed with dsRNA. They showed that the target gene expression in red-stained aphids was significantly lower when compare to the treated aphids that were not selected for dye color. This method has been also reported successful in oral delivery in the fever mosquito, *Aedes aegypti* (Singh et al., 2013). Utilization of dyes as a proxy for the dsRNA uptake is particularly useful for studies where silencing of the target gene does not lead to visible phenotype. Combining dyes with such dsRNAs would enhance chances of discovering molecular or physiological changes associated with the target gene silencing that is expected to be present at high frequency in the selected population of treated arthropods, relative to a general treated population where phenotype may be present at relatively low frequency and thus harder to identify.

Also, I demonstrated the positive correlation between dsRNA size and RNAi efficiency. Long dsRNA fragment of at least 400 bp is required to trigger high RNAi response in spider mite. This can be explained by: 1) longer dsRNA is required to be efficiently process by the RNAi machinery; 2) longer dsRNA is needed to generate more diverse population of siRNA that have greater coverage of target sequence; or 3) longer dsRNA fragments are absorbed more efficiently by cells than shorter fragments. I showed that the combination of two dsRNA fragments of 200 bp covering 400 bp of the *VATPase* sequence target didn't have additive effect compare to each fragment alone and thus, despite the expected more diverse siRNA population generated and the higher number of siRNA molecules, longer dsRNA might be required for efficient dsRNA processing or can be absorb better by mite tissues than shorter fragments. Furthermore, a study using siRNA (21 bp) or dsRNA (130 bp) injected in *T. urticae* has shown a higher RNAi efficiency associated with development of phenotype concomitant with *DLL* disruption with siRNA, indicating that small RNAs of limited diversity is not a limitation for RNAi (Khila and Grbić, 2007). Similar observation was made in the western corn rootworm. Using a 240 bp dsRNA and a 21 bp siRNA labelled with a fluorochrome, Bolognesi et al.,



(2012) demonstrated that only the long dsRNA was successfully absorbed, localizing fluorescence in epithelial cells of the western corn rootworm larvae. In addition, they showed that a dsRNA fragment with 100% complementarity to the target is more efficient in inducing an RNAi when compared to a chimeric dsRNA fragment with the same length but with only 21 bp complementarity to its target. Similar conclusions have been drawn in a study using the red flour beetle *Tribolium castaneum* (Miller et al., 2012). Although further experiments need to be carried out to complete characterization of *COPB2* in mite I showed the effectiveness of the soaking method. Furthermore, I initiated an understanding of RNAi process in *T. urticae* and provided tools to enhance its efficiency.

In summary, I developed optimized method for RNAi delivery and demonstrated the use of dyes to control dsRNA uptake and the requirement of a long fragment to enhance RNAi response. I also established a time- and cost-effective pipeline for functional analysis of mite genes, including a PCR method for template preparation and for synthesizing dsRNA fragments, RNA labeled probes, paving new avenues for reverse genetics approach in spider mite.

## 4.5 Reference

- Baum, J. A., Bogaert, T., Clinton, W., Heck, G. R., Feldmann, P., Ilagan, O., et al. (2007). Control of coleopteran insect pests through RNA interference. *Nat Biotech* 25, 1322–1326.
- Beament, J. L. (1951). The structure and formation of the egg of the fruit tree red spider mite, *Metatetranychus ulmi* Koch. *Ann. Appl. Biol.* 38, 1–24.
- Bensoussan, N., and Grbić, V. (2017). RNA interference in the two-spotted spider mite *Tetranychus urticae*. *Int. Organ. Biol. Integr. Control.* 124, 200–206. Available at: <http://journal.frontiersin.org/article/10.3389/fpls.2016.01105/full>.
- Bilgi, V., Fosu-Nyarko, J., and Jones, M. G. K. (2017). Using vital dyes to trace uptake of dsRNA by green peach aphid allows effective assessment of target gene knockdown. *Int. J. Mol. Sci.* 18, 80.
- Bolognesi, R., Ramaseshadri, P., Anderson, J., Bachman, P., Clinton, W., Flannagan, R., et al. (2012). Characterizing the mechanism of action of double-stranded RNA activity against western corn rootworm (*Diabrotica virgifera virgifera* LeConte). *PLoS One* 7, e47534.
- Ding, S. W., and Voinnet, O. (2007). Antiviral immunity directed by small RNAs. *Cell.* 130, 413–426.
- Fire, A., Xu, S., Montgomery, M. K., Kostas, S. A., Driver, S. E., and Mello, C. C. (1998). Potent and specific genetic interference by double-stranded RNA in *Caenorhabditis elegans*. *Nature.* 391, 806–811.
- Grbic, M., Leeuwen, T., Clark, R. M., Rombauts, S., Rouze, P., and Grbic, V. (2011). The genome of *Tetranychus urticae* reveals herbivorous pest adaptations. *Nature.* 479, 487–492.
- Hammond, S. M., Bernstein, E., Beach, D., and Hannon, G. J. (2000). An RNA-directed nuclease mediates post-transcriptional gene silencing in *Drosophila* cells. *Nature.* 404, 293–296.
- Isoe, J., Collins, J., Badgandi, H., Day, W. A., and Miesfeld, R. L. (2011). Defects in coatamer protein I (COPI) transport cause blood feeding-induced mortality in Yellow Fever mosquitoes. *Proc. Natl. Acad. Sci.* 108, 211–217.
- Jonckheere, W., Dermauw, W., Zhurov, V., Wybouw, N., Van den Bulcke, J., Villarroel, C. A., et al. (2016). The salivary protein repertoire of the polyphagous spider mite *Tetranychus urticae*: A quest for effectors. *Mol. Cell. Proteomics.* 15, 3594–3613.
- Khila, A., and Grbić, M. (2007). Gene silencing in the spider mite *Tetranychus urticae*:

- dsRNA and siRNA parental silencing of the *Distal-less* gene. *Dev. Genes Evol.* 217, 241–251.
- Kwon, D. H., Park, J. H., Ashok, P. A., Lee, U., and Lee, S. H. (2016). Screening of target genes for RNAi in *Tetranychus urticae* and RNAi toxicity enhancement by chimeric genes. *Pestic. Biochem. Physiol.* 130, 1–7.
- Kwon, D. H., Park, J. H., and Lee, S. H. (2013). Screening of lethal genes for feeding RNAi by leaf disc-mediated systematic delivery of dsRNA in *Tetranychus urticae*. *Pestic. Biochem. Physiol.* 105, 69–75.
- Mao, J., Zhang, P., Liu, C., and Zeng, F. (2015). Co-silence of the *coatomer β* and *v-ATPase A* genes by siRNA feeding reduces larval survival rate and weight gain of cotton bollworm, *Helicoverpa armigera*. *Pestic. Biochem. Physiol.* 118, 71–76.
- Meister, G., and Tuschl, T. (2004). Mechanisms of gene silencing by double-stranded RNA. *Nature.* 431, 343–349.
- Mello, C. C., and Conte, D. (2004). Revealing the world of RNA interference. *Nature.* 431, 338–342.
- Miller, S. C., Miyata, K., Brown, S. J., and Tomoyasu, Y. (2012). Dissecting systemic RNA interference in the red flour beetle *Tribolium castaneum*: Parameters affecting the efficiency of RNAi. *PLoS One* 7, e47431.
- Obbard, D. J., Gordon, K. H. ., Buck, A. H., and Jiggins, F. M. (2009). The evolution of RNAi as a defence against viruses and transposable elements. *Philos. Trans. R. Soc. B Biol. Sci.* 364, 99–115.
- Ramadan, N., Flockhart, I., Booker, M., Perrimon, N., and Mathey-Prevot, B. (2007). Design and implementation of high-throughput RNAi screens in cultured *Drosophila* cells. *Nat. Protoc.* 2, 2245–2264.
- Razi, M., Chan, E. Y. W., and Tooze, S. A. (2009). Early endosomes and endosomal coatomer are required for autophagy. *J. Cell Biol.* 185, 305–321.
- Singh, A. D., Wong, S., Ryan, C. P., and Whyard, S. (2013). Oral Delivery of double-stranded RNA in larvae of the yellow fever mosquito, *Aedes aegypti*: implications for pest mosquito control. *J. Insect Sci.* 13, 69.
- Suzuki, T., España, M. U., Nunes, M. A., Zhurov, V., Dermauw, W., Osakabe, M., et al. (2017a). Protocols for the delivery of small molecules to the two-spotted spider mite, *Tetranychus urticae*. *PLoS One* 12, e0180658.

- Suzuki, T., Nunes, M. A., España, M. U., Namin, H. H., Jin, P., Bensoussan, N., et al. (2017b). RNAi-based reverse genetics in the chelicerate model *Tetranychus urticae*: A comparative analysis of five methods for gene silencing. *PLoS One*. 12, e0180654.
- Wang, Y.-N., Wang, H., Yamaguchi, H., Lee, H.-J., Lee, H.-H., and Hung, M.-C. (2010). COPI-mediated retrograde trafficking from the Golgi to the ER regulates EGFR nuclear transport. *Biochem. Biophys. Res. Commun.* 399, 498–504.
- Whalon, M. E., Mota-Sanchez, D., and Hollingworth, R. (2016). Arthropod Pesticide Resistance Database, Michigan State University. Available at: <http://www.pesticideresistance.org/index.php>.
- Whitney, J. A., Gomez, M., Sheff, D., Kreis, T. E., and Mellman, I. (1995). Cytoplasmic coat proteins involved in endosome function. *Cell* 83, 703–13.
- Whyard, S., Singh, A. D., and Wong, S. (2009). Ingested double-stranded RNAs can act as species-specific insecticides. *Insect Biochem. Mol. Biol.* 39, 824–832.
- Zhou, G., Isoe, J., Day, W. A., and Miesfeld, R. L. (2011). Alpha-COPI coatomer protein is required for rough endoplasmic reticulum whorl formation in mosquito midgut epithelial cells. *PLoS One* 6, e18150.

## Chapter 5

### 5 Summary and Discussion

#### 5.1 *T. urticae* feeding and plant damage

The first objective of my thesis was to determine the immediate damage on host plant caused by *T. urticae* feeding. To date this study was the first to establish the direct consequence of mite feeding. Following individual mites, I established that the duration of a single feeding event ranged from a few minutes to more than half an hour, with an average time spent per feeding site of about 13 minutes. This finding was surprising, as the previous literature suggested (Liesering, 1960 and others in the field) that mites consume an average of 20 cells per minute. Upon feeding, there were no macroscopic changes at the feeding site. Thus, a chlorotic spot that is a typical plant symptom of spider mite feeding is not an immediate consequence of mite feeding, but rather results from the plant response triggered by mite feeding.

Furthermore, using a histochemical approach, I identified that plant damage caused directly by mite feeding is limited to a single mesophyll cell that was underneath the intact epidermal layer. My findings contrast the published images of macroscopic damage and epidermal injuries resulting from *T. urticae* feeding (Campbell et al., 1990; Park and Lee, 2002). The main difference between my report and previous studies was in the time when the analysis was performed. While others made their observations after days and even weeks post feeding, I was recording changes that were limited to the initial 10 minutes of mite feeding and were thus happening within the feeding event. Differences in the observed damage thus indicate that excessive cell death that is seen over longer period of time of mite feeding also depends on plant responses that influence the degree of tissue injury. Such indirect effects might be originated from mechanical or chemical damaged from the feeding cells that have a stressful impact on the organism or the cells and tissues adjacent to the punctured cell which can result in destruction of the stomatal apparatus (Sances et al., 1979) or a reduction of leaf thickness (Mothes and Seitz, 1981).

*T. urticae*, has been reported to feed preferentially on the lower epidermis (Foott, 1963; Morimoto et al., 2006; Osakabe et al., 2006), to avoid deleterious effects of UV (Ohtsuka and Osakabe, 2009) or the rain (Jeppson et al., 1975). In my experimental set up mite feeding was restricted to one side of the leaf. Regardless of the epidermis surface mites fed from, cells immediately underneath the epidermis were most frequently injured, despite the mite's ability to reach any leaf layer with the stylet, indicating no preference of cell type mites consume. Several reports have been suggested that metabolism activity (Mokronosov et al., 1973; Outlaw et al., 1976; Seeni and Gnanam, 1983) and protein content (Shen and Outlaw, 1989) was similar between cells from the spongy and the palisade layer relative to their chloroplast number suggesting similar nutrient quality in both cell type. In some cases, I observed a cluster of dead cells (a maximum of 3 dead cells) in the spongy and palisade layers upon mite feeding, but at very low frequency. Interestingly, when more than one cell was injured, damaged cells were localized on the stylet trajectory, making it possible that mite fed on these cells sequentially: after feeding on the first cell underneath the epidermis, mites may have punctured deeper, below the first empty cell.

The second objective of my thesis was to reconstitute *T. urticae* stylet pathway, as mites feeding from the internal leaf tissues resulted of non-visible damaged on the epidermis. This was a challenging task, as mites readily retract their stylets upon any disturbance. I successfully developed an experimental protocol that allowed the preparation of histological samples that capture mites in the feeding position, and have developed a fixation procedure that preserved the integrity of both plant and mite tissues that were previously frozen in liquid nitrogen. Using a histological cross section of a mite feeding on host plant, I visualized for the first time plant cells that were targeted by the *T. urticae* stylet. I estimated the length of the stylet of about 150  $\mu\text{m}$  which was consistent with the range observed by other authors (100-150  $\mu\text{m}$ ; Avery and Briggs, 1968; Ekka, 1969; Sances et al., 1979). The stylet length, mite density and host plant characteristic may have an impact on the depth and level of injuries (Mothes and Seitz, 1981; Sances et al., 1979; Summers and Stocking, 1972). For instance, the brown mite *B. rubrioculus* feeding from the upper epidermis is limited to the cells from the palisade layer estimated to be 90  $\mu\text{m}$  thick while its stylet was estimated to be 95  $\mu\text{m}$  (Summers and Stocking, 1972).

Likewise, in contrast to my observation of *T. urticae* stylet insertion following a by straight route into the mesophyll layer, the brown mite *B. rubrioculus* stylet is capable of lateral flexion, splaying outward to cut obliquely into the sidewalls of palisade cells which may increase the sphere of damage and more severe injuries in this mesophyll layer compare to *T. urticae* feeding habit. In addition, I observed stylet insertion between epidermal cells as the most frequent pattern, explaining the lack of visible injuries to these cells. In one case, the stylet was inserted through a stomata, a pattern that appears less frequent in *T. urticae* but seems to be an obligatory path for *T. lintearius* that feeds on gorse, a plant with very thick cuticle (Marriott et al., 2013). In this context, it will be interesting to determine if *T. urticae* as well uses stomatal leaf apparatus in hosts with thick cuticle. If *T. urticae* is able to modify its feeding, it may be a reflection of mite's ability to sense the physical properties of leaf surface and to adjust its feeding behavior accordingly. Lack of epidermal cellular injuries were observed when mites were feeding on apple or strawberry leaves (Sances et al., 1979; Tanigoshi and Davis, 1978). However, some authors have observed epidermal damage resulting from *T. urticae* feeding on cucumber and strawberry (Campbell et al., 1990; Park and Lee, 2002). Although, these observations were made days or week post feeding, time for which, plant response can influence the degree of injury.

Analysis of several independent serial cross sections didn't reveal damage in the cells neighboring the feeding cell as suggested by Kielkiewicz (1981) in strawberry leaves. Although, I was not able to see this feature, the time set for this experiment of 10 minutes of feeding and tissue processing might not allowed me to visualize this effect, if it is an indirect consequence of feeding. However, I observed cytological changes of cell content happened in the punctured cells: in most cells, there was a complete or partial removal of cell content or coagulated chloroplast were seen in cells in which the stylet was inserted, similar to cytological changes observed in strawberry, apple, citrus and cucumber (Albrigo et al., 1982; Park and Lee, 2002; Summers and Stocking, 1972; Tanigoshi and Davis, 1978).

Some authors have suggested action of salivary glands in the secretion of hydrolytic enzymes into plant cells for a pre-oral digestion. For instance, Mothes and Seitz (1981)

suggested destruction of the outer chloroplast membrane by salivary enzymes as only thylakoid granules were found in the esophagus and the ventriculus. Alternatively, enzymes may be secreted into the midgut lumen, however this hypothesis has not been demonstrated. In contrast, they propose sequential digestion in which, a first external pre-digestion within the plant cell is processed and subsequently, internal digestion takes place upon nutrient uptake into specialized cells, derived from midgut epithelium hydrolyzing thylakoid granules, chlorophyll and cell membrane by amylase activity. In this thesis, I brought new and strong evidence reinforcing a feeding model in which a pre-oral digestion occurred prior to the uptake of cellular content by the mite: 1) the stylet diameter of 2  $\mu\text{m}$  is small relative to several microns for plant cell organelles, and 2) the relatively long period of feeding time of about 13 minutes would support an existence of enzymatic breakdown of cellular content *in situ*. If pre-oral digestion exists, then the question remains if it is dependent on mite-produced enzymes that are secreted to the feeding cell by the stylet, or plant enzymes that are released from their storage compartments upon feeding (e.g. the central vacuole bursts upon stylet penetration), or there is involvement of digestive enzymes contributed by both interactive organisms. Likewise, histological section suggested a feeding model in which the mite uses the stylet as a channel for food uptake and salivary secretion. First, I showed that, no cellular debris or membrane were stained in the apoplast adjacent to the injured cell and secondly, in most of the section the stylet was protracted outside the mouth and visualized within the plant cell.

## 5.2 RNAi establishment and further optimization in *T. urticae* through soaking in dsRNA

The second part of my thesis was to further develop RNAi as a reverse genetic tool that is required for the functional characterization *T. urticae* genes and to prepare large-scale systematic RNAi screens as a first step towards the development of specific RNA-based pesticide.

As previously demonstrated, injection of dsRNA into *T. urticae* female abdomen resulted in RNAi in embryos and caused developmental aberrations associated with downregulation of the targeted gene (Khila and Grbic, 2007). Moreover, sequence



analysis of the *T. urticae* genome uncovered a complete RNAi machinery. Only recently, Kwon et al., (2013) demonstrated efficient RNAi through oral delivery using a floating leaf disc in solution of dsRNA. However, this method was not suitable for high throughput screening, as it requires a lot of dsRNA quantity that needs to be refreshed on a daily basis. In our laboratory, a soaking method was under development, consisting of the immersion of synchronized adult female mites into a solution of dsRNA (Suzuki et al., 2017).

The objective of my thesis was to further develop the RNAi soaking method. I first used the *VATPase* as a target gene, as successful silencing of this gene in other arthropods systems induced to a measurable fitness reduction (Baum et al., 2007; Kwon et al., 2013; Upadhyay et al., 2011; Whyard et al., 2009; Zhu et al., 2011). Moreover, the oral delivery method using leaf disc floating on dsRNA against *TuVATPase* was successful to trigger RNAi in *T. urticae* (Kwon et al., 2013). I established that RNAi had incomplete phenotypic penetration, leading to the efficient silencing of the target in only a portion of the treated mites. I further confirmed that the low RNAi phenotypic penetration was intrinsic to the delivery method and was not due to the potential genetic variation in loci that could affect RNAi response among treated mites. Subsequently, I investigated the individual parameters of the delivery method, to see if I can increase the RNAi efficiency. I first established *COPB2*, involved in vesicular trafficking, as additional target for RNAi as it wasao *et* 2011) and in *T. urticae* (Kwon et al., 2013). RNAi targeting both *VATPase* and *COPB2* resulted in visible phenotypes, dark and red mite body color, respectively. Using these phenotypes, I tested different parameters to increase RNAi efficiency. First, I developed a method consisting of a mixture of dsRNA and a food dye, to preselected mites that have ingested dsRNA and enriched the pool of mites responding to RNAi. Second, I demonstrated that longer dsRNA fragments are more efficient in triggering RNAi in spider mites. Combining these two changes into a revised protocol, I was able to achieve RNAi in more than 95% of preselected treated mites.

A critical remaining issue for the efficacy of gene silencing is the differential accessibility of tissues to supplied dsRNA, especially since delivery of fluorescently labeled dsRNA fragments demonstrated that most of the fluorescence remained in the

mite gut (Suzuki et al., 2017). To address the accessibility of the tissue to dsRNA, there is a need to assess the ability of dsRNAs to silence a set of test genes for which the expression patterns have been defined in a specific domain in the mite body. I have previously determined the expression patterns of several genes via whole mount *in situ* hybridization (Appendix 4) that identified different domains within the mite body. By delivering dsRNA directed against each of those genes, one can compare the effectiveness of dsRNA penetration to each of these domains by quantifying the extent of gene downregulation. Based on these results, one can select gene targets, expressed in the gut and/or outside the gut as a model target genes to compare the efficiency of dsRNA delivery. Moreover, chemically modify dsRNA and carrier such as lipofectamine could be tested to enhance RNAi response.

Another interesting future initiative would be to test the ability to silence multiple genes within a gene family by targeting conserved sequence within the coding region. To specifically test the ability to silence multiple members of the gene family, dsRNAs against conserved sequences of the members of the gene family could be designed and tested for their effect by monitoring the expression of individual family members via locus-specific RT-qPCR. These results will be a useful method for functional analysis of gene families in *T. urticae*.

Understanding the molecular mechanisms underlying the successful adaptation of *T. urticae* on a broad range of plant species has become essential to understanding the mutual interaction between plants and spider mites. The availability of efficient reverse genetic tools that are currently under development for spider mites, combined with resources available for plant models such *Arabidopsis* and the tomato host plant, will help reveal the fundamental processes governing plant-spider mite interactions.

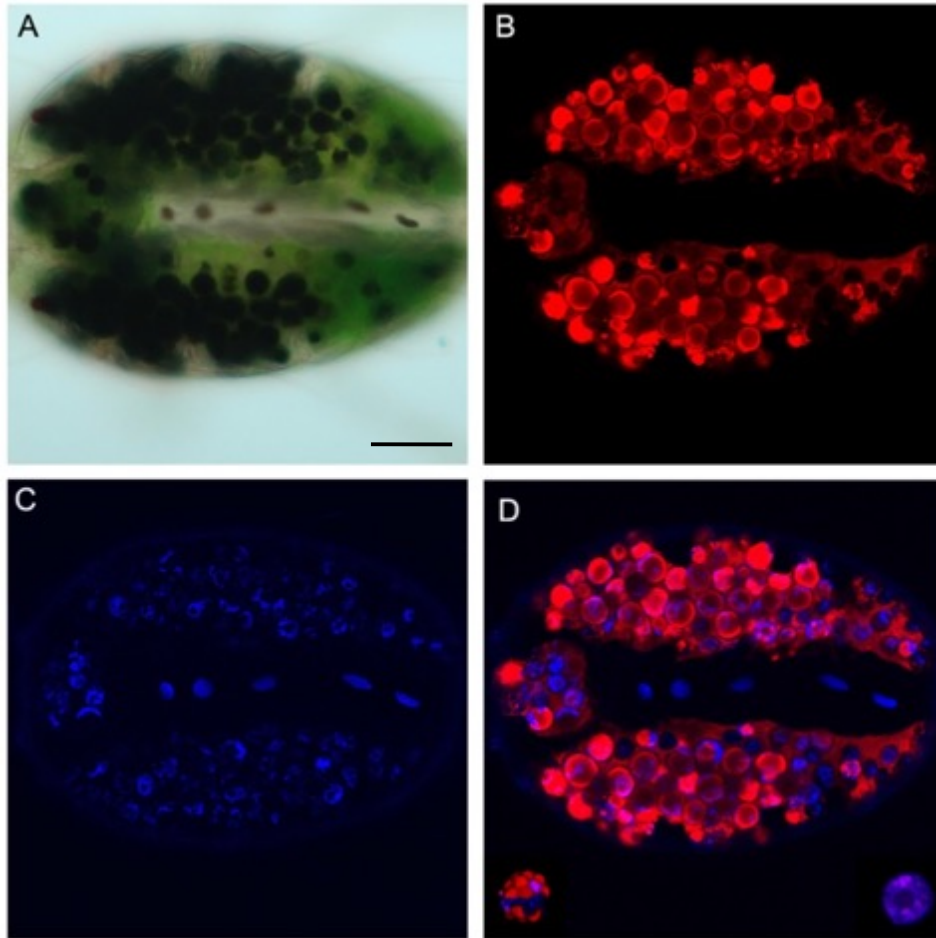
### 5.3 Reference

- Albrigo, L., Childers, C., and Syvertsen, J. (1981). Structural damage to citrus leaves from spider mite feeding. *Proc. Int. Soc. Citriculture* 2, 649–652.
- Avery, D. J., and Briggs, J. B. (1968). The aetiology and development of damage in young fruit trees infested with fruit tree red spider mite, *Panonychus ulmi* (Koch). *Ann. Appl. Biol.* 61, 277–288.
- Baum, J. A., Bogaert, T., Clinton, W., Heck, G. R., Feldmann, P., Ilagan, O., et al. (2007). Control of coleopteran insect pests through RNA interference. *Nat Biotech* 25, 1322–1326.
- Campbell, R. J., Grayson, R. L., and Marini, R. P. (1990). Surface and ultrastructural feeding injury to strawberry leaves by the twospotted spider mite. *Hortscience*. 25, 948–951.
- Ekka, I. (1969). *The Rearing of the Two-Spotted Spider Mite (Tetranychus urticae Koch) on Artificial Diets*. Ph. D. McGill University.
- Foott, W. H. (1963). Competition between two species of mites.: II. Factors influencing intensity. *Can. Entomol.* 95, 45–57.
- Jeppson, L. R., Keifer, H. H., and Baker, E. W. (1975). *Mites injurious to economic plants*. Berkeley: University of California Press.
- Kielkiewicz, M. (1981). *Physiological, anatomical and cytological changes in leaves of two strawberry varieties (Fragaria grandiflora Duch) resulting from feeding by the two-spotted spider mite (Tetranychus urticae Koch)*. Dissertation, Agricultural University of Warsaw.
- Kwon, D. H., Park, J. H., and Lee, S. H. (2013). Screening of lethal genes for feeding RNAi by leaf disc-mediated systematic delivery of dsRNA in *Tetranychus urticae*. *Pestic. Biochem. Physiol.* 105, 69–75.
- Liesering, R. (1960). Beitrag zum phytopathologischen Wirkungsmechanismus von *Tetranychus urticae* (Koch) (Tetranychidae, Acari). *Z. Naturforsch.* 67, 524–542.
- Marriott, J., Florentine, S., and Raman, A. (2013). Effects of *Tetranychus lintearius* (Acari: Tetranychidae) on the structure and water potential in the foliage of the invasive *Ulex europaeus* (Fabaceae) in Australia. *Int. J. Acarol.* 39, 275–284.
- Mokronosov, A., Bagautdinova, R., Bubnova, E., and Kobeleva, I. (1973). Photosynthetic metabolism in palisade and spongy tissues of the leaf. *Sov. Plant Physio.* 20, 1013–1018.

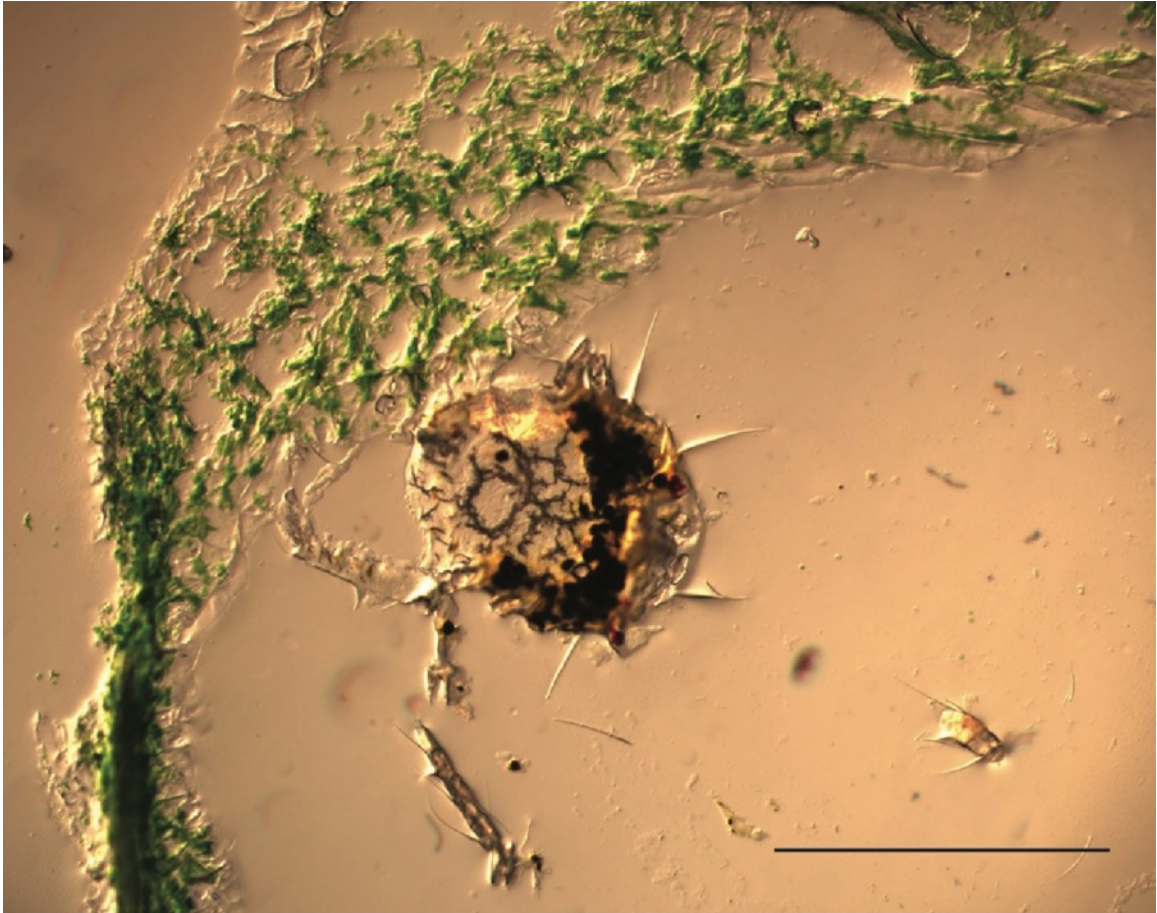
- Morimoto, K., Furuichi, H., Yano, S., and Osakabe, M. (2006). Web-mediated interspecific competition among spider mites. *J. Econ. Entomol.* 99, 678–684.
- Mothes, U., and Seitz, K. a. (1981). Fine structure and function of the prosomal glands of the two-spotted spider mite, *Tetranychus urticae* (Acari, Tetranychidae). *Cell Tissue Res.* 221, 339–349.
- Ohtsuka, K., and Osakabe, M. M. H. (2009). Deleterious effects of UV-B radiation on herbivorous spider mites: they can avoid it by remaining on lower leaf surfaces. *Environ. Entomol.* 38, 920–9.
- Osakabe, M., Hongo, K., Funayama, K., and Osumi, S. (2006). Amensalism via webs causes unidirectional shifts of dominance in spider mite communities. *Oecologia.* 150, 496–505.
- Outlaw, W. H., Schmuck, C. L., and Tolbert, N. E. (1976). Photosynthetic carbon metabolism in the palisade parenchyma and spongy parenchyma of *Vicia faba* L. *Plant Physiol.* 58, 186–189.
- Park, Y.-L., and Lee, J.H. (2002). Leaf cell and tissue damage of cucumber caused by twospotted spider mite (Acari: Tetranychidae). *J. Econ. Entomol.* 95, 952–957.
- Sances, F. V, Wyman, J. A., and Ting, I. P. (1979). Morphological responses of strawberry leaves to infestations of twospotted spider Mite. *J. Econ. Entomol.* 72, 710–713.
- Seeni, S., and Gnanam, A. (1983). Photosynthesis in cell Suspension culture of a C4 plant, *Gisekia pharnaceoides* L. *Plant Cell Physiol.* 24, 1033–1041.
- Shen, L., and Outlaw, W. H. (1989). Two-dimensional protein profiles of palisade parenchyma and of spongy parenchyma of *Vicia faba* leaf. *Physiol. Plant.* 77, 599–605.
- Summers, F. M., and Stocking, C. R. (1972). Some immediate effects on almond leaves of feeding some by *Bryobia rubrioculus* (Scheuten). *Acarologia.* 14, 170–178.
- Suzuki, T., España, M. U., Nunes, M. A., Zhurov, V., Dermauw, W., Osakabe, M., et al. (2017). Protocols for the delivery of small molecules to the two-spotted spider mite, *Tetranychus urticae*. *PLoS One* 12, e0180658.
- Tanigoshi, L. K., and Davis, R. W. (1978). An Ultrastructural study of *Tetranychus mcdanieli* feeding injury to the leaves of “Red Delicious” apple (Acari: Tetranychidae). *Int. J. Acarol.* 4, 47–51.
- Upadhyay, S. K., Chandrashekar, K., Thakur, N., Verma, P. C., Borgio, J. F., Singh, P. K., et al. (2011). RNA interference for the control of whiteflies (*Bemisia tabaci*) by oral route. *J. Biosci.* 36, 153–161.

- Whyard, S., Singh, A. D., and Wong, S. (2009). Ingested double-stranded RNAs can act as species-specific insecticides. *Insect Biochem Mol Biol.* 39, 824–832.
- Zhu, F., Xu, J., Palli, R., Ferguson, J., and Palli, S. R. (2011). Ingested RNA interference for managing the populations of the Colorado potato beetle, *Leptinotarsa decemlineata*. *Pest Manag. Sci.* 67, 175–182.

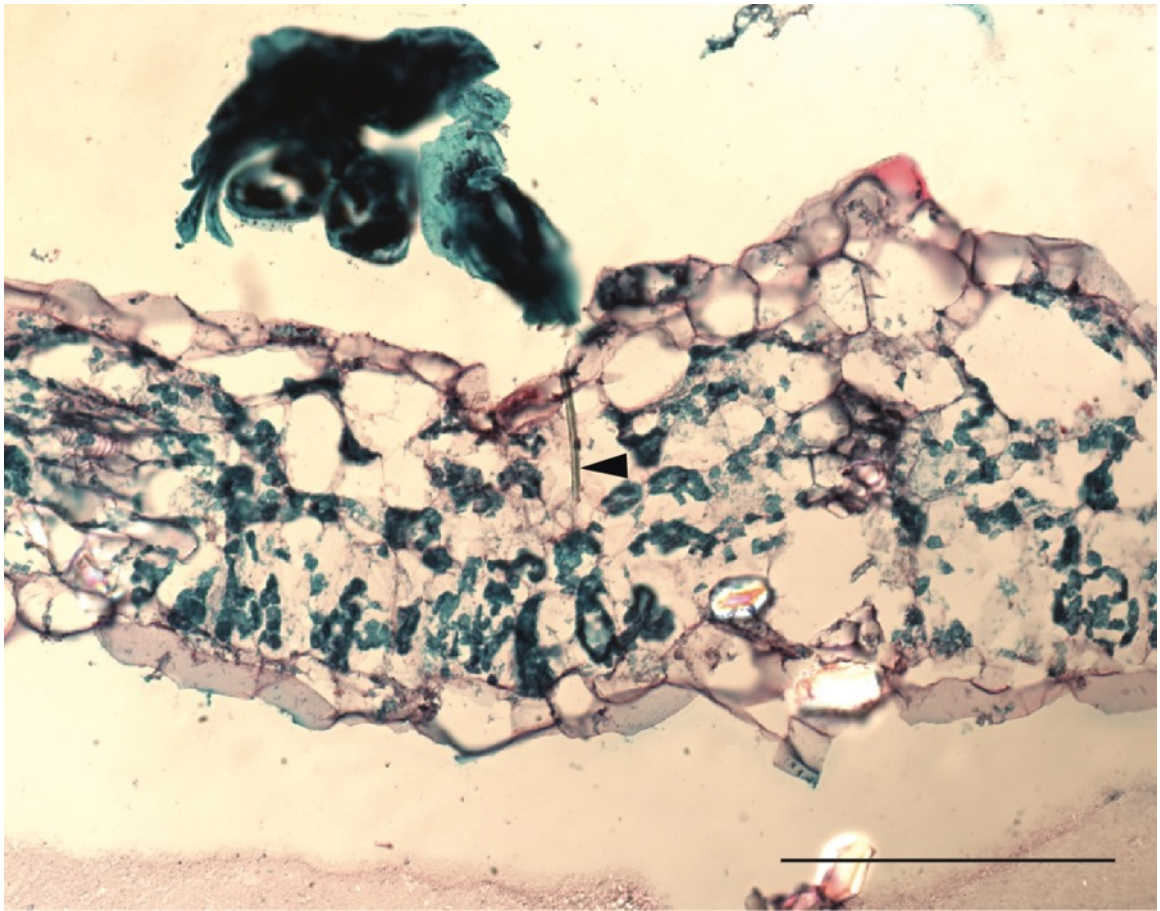
## 6 List of Appendices



**Appendix 1: Brightfield and confocal microscopy observation of fecal pellets and crystals of guanine in *T. urticae*.** (A) Dorsal view of *T. urticae* female with the mouth oriented to the left observed in brightfield. (B) Fecal pellet representing the chlorophyll degradation visualized with confocal microscopy using 633 nm wavelength excitation and a LP of 650 nm. (C) Crystals of guanine presents mostly in the excretory organ visualized with confocal microscopy using 543 nm wavelength excitation and a LP of 650 nm. (D) Merge of autofluorescence from B and C. (scale bar applies in all panel: 100  $\mu\text{m}$ ).

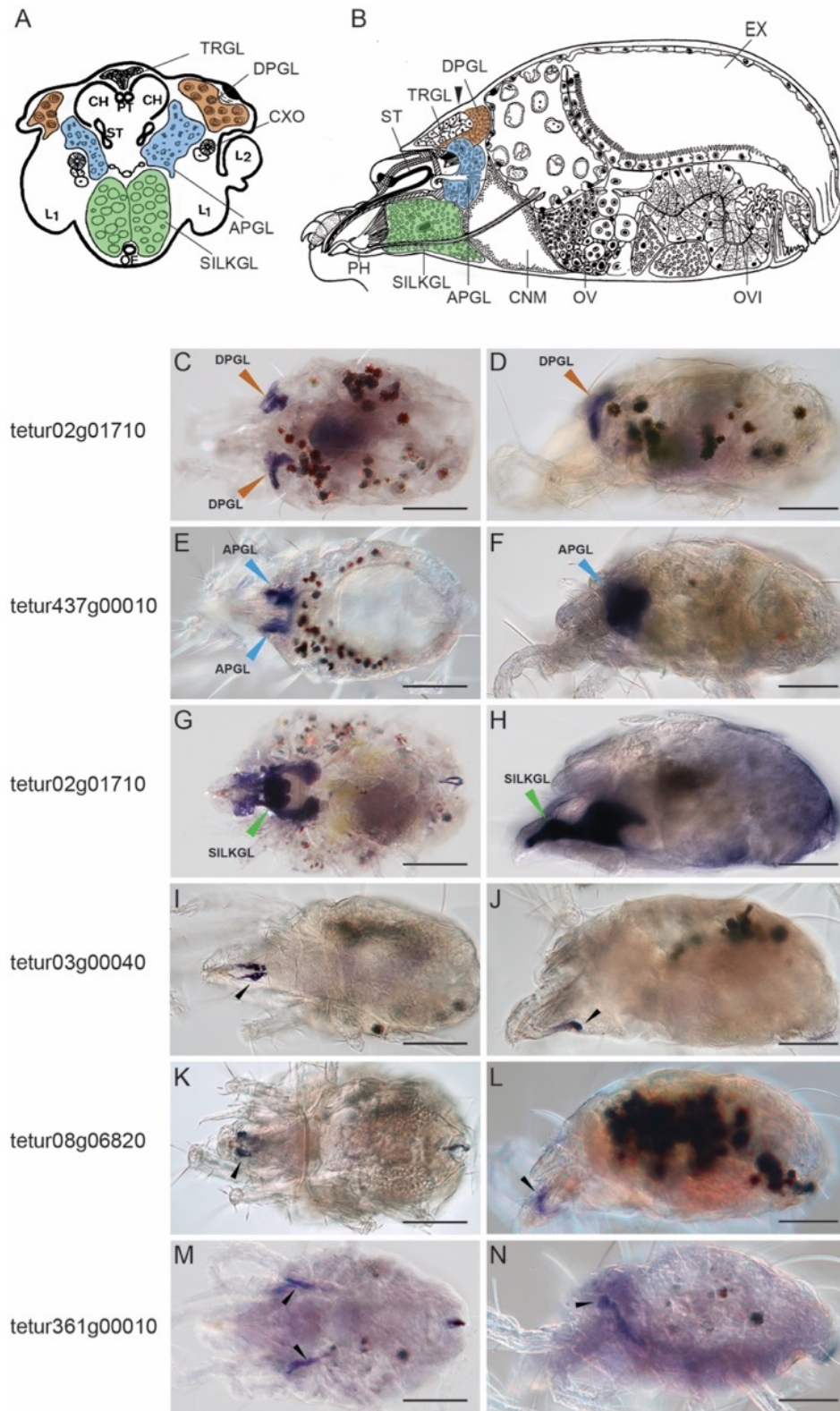


**Appendix 2: Representative picture of a cryosection of a mite feeding on a bean leaf previously frozen and embedded in optimal cutting temperature compound (OCT compound). The leaf section is on the top and part of the body mite with detached legs is on the bottom. The section thickness is about 50  $\mu\text{m}$ . (Scale bar: 500  $\mu\text{m}$ ).**



**Appendix 3: Representative picture of a microtome section of a mite feeding on a bean leaf previously frozen, fixed, dehydrated and embedded in paraffin. The arrow indicated the stylet within the plant tissue. The section is about 10 $\mu$ m thick. (Scale bar: 250  $\mu$ m.)**





**Appendix 4: Expression pattern of selected genes, highly expressed in mite's head using whole-mount RNA *in situ* hybridization.** (A) Schematic representation of a cross section of adult *T. urticae* female prosoma between legs 1 and 2 (Adapted from Mothes and Seitz, 1981). (B) Schematic representation of a sagittal section of a female *T. urticae* (adapted from Alberti and Crooker, 1985). In these two diagrams, the dorsal podocephalic glands (DPGL) are colored in orange, the anterior podocephalic glands (APGL) are colored in blue and the silk glands (SILKGL) are colored in green. The black arrow in the Figure B indicates the location of the section in the prosoma corresponding to the Figure A. (C-N) Expression patterns of selected genes using *in situ* hybridization with an antisense RNA probe DIG labelled. The purple signal was developed using anti DIG antibodies conjugated with AP enzyme in presence of NBT and BCIP substrates. On the far left the tetur ID corresponding to each panel. Figures C and E, dorsal view; Figure G, I, K and M, ventral view; Figures D, F, H, J, L and N, lateral view. On the panels C and D, the orange arrows show the signal development corresponding to DPGL, (tetur02g01710) whereas in the panel E and F, the signal corresponds to the APGL and shown with the green arrows, (tetur437g00010). In panels G and H, the green arrows indicate the silk glands, (tetur02g01710). The black arrows in panels I to N show expression domain in non-identified organs. CNM: central nervous mass; OV: ovaries; OVI: oviduct; EX: excretory organ; TRGL: tracheal gland; ST: stylet; PH: pharynx; CXO: coxal organ. The bars in panels C to N indicates 100  $\mu$ m.

## Curriculum Vitae

**Name:** Nicolas Bensoussan

**Post-secondary Education and Degrees:** Université Paul Sabatier  
Toulouse, France  
2007-2009 B.A.

Université Paul Sabatier  
Toulouse, France  
2009-2011 M.A.

The University of Western Ontario  
London, Ontario, Canada  
2012-2017 Ph.D.

**Awards:** Plant biology conference  
Second price for poster presentation  
2015

International conference of  
Travel award: 1500€  
2017

**Related Work Experience** Teaching Assistant  
The University of Western Ontario  
2012-2017

- Introduction in Biology (1201)
- Scientific methods in Biology (2290)
- Molecular Cell Biology of Stress (3355)

### Publications:

**Bensoussan, N.**, and Grbić, V. (2017). RNA interference in the two-spotted spider mite *Tetranychus urticae*. *Int. Organ. Biol. Integr. Control* 124, 200–206.

Suzuki, T., Nunes, M. A., España, M. U., Namin, H. H., Jin, P., **Bensoussan, N.**, et al. (2017b). RNAi-based reverse genetics in the chelicerate model *Tetranychus urticae*: A comparative analysis of five methods for gene silencing. *PLoS One* 12, e0180654.

**Bensoussan N**, Santamaria M.E, Zhurov V, Diaz I, Grbic M, Grbic V. (2016). Plant-herbivore interaction: dissection of the cellular pattern of *Tetranychus urticae* feeding on the host plant. *Front Plant Sci.* 7, 1105.

### **Selected presentation**

**Nicolas Bensoussan** and Vojislava Grbić. (2017). RNA interference in the two-spotted spider mite *Tetranychus urticae*. International Organisation for Biological and Integrated Control. Niagara Falls. On. (**Award: 1500€**)

Maria Nunes, **Nicolas Bensoussan**, Pengyu Jin, Takeshi Suzuki, María Urizarna España, Miodrag Grbic, Vojislava Grbic. (2017). Genetic variability of RNAi pest control. Phallona workshop. London. ON

**Nicolas Bensoussan**, Vladimir Zhurov, Miodrag Grbić and Vojislava Grbić. (2016). Characterization of the feeding apparatus and salivary glands associated with feeding in the two-spotted spider mite, *Tetranychus urticae*. Phallona workshop. London. ON

Maria Nunes, **Nicolas Bensoussan**, Pengyu Jin, Takeshi Suzuki, María Urizarna España, Miodrag Grbic, Vojislava Grbic. (2016). Genetic variability of RNAi pest control. Ontario Pest Management Conference. Guelph.

**Nicolas Bensoussan** and Vojislava Grbic. (2016) Plant-herbivore interaction: dissection of the cellular pattern of *Tetranychus urticae* feeding on the host plant. Biology Graduate Research Forum. London. On

**Nicolas Bensoussan**, Estrella Santamaria, Vojislava Grbić. (2015) Characterization of the plant damage resulting from the feeding of spider mite *Tetranychus urticae*. The Phallona Interdisciplinary Science Showcase. London ON (PhD. Work)

**Nicolas Bensoussan**, Estrella Santamaria, Vojislava Grbić. (2015) New insights into the spider mite mouthparts, their mode of action and their effect on plant tissues associated with feeding. Canadian Society of Plant Biologists. University of Toronto. ON (PhD. Work). **Award: Second price**

**Nicolas Bensoussan**, Estrella Santamaria, Vladimir Zhurov, Vojislava Grbić. (2014). Toward the characterization of the two-spotted spider mite plant feeding pattern and associated damage. Poster presentation. Sustainability and the Environment Research Showcase. University of Western Ontario. London, ON. (M.Sc. work)

**Nicolas Bensoussan**, Estrella Santamaria, Vladimir Zhurov, Vojislava Grbić. (2013). Toward the characterization of the two-spotted spider mite plant feeding pattern and associated damage. Canadian Society of Plant Biologists. Mississauga, ON. Poster presentation (M.Sc. work).